AD_____

Award Number: W81XWH-05-1-0053

TITLE: Epigenetic Characterization of Ovarian Cancer

PRINCIPAL INVESTIGATOR: Susan K. Murphy, Ph.D.

CONTRACTING ORGANIZATION: Duke University Medical Center
Durham, NC 27710

REPORT DATE: December 2008

TYPE OF REPORT: Final

PREPARED FOR: U.S. Army Medical Research and Materiel Command
Fort Detrick, Maryland 21702-5012

REPORT DOCUMENTATION PAGE

Form Approved
OMB No. 0704-0188

1. REPORT DATE	2. REPORT TYPE	3. DATES COVERED
1 Dec 2008	Final	15 Nov 2004 – 14 Nov 2008

4. TITLE AND SUBTITLE

Epigenetic Characterization of Ovarian Cancer

5a. CONTRACT NUMBER

5b. GRANT NUMBER
W81XWH-05-1-0053

5c. PROGRAM ELEMENT NUMBER

6. AUTHOR(S)

Susan K. Murphy, Ph.D.

E-Mail: murph035@mc.duke.edu

5d. PROJECT NUMBER

5e. TASK NUMBER

5f. WORK UNIT NUMBER

7. PERFORMING ORGANIZATION NAME(S) AND ADDRESS(ES)

Duke University Medical Center
Durham, NC 27710

8. PERFORMING ORGANIZATION REPORT NUMBER

9. SPONSORING / MONITORING AGENCY NAME(S) AND ADDRESS(ES)
U.S. Army Medical Research and Materiel Command
Fort Detrick, Maryland 21702-5012

10. SPONSOR/MONITOR'S ACRONYM(S)

11. SPONSOR/MONITOR'S REPORT NUMBER(S)

12. DISTRIBUTION / AVAILABILITY STATEMENT
Approved for Public Release; Distribution Unlimited

13. SUPPLEMENTARY NOTES

14. ABSTRACT

The overall objective of this research was to identify genes that are aberrantly methylated in epithelial ovarian cancer. Our approach was to treat or mock treat primary normal or tumor cultured cells with drugs that inhibit DNA methyltransferase activity and then perform microarray analysis to identify genes that are likely to exhibit methylation-mediated silencing. We also employed similar analysis of 43 ovarian cell lines. Two major criteria identified genes likely to be methylated: maximum fold-change in expression following drug treatment, and a high standard deviation in expression among untreated cells. These criteria were validated using a gene set known to exhibit methylation in other cancers and led to prediction of a total of 360 methylated genes in ovarian cancer, among which 32 were validated. Genes involved in TGF-beta pathway activity were over-represented among the candidates, and their methylation status was confirmed. Pathway activity was found to increase when DNA methyltransferase activity is inhibited, indicating coordinate epigenetic suppression of this pathway in ovarian cancer.

15. SUBJECT TERMS
Ovarian cancer, DNA methylation, primary culture, 5-azacytidine, Pyrosequencing, TGF-beta pathway

16. SECURITY CLASSIFICATION OF:			17. LIMITATION OF ABSTRACT	18. NUMBER OF PAGES	19a. NAME OF RESPONSIBLE PERSON
a. REPORT	b. ABSTRACT	c. THIS PAGE			USAMRMC
U	U	U	UU	105	19b. TELEPHONE NUMBER *(include area code)*

Table of Contents

INTRODUCTION

The purpose of this research project was to identify genes on a genome-wide scale that are epigenetically deregulated in ovarian cancer. The approach used was to identify genes targeted by DNA methylation in ovarian cnacer by utilizing microarray data generated from established cell lines as well as primary cultures from ovarian cancers of serous histology that were treated with a chemical inhibitor of DNA methyltransferase enzymes. A subset of the identified genes was examined for changes in promoter region methylation status to verify that they were indeed epigentically silenced in the original cancers. This information was used to determine the prevalence of that epigenetic deregulation in a larger sample of frozen ovarian cancer specimens and to identify particular patterns of epigenetic deregulation throughout the genome that provide insight into ovarian cancer etiology. The present report represents a final account of the research following completion of a one year no-cost extension to the project.

BODY

Over the past year during the no-cost extension period, we have completed the aims of the proposal. A summary of the work accomplished during the course of this project is detailed below.

Task 1. Optimize treatment of cells with 5-AzaC.

Completed as described in prior progress reports.

Task 2. Testchip analysis.

Completed as described in prior progress reports.

Task 3. GeneChip U133A Plus 2.0 analysis of five 5-azaC treated primary cultures of normal OSE and five serous ovarian carcinomas.

Completed as detailed in the 2006 and 2007 progress reports, and described in the draft manuscript appended to this report.

Task 4. Validation of gene hypermethylation status.

Completed as detailed below and in the appended draft manuscript.

Updates on genes presented in the 2006 and 2007 progress reports:

CENP-A. We reported that we had identified extremely site-specific partial methylation of the *CENP-A* (centromere variant protein A) transcription start site that was invariant among malignant and non-malignant tissues and was present in prenatal and postnatal tissues. Detailed results were provided in the 2006 and 2007 progress report showing that CENP-A exhibits what appears to be an allele-specific methylation pattern (it is 40-60% methylated in all tissues examined) and is also monoallelically expressed in many conceptal tissues in a manner that is not parent-of-origin dependent. CENP-A is therefore not an imprinted gene. We reported in 2007 that in synchronized cells, CENP-A methylation fluctuates with phases of the cell cycle in a

manner that is correlated with the levels of CENP-A transcription. We began the CENP-A project studying methylation using manual radiolabeled terminator cycle sequencing. As detailed in the 2007 progress report and request for a no-cost extension of this project, the reagents for this methodology were permanently discontinued by the manufacturer, necessitating an aternative approach to perform quantitative methylation analyses. *Support from the DoD enabled our acquisition of a Biotage Pyromark MD Pyrosequencing instrument* which we have now been using for methylation analysis. At the time of transition, we had only partially completed the *CENP-A* methylation analysis. We therefore have worked on designing a Pyrosequencing assay for *CENP-A* in order to complete the experiments and demonstrate reproducibility of the findings.

Development and optimization of Pyrsoequencing assays has been much more difficult than we had anticipated. Aside from the inherent obstacles of designing primers that sit in CG-rich sequence, the assay is limited by the temperature of the Pyrsoequencing reaction itself, which is carried out at 28 degrees C. This temperature is extremely permissive for mispriming events; therefore the initial assay design must take this into account, particularly for the biotinylated PCR primer (a biotin tag is incorporated at the 5' end to allow for retrieval of single stranded PCR amplicons that serve as template for the Pyrosequencing reaction) and sequencing primer. Our optimization of the PCR reaction includes testing the PCR conditions for temperature, MgCl2 concentration, primer concentration, potential benefit of PCR additives and cycling conditions. Ultimately, a single band must be produced from the reaction as visualized by agarose gel electrophoresis to have optimal chance of a successful run by Pyrosequencing.

Once the PCR conditions are optimized, we then generate standard curves for the reaction to show the linearity of methylation detection over a range of predefined methylation levels. While this is relatively easy to perform for a normally unmethylated region, regions that have inherent normal methylation (like *CENP-A* or imprint regulatory elements) are much more challenging. This is because of the unavailability of completely unmethylated DNA specimens for these particular regions. Our first attept to overcome this deficit was to use whole genome amplification. Here, the amplified specimen is theoretically devoid of methylation, but contains amplicons representing the entire genome. Dividing the specimen in half, then treating half with *SssI* DNA methyltransferase while mock treating the other half produces the unmethylated and methylated versions of the same genomic DNA. Defined mixtures of these specimens were prepared either prior to or following bisulfite modification, followed by Pyrsoequencing. Unfortunately, this produced less-than-desirable reproducibility in standard curve generation, owing to the inability to *accurately* quantify (using a Nanodrop spectrophotometer) the amplified genomic DNA no matter the particular step in which we tried. We therefore opted to utilize an alternative method based on a prior report [1]. This technique involves producing amplicons of the region of interest from normal human genomic DNA or universally methylated genomic DNA that has been bisulfite modified. ligating the amplicons into plasmids, bacterial transformation and selecting of individual clones for sequencing. The idea is to identify clones that exhibit a fully methylated profile and clones that exhibit a completely unmethylated profile. Once these clones are identified, the plasmids are grown up using mid-scale plasmid preps. As we found out, mini preps do not work well for this technique, because accurate quantification is essential for generating the defined mixtures of methylated and unmethylated DNA necessary for standrad curve analysis. Once the plasmids are quantified, we produced mixtures of methylated:unmethylated in the following ratios: 0:100, 25:75, 50:50, 75:25, 100:0. These mixtures then serve as template for PCR amplification and subsequent Pyrosequencing. The standard curve generated for the *CENP-A* Pyrosequencing assay using this method is shown in **Figure 1**. We achieved excellent concordance between the input value and observed value, with $R^2 = 0.997$.

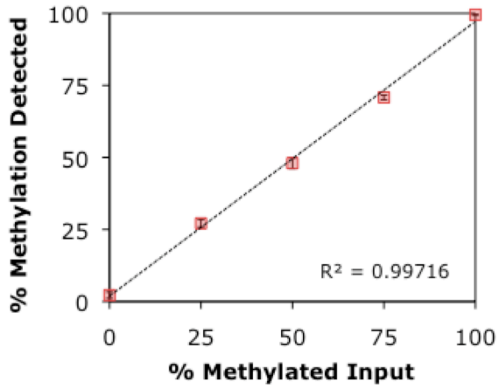

FIGURE 1. Pyrosequencing standard curve for *CENP-A* promoter region. Results are presented as the average of three independent assays (+/- SD). Dotted line, trend line.

We repeated the *CENP-A* experiment again in a panel of cell lines and selected those for further analysis that showed evidence of synchronization by a shift downward in the number of cells in S phase following serum starvation (**Figure 2,** right y-axis). Analysis of synchronized HUFF and CCD1138sk fibroblast cells by Pyrosequencing showed good agreement in methylation fluctuations that we had observed using the radiolabeled terminator method of sequencing as reported in the 2007 progress report. There was up to a 90% increase in the methylation status of *CENP-A* following serum starvation, which was followed in the HUFF cells by a further ~30% increase in methylation 6 hours later while *CENP-A* transcription decreased ~30%. Over the next 18 hours, *CENP-A* transcription increased ~30% while methylation decreased ~40%, showing a clear inverse relationship between methylation and *CENP-A* transcription. Since the doubling time of HUFF cells is ~24 hours, and the increase in S phase cells occurred after the 6 hour time point, *after CENP-A* methylation increased, such increased methylation cannot be attributed to a doubling of DNA content within these cells. While the CCD-1138Sk skin fibroblast cells showed wide shifts in methylation (from nearly completely methylated at time 0 to completely unmethylated at 6 hours following serum refeeding), *CENP-A* transcription only slightly increased when methylation declined, although the percentage of cells entering S phase was increasing at this time. It is presently unclear why *CENP-A* transcription did not increase in this cell line. Although there are differences in the overall levels of methylation from our first experiments to these that we analyzed using Pyrosequencing, our initial conclusions are supported by these more recent experiments in that methylation rapidly fluctuates during the cell cycle and this appears to inversely coincide with *CENP-A* transcription. We are preparing a

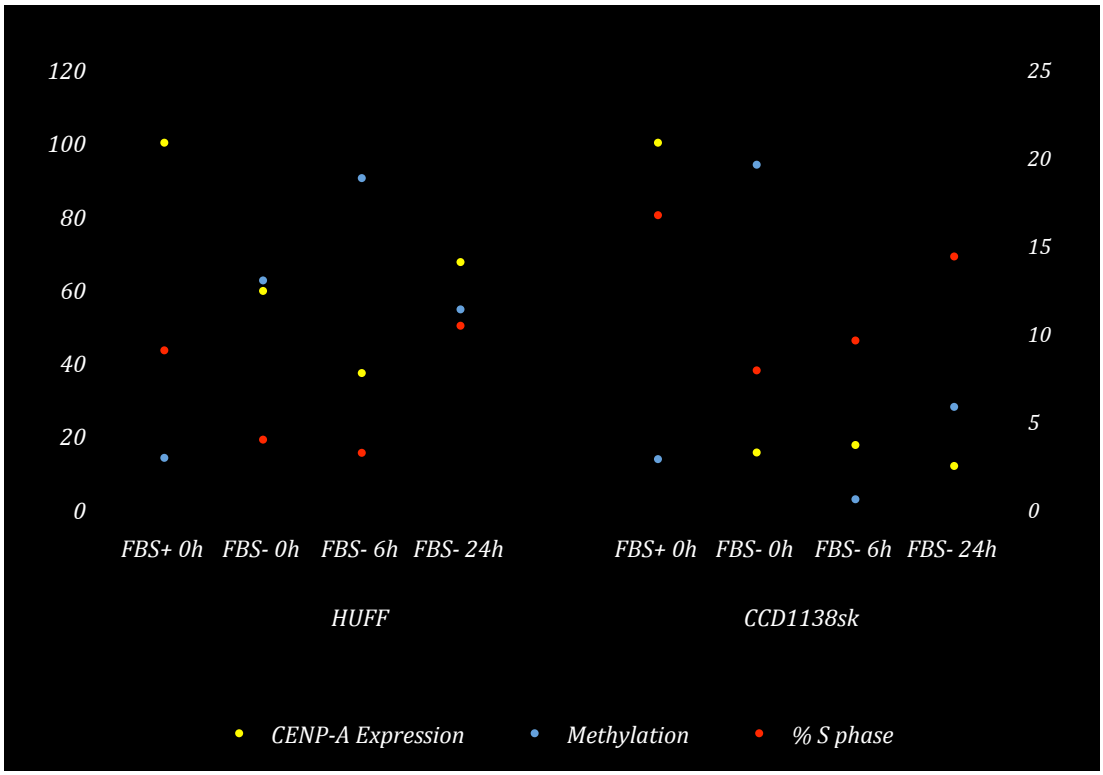

Figure 2. Analysis of serum-starved and re-fed synchronized human fibroblast cells for percentage of cells in S phase (flow cytometry), *CENP-A* methylation (Pyrosequencing) and *CENP-A* transcription (quantitative RT-PCR). Control cells (FBS+) represent a typical cycling population of the cells analyzed. Serum was removed for 24 hours after the cells reached ~60% confluence, followed by addition of 20% FCS for the remainder of the experiment. Methylation analysis was performed using Pyrosequencing.

manuscript for publication.

CDH4 (Retinal cadherin). In the 2006 and 2007 progress reports, we had described analysis of *CDH4* for methylation in ovarian cancer. This gene was predicted to be methylated from work done in collaboration with Dr. Terrence Furey, a computional biologist at Duke University with whom I have an ongoing collaboration. A manuscript detailing this work and acknowledging the DoD OCRP for support was submitted for publication first to *Oncogene* (rejected) and then to *Molecular Cancer Research* and is included in the Appendix. Although the manuscript was sent out for review it was ultimately rejected by *Molecular Cancer Research*, largely due to a lack of CDH4 protein analysis. We had actually attempted to detect CDH4 protein both by Western blotting and flow cytometry using available antibodies but only achieved nonspecific results. The person performing these experiments is highly skilled at both techniques so we do not believe this was due to experimental error. We are therefore revising the manuscript for resubmission elsewhere by addressing the other relatively minor reviewer concerns.

Analysis of microarray data and gene validation

Our major accomplishment over the duration of this project has been the generation and validation of genes methylated in ovarian cancer from analysis of microarray data from the primary ovarian cancers that underwent culture and treatment/mock treatment with 5-azacytidine. Our analysis also included microarray data generated from established ovarian cell lines as described in last year's progress report. We are currently working on revising the draaft of the manuscript that details these results, including validation of several genes using the Biotage Pyromark MD Pyrosequencing instrument. The current draft version of the manuscript and figures are provided in the Appendix and thus the details will not be presented here. This manuscript is in early revision stages and thus should not be interpreted as being a final draft. We are still analyzing genes by Pyrosequencing and if successful, this data will also be included in the manuscript.

One unforeseen complication we encountered during the extension period is the amount of effort and time required to design, optimize and validate the Pyrosequencing assays for DNA methylation. We have had extensive technical training and support from Biotage in this matter that has helped tremendously, but still the process is painstakingly slow in many cases. This is due to the fact that the Pyrosequencing reaction is necessarily carried out at 28 degrees celsius, a temperature that is very permissive for mispriming events. Great care must be taken in assay design to insure that the sequencing and biotinylated primers do not have alternative potential annealing sites on the amplicon produced. It is also essential that the PCR produces single robust amplicons as visulaized on an agarose gel. While we have been quite successsful at developing a number of assays, many others have been frustratingly difficult. We therefore will submit our manuscript for publication with a combination of MS-PCR and Pyrosequencing data, but are hoping to increase the number of genes analyzed by Pyrosequencing prior to the submission date since we believe this data is much more reliable, we have demonstrated its reproducibility, and it offers the great advantage of being able to quantitatively analyze individual CpG dinucleotides with endogenous controls for bisulfite conversion included in each reaction. We have included a figure in the Appendix that shows representative results for methylation-speciifc PCR which we have just compiled and that have not yet been incorporated into the manuscript.

We have also analyzed several additional genes by Pyrosequencing that were from the 360 predicted genes detailed in the appended manuscript (Item 2) and shown to exhibit evidnece of methylation from MS-

PCR analysis. We have designed Pyrosequencing assays for CD44, CD133 and CXCL12 and these are still in the process of optimization. We recently published a paper in *Oncogene* [2] showing that CD133 is regulated by DNA methylation and its expression is associated with a cancer stem cell phenotype. CD44 has also recently been identified as demarcating ovarian cancer cells with cancer stem cell phenotypes [3], and has previously been reported to be subject to methylation-mediated regulation [4-8]. Our prior CD133 analysis utilized the radiolabeled dideoxy terminator sequencing method that is no longer possible; we are therefore interested in being able to analyze CD133 methylation by Pyrosequencing. Both CD133 and CD44 were among the 360 predicted methylated genes in this study. We have developed Pyrosequencing assays for

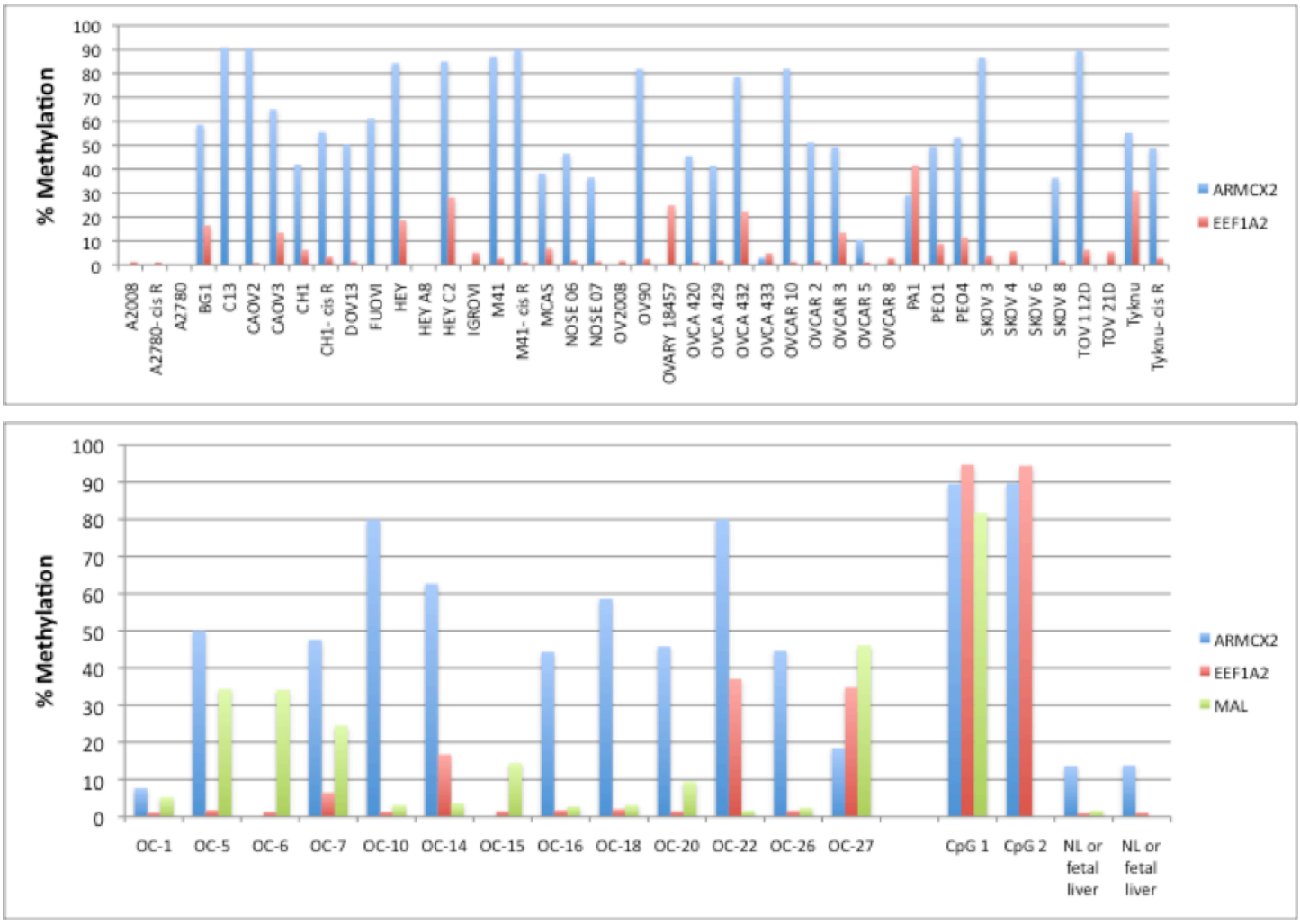

Figure 3. Pyrosequencing to quantify methylation at the *ARMCX2, EEF1A2* and *MAL* gene promoters (average of duplicate runs shown). Top, results obtained for our panel of ovarian cell lines. Bottom, results obtained from analysis of tumors that were used to establish primary cultures for treatment with 5-AzaC. CpG, universally methylated DNA; NL, normal lymphocytes.

three other genes from the 360 predicted to be methylated: *ARMCX2*, *EEF1A2* and *MAL*. We had previously found that *MAL* exhibits hypermethylation in ovarian cancer (prior to realizing it was one of our predicted genes!) using MS-PCR and radiolabeled bisulfite sequencing. We have analyzed DNA from the tumors used to establish the primary cultures for this project and cell lines for the methylation status of these genes. The results are presented in Figure 3. This work, although beyond what is required, will continue and will either be

incorporated into the manuscript already drafted (Appendix Item 2) or will form the basis for another manuscript.

To further aid identification of the genes throughout the genome that are aberrantly methylated in ovarian cancer, we have collaborated with Dr. Simon Gregory in using comparative methylation hybridization using high resolution (100 kb) genome tiling path arrays of the human genome. We have performed work using two established ovarian cancer cell lines to identify aberrantly methylated loci as described in the 2007 progress report. A manuscript detailing this work is being prepared by Jessica Connelly, a postdoctoral researcher in Dr. Gregory's laboratory. A poster recently presented at the 2008 American Society of Human Genetics meeting is appended to this final report, and a manuscript is in preparation detailing this work. This manuscript will acknowledge support from the DoD since most of the validation of methylation for the hybridization data was performed in the Murphy laboratory.

Task 5. Perform 5-azaC treatment and GeneChip U133A Plus 2.0 analysis of five each clear-cell, mucinous, and endometrioid tumors.

Restructured to focus on serous ovarian cancers because of the unfortunate lack of availability of the other histologic types as detailed in the 2007 progress report.

Task 6, Determine methylation status of the genes in N=43 normal ovaries that are hypermethylated in ovarian cancer.

This task was related to specific aim 3 of the grant, which was omitted per the DoD review.

KEY RESEARCH ACCOMPLISHMENTS

Year 1:

- Optimization of 5-azaC treatment completed; standard protocol has been established.
- Gene reactivation was confirmed in ovarian cancer cell lines.
- Protocol for culture of primary normal ovarian surface epithelial cells established.
- Ongoing collection and 5-azaC treatment of NOSE cells from surgery.
- Criteria for primary cancer specimen collection established, ongoing collection.
- RNA check and microarray hybridization (Affymettrix U133 Plus 2.0) has been performed for three serous epithelial ovarian cancer specimens.
- Annotation of genes containing promoter CpG islands was performed for the Affymetrix Array probe sets.
- One endometrioid cancer and a fourth serous cancer have been treated. The serous specimen is awaiting confirmation of the epithelial component of the cultured cells prior to array analysis and the endometrioid specimen has been confirmed.

Year 2:

- Sample accrual for ovarian tumor specimens has increased from 13 to 32 over the last funding period.
- Sample accrual for normal OSE has increased from 19 to 31 over the last funding period. 14 of these have been treated with 5-azaC and these have been divided into two pools, RNA has been prepared, and they are awaiting microarray hybridization.
- Frozen tumor and cells derived from these tumors (treated, mock-treated and untreated in most cases) has been banked for future analysis.
- RNA check and microarray hybridization (Affymettrix U133 Plus 2.0) has been performed for nine serous epithelial ovarian cancer specimens during this funding period, for a total of twelve serous cancers that have been microarrayed following 5-azaC treatment.
- One endometrioid cancer has been microarrayed following 5-azaC treatment.
- Microarray analysis indicates that there is a large cluster of genes with promoter CpG islands that are transcriptionally upregulated following 5-azaC treatment.
- Microarray analysis also indicates that there are a large number of genes that are transcriptionally downregulated following 5-AzaC treatment.
- DNA methylation anlaysis of one cell cycle gene, *CENPA*, showed that the region upstream of the transcription start site is methylated from 40-60% in an extremely site-specific manner.
- Computational predictions identified *CDH4* as a candidate methylated gene in ovarian cancer; molecular analysis confirmed this prediction and demonstrated a functional role for this retinal cadherin gene in epithelial ovarian cancer cells.
- Funded by the Duke Division of Gynecologic Oncology, we have recently obtained microarray data for 42 ovarian cell lines we have accrued (40 malignant and 2 spontaneously immortalized OSE lines) that were treated/mock treated with the DNMT inhibitor decitabine. These data will be used for comparative purposes with the primary tumor microarray data obtained from this project to help identify and analyze genes that are aberrantly methylated in ovarian cancer.

Year 3:

- Microarray data has been generated for two pooled normal ovarian surface epithelium specimens and two serous borderline ovarian tumors. The similarity in microarray data for the serous epithelial ovarian cancers indicated that additional microarrays may not yield additional useful information. We therefore opted to terminate collection of specimens (although still pursuing other histologies, to no avail) and focus on the analysis of the genes predicted to be methylated from the microarray analysis.
- A review article describing links between the environment, epigenetic changes and cancer was published.
- A manuscript describing a computational algorithm to predict genes methyated in cancer, and validation of the method, was published in *Bioinformatics*.
- A manuscript detailing methylation of *CDH4* was submitted for publication.
- *CENP-A* promoter methylation was shown to fluctuate with the cell cycle based on cell synchronization experiments; *CENP-A* expression levels coincide with this fluctuation based on analysis of human fibroblast cell lines.
- Analysis of microarray data from primary cancer specimens and ovarian cancer cell lines indicates that genes in the TGF-beta signaling pathway are frequently downregulated in epithelial ovarian cancer.

- Analysis of TGF-beta pathway genes for promoter methylation by methylation-specific PCR in primary ovarian cancers and in ovarian cancer cell lines verifies that promoter methylation is present at multiple TGF-beta pathway genes in a substantial number of specimens.
- BAC DNA tiling path methylation array experiments were performed on two ovarian cancer cell lines; promoter methylation was verified by methylation-specific PCR of a subset of genes for which the comparative methylation hybridization array data suggested methylation.
- A no-cost extension and rebudget request were approved for this project to allow us to perform quantitative DNA methylation analysis for the genes we have predicted to be methylated in ovarian cancer.

Year 4 (no-cost extension year)

- The *CDH4* manuscript was revised and again submitted for publication.
- A Biotage Pyromark MD Pyrosequencing instrument was purchased, and we received training in instrument use and assay design from Biotage.
- We validated our findings presented previously for *CENP-A* using Pyrosequencing that show dramatic fluctuations in methylation during cell cycle progression and are now preparing a manuscript for publication.
- We developed and validated Pyrosequencing assays for anlaysis of TGF-beta pathway-related genes that were predicted to be methylated in ovarian cancer based on our micorarray-based computational analyses.
- We have completed a draft manuscript that describes the analyses of the primary cell cultures, cell lines and primary cancers with the major findings that there is methylation-mediated coordinate suppression of the TGF-beta pathway, that methylation appears to accrue with age therefore increasing the likelihood of TGF-beta pathway deregulation, and that the genes targeted by methylation in ovarian cancer appear to demarcate a CpG Island Methylator Phenotype, previously described in colon cancer.
- A manuscript is in preparation detailing the BAC DNA tiling path methylation experiments and this work was presented at the 2008 American Society of Human Genetics meeting.
- We have developed additional Pyrosequencing assays for three other genes (*ARMCX2, EEF1A2* and *MAL*) of the 360 that were predicted to be methylated and validated thir methylation status in ovarian cnacer cell lines and in the primary ovarian tumors that were used to establish the primary cultures for analysis in this project.

REPORTABLE OUTCOMES

Research publications:

(1) Goh, L., Murphy, S. K., Mukherjee, S. and T. S. Furey. 2007. *Genomic sweeping for hypermethylated genes*. Bioinformatics 23:281-288.
(2) Weidman, J. R., Dolinoy, D. C., Murphy, S. K., and R. L. Jirtle. 2007. *Cancer susceptibility: epigenetic manifestation of environmental exposures.* The Cancer Journal 13:9-16.
(3) Murphy, S. K., Huang, Z., Simel, L. S., Goh, L. and T.S. Furey. *CDH4: a novel target of hypermethylation in ovarian cancer predicted through computational analysis*. (Under revision).

(4) *Baba, T., Convery, P., Matsumura, N., Whitaker, R. S., Perry, T., Huang, Z., Bentley, R. C., Mori, S., Fujii, S., Marks, J. R., Berchuck, A. and S. K. Murphy. 2008. Epigenetic regulation of CD133 and tumorigenicity of CD133(+) ovarian cancer cells. Oncogene (Advance Online Publication, October 6).
(5) *Matsumura, N., Huang, Z., Baba, T., Lee, P. S., Mori, S., Chang, J., Kuo, W., Gusberg, A. H., Whitaker, R. S., Gray, J. W., Fujii, S., Berchuck, A. and S. K. Murphy. YY1/E2F3 modulates antimicrotubule drug response in epithelial ovarian cancer. Molecular Cancer Research (in press).
(6) *Horne, H., Lee, P. S., Murphy, S. K., Alonso, M. A., Olson, J. A. and J. R. Marks. Inactivation of the MAL gene in breast cancer is a common event and predicts benefit from adjuvant chemotherapy. Molecular Cancer Research (in press).
(7) Huang, Z. and S. K. Murphy. Site-specific methylation of CENP-A promoter fluctuates during cell cycle progression. (In preparation)
(8) Connelly, J. J., Huang, Z., Biscocho, D., Gregory, S., and S. K. Murphy. Genome-wide targets of aberrant methylation in epithelial ovarian cancer cells. (In preparation)
(9) Matsumura, N., Huang, Z., Kroyer, D., Perry, T., Fujii, S., Berchuck, A. and S. K. Murphy. Transcriptome analysis reveals coordinate methylation-mediated suppression of genes associated with TGF-beta pathway activity in epithelial ovarian cancers. (In preparation)

* related to, but not directly funded by this project

Meeting Abstracts

2007 Reporting Period

(1) Murphy, S. K., Huang, Z., Goh, L., Simel, L. R., Wen, Y., Berchuck, A., and T. S. Furey. Computational Modeling Correctly Predicts Methylation-Mediated Silencing of R-CADHERIN in Ovarian Cancer. 38th Annual Society of Gynecologic Oncologist's Annual Meeting; San Diego, California, Abstract 117.
(2) Murphy, S. K., Huang, Z., Goh, L., Simel, L., Wen, Y., Berchuck, A. and T. S. Furey. Computational Modeling Correctly Predicts Methylation-Mediated Silencing of R-CADHERIN in Ovarian Cancer. Helene Harris Memorial Trust 11th International Biennial Forum on Ovarian Cancer; Lake Como, Italy.
(3) Matsumura, N., Huang, Z., Berchuck, A. and S. K. Murphy. Transcriptome analysis of DNA methylation status in ovarian cancer – correlation of aggressiveness and TGFb pathway. The 66th Annual Meeting of the Japanese Cancer Association, Yokohama, Japan; Abstract 10062.

2008 Reporting Period

(1) Matsumura, N., Huang, Z., Perry, T., Kroyer, D., Baba, T., Mori, S., Fujii, S., Berchuck, A. and S. K. Murphy. 2008. *Methylation in ovarian cancer is related to poor prognosis and suppression of the TGF-beta signaling pathway*. Society of Gynecologic Oncologists 39th Annual Meeting, Tampa, FL. Abstract #236.

(2) Huang, Z., Matsumura, N., Perry, T., Kroyer, D., Baba, T., Mori, S., Fujii, S., Berchuck, A. and S. K. Murphy. 2008. *Methylation in ovarian cancer is related to poor prognosis and suppression of the TGF-beta signaling pathway.* AACR Annual Meeting; San Diego, CA. Abstract 2644.

(3) Biscocho, D., Connelly, J.J., Huang, Z., Gregory, S. G. and S. K. Murphy. 2008. *Genome-wide targets of aberrant methylation in serous epithelial ovarian cancer.* American Society of Human Genetics Annual Meeting; Philadelphia, PA. Abstract #1204.

(4) Yamamura, S., Matsumura, N., Mandai, M., Baba, T., Hamanishi, J., Yamaguchi, K., Konishi, I., Huang, Z., Berchuck, A., and S.K. Murphy. 2008. *BIGH3, target of methylation in ovarian cancer, is up-regulated in omental metastasis.* Japanese Cancer Association, Nagoya, Japan.

(5) Matsumura, N., Murphy, S. K., Mandai, M., Fukuhara, K., Suzuki, A., Higuchi, T., Takakura, K. and S. Fujii. 2008. *Methylation in ovarian cancer is related to poor prognosis and suppresses TGF beta pathway.* 60th Annual Congress of the Japan Society of Obstetrics and Gynecology; Yokohama, Japan.

(6) Matsumura, N., Yamaguchi, K., Yamamura, S., Mandai, M., Fujii, S., Konishi, I., Huang, Z., Berchuck, A. and S. K. Murphy. [Translated from Japanese] *Bioinformatics approach to identify chemotherapy-sensitive molecular mechanisms and novel molecular-targeted drugs for the treatment of ovarian cancer.* Will be presented as a plenary presentation at the 2009 61st Annual Congress of the Japan Society of Obstetrics and Gynecology; Kyoto, Japan.

Degrees and Employment

(1) **Matsumura, N., M.D., Ph.D.** partially fulfilled the requirements for his Ph.D. from Kyoto University in Japan through work he performed on this project while he served as a visiting scientist in the Murphy laboratory from 2005 to 2007. Dr. Matsumura is currently on faculty at Kyoto University where he has developed an independent research program and has continued our collaboration on this project.
(2) **Goh, L**., **Ph.D.,** completed her postdoctoral research and was first author on the computational prediction paper leading to identification of *CDH4* as an aberrantly methylated gene in ovarian cancer. She has applied for and secured an Assistant Professor position at the Duke – National University of Singapore Graduate Medical School, where she is continuing to work on computational analysis of DNA methylation in ovarian cancer as a collaborator.
(3) **Jessica Connelly, Ph.D.**, completed her postdoctoral research in the laboratory of Dr. Simon Gregory and received additional mentoring related to this project from Dr. Murphy over the last three years. This project has formed a substantial component of her postdoctoral training. She has obtained a faculty position at the University of Virginia, Charlottesville where she plans to continue working on analysis of DNA methylation in coronary disease.

Tissue repository. The primary cancer specimens collected for the purposes of this project were stored as frozen tissues and as cell pellets following expansion in culture. We have stored cell pellets from untreated, mock-treated, and 5-azacytidine treated cells to allow for ongoing analysis of genes that are affected by DNA methylation in ovarian cancers.

Funding applied for (partially) resulting from this project:

(1) NIH/NCI: 1 R01CA122424 (Murphy, PI)
Total requested amount: $ 1,940,020
Proposed award period: 07/01/07 – 06/30/12
Title: Multidisciplinary Attack on Silent Killer: Ovarian Methylome Revealed

(2) DoD BCRP: Synergistic Idea Award (Murphy and Schildkraut, Co-PIs)
Total requested amount: $ 736,080
Proposed award period: 11/01/07 – 10/31/09
Title: Inheritance of BRCA1 Methylation

(3) Duke Comprehensive Cancer Center / American Cancer Society (Murphy, PI)
Total requested amount: $20,000
Proposed award period: 12/01/07-12/31/07
Title: Aberrant DNA Methylation in Ovarian Cancer: Inducers and Protectors

(4) DoD OCRP: Translational Research Partnership Award (Murphy and Berchuck, Co-PIs)
Total requested amount: $ 553,603
Proposed award period: 9/30/09 – 9/29/12
Title: Characterization of CD133+ Ovarian Cancer Cells

(5) NIH/NCI: 1R01CA1140500 (Murphy, PI)
Total requested amount: $1,560,000
Proposed award period: 7/1/09 – 6/30/13
Title: Deregulation of an Imprinted Gene Network in Ovarian Cancer

Personnel Receiving Pay for this Project

Susan K. Murphy, Ph.D.
Andrew Berchuck, M.D.
Jeff Marks, Ph.D.
Ed Iversen, Ph.D.
Zhiqing Huang, M.S. (Research Analyst II)
Teresa Nichols, B.S. (Research Tech I)
Lauren Simel, B.S. (Research Tech I, replaced Nichols, now in nursing school)
Tiffany Perry, B.S. (Research Tech I, replaced Simel, now in medical school)
Darby Kroyer, BS (Research Tech I, replaced Perry, now in medical school)

Personnel that Contributed to the Project Without Pay

Noriomi Matsumura, M.D., Ph.D.
Liang Goh, Ph.D.
Terry Furey, Ph.D.
Jessica Connelly, Ph.D.

Dhani Biscocho
Simon Gregory, Ph.D.
Carole Grenier, B.S.
Cara Davis
Yaqing Wen, B.S.

CONCLUSIONS

This project has achieved a number of remarkable findings. First, we have identified a gene, through our initial computational analysis, that exhibits extremely site-specific methylation that fluctuates dramatically through the cell cycle. This necessarily implies that there is *active* loss and gain of methylation that occurs, since these events take place *prior* to cell division. Such an exciting finding has major implications for our understanding of just how rapidly DNA methylatin can change, and indicates that our paradigm view of DNA methylation may need to be reassessed to accommodate the finding that changes in methylation may be a highly dynamic process.

The major outcome of our research has led to the identification and validation of a large number of genes that are targeted by DNA methylation as a mechanism to repress their transcription. Importantly, we have identified methylation of a substantial number of genes that participate in the activity of the TGF-beta pathway and confirmed the relationship between DNA methylation and suppression of pathway activity. Interestingly, the accumulation of DNA methylation and pathway suppression seem to be a function of increasing age, providing a potential explanation for the increased incidence of ovarian cancer as women age. In addition, our data support that there is a CpG Island Methylator Phenotype (CIMP) in ovarian cancer, since we observe coordinate methylation of a large number of genes in both ovarian cancer cell lines and primary ovarian cancers.

The importance of these findings lies not only in the contribution of knowledge about the gene set that becomes epigenetically deregulated in ovarian malignancies and the CIMP phenotype, but may have direct application to patient care. We hope to develop a 'methylation chip' that can be used as a tool to improve early diagnosis as well as for therapeutic decision making, that will take into account the epigenetic profile of the individual tumor and how the methylation and expression status of the affected genes in that tumor will in turn affect response to therapy and prognosis. With a large number of validated genes in hand, it may be possible to now bring this to fruition, although we will still need to identify the gene set that demonsrates specificity to ovarian cancer. Our finding that TGF-beta pathway suppression is a common feature among ovarian cancer patients combined with the fact that this suppression is epigenetically mediated suggests the potential to intervene in this process, either through epigenetic-based therapies (e.g., Valproic Acid [9]) or through intervention using drugs that target the pathway [10, 11]. In conclusion, our research has contributed substantial new findings (including one that may be paradigm-shifting) using a comprehensive, genome-wide approach that demonstrate how epigenetic changes contribute to the development of epithelial ovarian cancer, results that we envision will ultimately improve the ability to diagnose and treat this disease.

REFERENCES

1. Wong, H.L., et al., *Rapid and quantitative method of allele-specific DNA methylation analysis.* Biotechniques, 2006. **41**(6): p. 734-9.
2. Baba, T., et al., *Epigenetic regulation of CD133 and tumorigenicity of CD133+ ovarian cancer cells.* Oncogene, 2008.
3. Zhang, S., et al., *Identification and characterization of ovarian cancer-initiating cells from primary human tumors.* Cancer Res, 2008. **68**(11): p. 4311-20.
4. Abecassis, I., et al., *Re-expression of DNA methylation-silenced CD44 gene in a resistant NB4 cell line: rescue of CD44-dependent cell death by cAMP.* Leukemia, 2008. **22**(3): p. 511-20.
5. Woodson, K., et al., *CD44 and PTGS2 methylation are independent prognostic markers for biochemical recurrence among prostate cancer patients with clinically localized disease.* Epigenetics, 2006. **1**(4): p. 183-6.
6. Wang, Y., et al., *Multiple gene methylation of nonsmall cell lung cancers evaluated with 3-dimensional microarray.* Cancer, 2008. **112**(6): p. 1325-36.
7. Patra, S.K. and S. Bettuzzi, *Epigenetic DNA-methylation regulation of genes coding for lipid raft-associated components: a role for raft proteins in cell transformation and cancer progression (review).* Oncol Rep, 2007. **17**(6): p. 1279-90.
8. Sato, S., et al., *Silencing of the CD44 gene by CpG methylation in a human gastric carcinoma cell line.* Jpn J Cancer Res, 1999. **90**(5): p. 485-9.
9. Duenas-Gonzalez, A., et al., *Valproic acid as epigenetic cancer drug: preclinical, clinical and transcriptional effects on solid tumors.* Cancer Treat Rev, 2008. **34**(3): p. 206-22.
10. Redondo, S., C.G. Santos-Gallego, and T. Tejerina, *TGF-beta1: a novel target for cardiovascular pharmacology.* Cytokine Growth Factor Rev, 2007. **18**(3-4): p. 279-86.
11. Saunier, E.F. and R.J. Akhurst, *TGF beta inhibition for cancer therapy.* Curr Cancer Drug Targets, 2006. **6**(7): p. 565-78.

APPENDICES

ITEM 1: Murphy, S. K., Huang, Z., Simel, L. R., Goh, L., Berchuck, A. and T. S. Furey. *CDH4* (R-Cadherin): a novel computationally predicted target of hypermethylation in ovarian cancer. (Draft Manuscript)

ITEM 2: Matsumura, N., Huang, Z., Perry, T., Kroyer, D., Baba, T., Mori, S., Fujii, S., Marks, J. R., Berchuck, A. and S. K. Murphy. Transcriptome analysis reveals coordinate methylation-mediated suppression of genes associated with TGF-beta pathway activity in epithelial ovarian cancers. (Draft Manuscript)

ITEM 3: Representative methylation-specific PCR results related to the above manuscript.

ITEM 4: Biscocho, D., Connelly, J.J., Huang, Z., Gregory, S.G. and S.K. Murphy. 2008. *Genome-wide targets of aberrant methylation in serous epithelial ovarian cancer.* American Society of Human Genetics Annual Meeting; Philadelphia, PA. (Poster)

ITEM 5: Matsumura, N., Huang, Z., Perry, T., Kroyer, D., Baba, T., Mori, S., Fujii, S., Berchuck, A. and S. K. Murphy. 2008. Methylation in ovarian cancer is related to poor prognosis and suppression of the TGF-beta signaling pathway. Society of Gynecologic Oncologists 39th Annual Meeting, Tampa, FL. Abstract #236.

ITEM 6: Huang, Z., Matsumura, N., Perry, T., Kroyer, D., Baba, T., Mori, S., Fujii, S., Berchuck, A. and S. K. Murphy. 2008. *Methylation in ovarian cancer is related to poor prognosis and suppression of the TGF-beta signaling pathway.* AACR Annual Meeting; San Diego, CA. Abstract 2644.

ITEM 7: Biscocho, D., Connelly, J.J., Huang, Z., Gregory, S.G. and S.K. Murphy. 2008. *Genome-wide targets of aberrant methylation in serous epithelial ovarian cancer.* American Society of Human Genetics Annual Meeting; Philadelphia, PA. Abstract 1204.

ITEM 8: Yamamura, S., Matsumura, N., Mandai, M., Baba, T., Hamanishi, J., Yamaguchi, K., Konishi, I., Huang, Z., Berchuck, A., and S.K. Murphy. 2008. BIGH3, target of methylation in ovarian cancer, is up-regulated in omental metastasis. Japanese Cancer Association, Nagoya, Japan.

ITEM 9: Matsumura, N., Murphy, S. K., Mandai, M., Fukuhara, K., Suzuki, A., Higuchi, T., Takakura, K. and S. Fujii. 2008. Methylation in ovarian cancer is related to poor prognosis and suppresses TGF beta pathway. 60th Annual Congress of the Japan Society of Obstetrics and Gynecology; Yokohama, Japan.

ITEM 10: Matsumura, N., Yamaguchi, K., Yamamura, S., Mandai, M., Fujii, S., Konishi, I., Huang, Z., Berchuck, A. and S. K. Murphy. [Title translated from Japanese] Bioinformatics approach to identify chemotherapy-sensitive molecular mechanisms and novel molecular-targeted drugs for the treatment of ovarian cancer. Will be presented as a plenary presentation at the 2009 61st Annual Congress of the Japan Society of Obstetrics and Gynecology; Kyoto, Japan.

January 4, 2008
Original

CDH4 (*R-Cadherin*): a novel computationally predicted target of hypermethylation in ovarian cancer

Susan K. Murphy[1,2*], Zhiqing Huang[1], Lauren R. Simel[1], Liang Goh[2], Andrew Berchuck and Terrence S. Furey[2]

1 Department of Obstetrics and Gynecology, Division of Gynecologic Oncology, Duke University, Durham, NC USA 27708
2 Duke Institute for Genome Sciences and Policy, Durham, NC USA 27708

This work was supported by a grant to SKM from the DoD Ovarian Cancer Research Program, award number W81XWH-05-1-0053.

Key Words: R-cadherin, *CDH4*, methylation, ovarian cancer
Running Title: *CDH4* methylation in ovarian cancer

* Corresponding author
2185 F-CIEMAS
Box 91012
101 Science Drive
Durham, North Carolina 27708
(919) 681-3423
FAX: (919) 684-5336
murph035@mc.duke.edu
epigen001@mac.com

ABSTRACT

We previously developed a machine learning-based algorithm that predicted *Retinal Cadherin* (*CDH4)* as a gene prone to methylation in cancer. Gene expression microarrays indicate that *CDH4* is highly expressed in normal ovarian surface epithelium relative to most primary serous epithelial ovarian cancers. We found that the *CDH4* promoter exhibits methylation in 56% of primary ovarian cancers. *CDH4* promoter methylation is also present in 23 of 35 ovarian cancer cell lines analyzed, and methylation correlates with transcriptional silencing. Methylation was pharmacologically reversed using DNA methyltransferase inhibitors, leading to increased *CDH4* transcription in two of four tested cell lines with promoter methylation. siRNA-mediated knockdown of *CDH4* in ovarian cancer cell lines led to inhibition of cellular proliferation, reduced anchorage-independent growth and reduced cell motility. *CDH4* knockdown also decreased cell-cell adhesion and increased cell scattering, phenotypes that can promote cancer cell metastasis. Our results indicate a complex and previously unappreciated role for CDH4 and its epigenetic inactivation in the molecular pathogenesis of ovarian cancer.

INTRODUCTION

Ovarian cancer is the leading cause of death from gynecologic malignancies, with metastatic spread common at first diagnosis. This is due to the lack of a screening test for early stage disease (1) together with vague symptoms that are often attributed to other more common ailments (2). Inherited alterations in *BRCA1* and *BRCA2* account for about 10% of ovarian cancer cases (3) and the underlying cause(s) for the remainder are largely unknown. It is now clear that epigenetic alterations, including DNA methylation and histone modifications, have a profound influence on the initiation and progression of malignancy (4, 5). Aberrant methylation of cytosines at the promoter region of genes is one mechanism that is commonly found in cancer cells to reduce or silence gene transcription. This event occurs in a highly gene-specific and tumor-specific manner (6, 7), yet very little is known about how and why particular genes are targeted for methylation and if the context of the surrounding nucleotide sequence contributes to this targeting.

Previously, we developed a computational algorithm called *cluster_boost* to determine if sequence features extracted from a training set of genes known to be methylated in cancer could identify other such genes (8). In this report, we investigate in ovarian cancer the methylation status and role of *RETINAL CADHERIN* (*CDH4*), one of the genes computationally predicted to be methylated by *cluster_boost*. *CDH4* encodes a 916 amino acid, type I single span membrane protein and is a member of the cadherin superfamily that mediate cell-cell adhesion and cell signaling. Our objective was to

determine if *CDH4* is targeted by promoter methylation in epithelial ovarian cancers and to better understand the role of CDH4 in ovarian carcinogenesis.

RESULTS AND DISCUSSION

Comparison of the expression patterns of *CDH4* in normal and malignant ovarian tissues using gene expression microarrays (9) indicated that *CDH4* is highly expressed in normal ovarian surface epithelium with decreased expression prominent in the majority of serous borderline tumors (tumors of low malignant potential) and malignant tissues (Figure 1A). Furthermore, the difference in *CDH4* expression in advanced ovarian cancers is significant between women living less than 3 years post diagnosis versus those living longer than 7 years, with higher expression in short-term survivors ($p= 0.0008$, 95% CI, -0.39—0.11; two-tailed unpaired t test). *CDH4* expression was also lower in tumors from women with a complete clinical response to treatment (N=34; defined as having a CA125 level < 35 U/ml, normal CT scan and office examination with no evidence of disease one month following completion of primary chemotherapy) versus women with an incomplete clinical response (N=22; $p=0.002$, 95% CI, 0.09-0.38; two tailed unpaired t test; not shown). *CDH4* spans ~685 kb of genomic distance at chromosome 20q13.3 and is encoded by 15 exons. There are 13 CpG islands annotated within the *CDH4* locus, with the largest located at the promoter. This CpG island is 2001 bp in length, with 230 CpG dinculeotides and an observed to expected CpG ratio of 1.05 (10). We used methylation-specific PCR to examine the methylation status of CpG dinucleotides flanking the *CDH4* transcription start site. We found that *CDH4* does not exhibit methylation in normal peripheral blood lymphocytes (N=23), but in 28 of 52 (56%) ovarian cancer specimens, promoter methylation was detected. We also found

CDH4 methylation in 23 of 35 (66%) of the established ovarian cancer cell lines we examined (representative results shown in Figure 1B).

DNA methylation-mediated silencing of gene expression is potentially reversible using pharmacological agents that inhibit the activity of the DNA methyltransferase (DNMT) enzymes. We therefore treated four ovarian cancer cell lines that exhibited *CDH4* methylation with the DNMT inhibitors, 5-azacytidine (AzaC) and 5-aza 2-deoxycytidine (DAC). Quantitative bisulfite sequencing revealed cell-dependent responses to these treatments (Figure 2A; representative sequences shown in Figure 2C). OVCAR3 and SKOV3 showed little to no decrease in methylation in response to treatment with DAC. Treatment of SKOV3 cells with AzaC reduced methylation ~20%, but this was insufficient to allow for reactivation of *CDH4* transcription as detected by RT-PCR (Figure 2B). DAC treatment of CAOV2 and SKOV4 cells reduced methylation to ~20% and 55%, respectively, and resulted in increased *CDH4* transcription. AzaC treatment also reduced methylation in these cell lines, but was not sufficient to reactivate expression (Figure 2B).

We examined the level of expression of *CDH4* in 43 ovarian cell lines (41 cancer cell lines and two spontaneously immortalized normal ovarian surface epithelium lines) with respect to the methylation status of the transcription start site using microarray data and MS-PCR. We first validated that the microarray expression levels of *CDH4* for a subset of these cell lines (N=23) correlated with *CDH4* gene expression using an

independent method - quantitative real time RT-PCR for *CDH4*, normalized to *ACTB* run in parallel as an endogenous control for RNA loading for each sample. The results showed good agreement between the two methods in quantifying expression of *CDH4* (Spearman r = 0.81, 95% CI, 0.59 to 0.92; $p<0.0001$; data not shown). From methylation analysis, the cell lines are divided into two groups: those with low *CDH4* expression and evidence of methylation at the promoter and those with higher *CDH4* expression and no methylation (Figure 2D); this association is statistically significant ($p<0.0001$, two-tailed unpaired t test). The two normal ovarian surface epithelium cell lines, NOSE-06 and NOSE-07, had higher levels of *CDH4* transcripts and were unmethylated.

To determine how CDH4 might contribute to ovarian cell biology, we used siRNA knockdown to repress the level of *CDH4* transcription and followed this with measures of cell behavior. Transient transfection of *CDH4*-specific siRNAs reduced transcript levels more than 70% (although in most cases >90%) as measured by quantitative real time RT-PCR and normalized to *ACTB* (not shown). *CDH4* knockdown led to reduced cell proliferation, measured in quadruplicate, in NOSE-06, HEY, HEYC2, HEYA8, PEO1, OVCA429 and OVCA433 ($p=0.01$, two-tailed paired t test), with a range of reduction from 4% (in the normal OSE line) to 39% (Figure 3A). Anchorage-independent growth was also repressed following knockdown of *CDH4,* up to 71% of that observed in cells receiving the control siRNAs in HEY, HEYC2 and PEO1 cells, but not in HEYA8 cells ($p=0.10$, two-tailed paired t test; Figure 3B).

We next assessed the effect of *CDH4* knockdown on cell migration, using a 'wound healing assay' in which a confluent monolayer of cells is disrupted by inducing a gap with the tip of a sterile pipet by scraping it across the monolayer. The migration of cells from each edge of the 'wound' inward to fill this gap is then monitored. In the four cell lines analyzed (HEY, HEYA8, OVCA429 and OVCA433), *CDH4* knockdown resulted in a marked delay in return to confluence (Figure 4A, OVCA429 cells shown). Upon closer examination, the monolayer in the *CDH4* knockdown cells exhibited increased disorganization as compared to the cells receiving control siRNAs, and there was an increase in cell scattering behavior, evident five hours after wound induction for the OVCA429 cell line. In this case, cells appeared to be released from the remainder of the monolayer, with increased numbers of cells that no longer maintain cell-cell contacts. This was observed in each of the four cell lines but was most prominent in the OVCA433 and OVCA429 cells because of their 'cobblestone' appearance that is typical of ovarian epithelial cells (Figure 4B).

We have shown here that *CDH4* is subject to promoter methylation in serous epithelial ovarian cancers, a characteristic predicted from computational analysis. Promoter methylation is pharmacologically reversible, leading to increased *CDH4* transcription. *CDH4* was previously shown to be methylated at high frequency in colorectal and gastric cancers (11), although it was not included as a member of our *cluster_boost* training set. In these malignancies, *CDH4* methylation was present in tissue proximal to the malignancy, suggesting that methylation is an early event in the

carcinogenic process. It is presently unclear if this also holds true for ovarian cancer, although the data in Figure 1A suggest that *CDH4* is downregulated in most Stage I and II malignant ovarian tissues. We have also found that elevated CDH4 expression is associated with poor clinical outcome, and *in vitro* assays indicate that CDH4 contributes to a more aggressive cell phenotype. This is consistent with a prior report in which abnormal expression of CDH4 led to loss of E-cadherin interaction with p120 and deregulation of cell signaling in a human epidermoid carcinoma cell line (12). Finally, *CDH4* knockdown in ovarian cancer cell lines caused cell scattering behavior and monolayer disorganization. This finding may have substantial implications for *in vivo* tumor behavior in the context of *CDH4* repression, whether by epigenetic deregulation or other means. In conclusion, we have shown that CDH4 plays a role in the phenotype of ovarian cancer and contributes to the heterogeneity of this disease. Additional work is required to more precisely define the role of *CDH4* in ovarian carcinogenesis and the functional consequences of epigenetic inactivation *in vivo*.

MATERIALS AND METHODS

Tissue specimens and cultured cells. All tissue specimens were obtained with patient consent and were used under a protocol approved by the Duke Institutional Review Board. Patient characteristics for primary ovarian specimens that underwent microarray analysis, and the microarray data generated from those specimens have been previously described (9). Established ovarian cancer cell lines were maintained in 1X RPMI1640 medium with L-glutamine (Invitrogen, Carlsbad, CA) supplemented with 10% FBS and 1% Penicillin/Streptomycin (Mediatech; Herndon, VA) in a 37°C humidified chamber with 5% atmospheric CO_2.

Gene expression microarrays. Microarray hybridization for 43 ovarian cell lines (41 cancer and two spontaneously immortalized normal OSE lines, NOSE-06 and NOSE-07) was performed using the Affymetrix U133A High Throughput Arrays (Affymetrix; Santa Clara, CA, USA) by the Duke DNA Microarray Facility. The quality and integrity of the RNA was assessed using the Agilent Bioanalyzer (Santa Clara, CA) prior to array hybridization. Log-transformed gene expression values were calculated using the robust multiarray analysis (RMA) algorithm (13) implemented in the Bioconductor (http://www.bioconductor.org) extensions to the *R* statistical programming environment (14).

Methylation analysis. Genomic DNA was purified using Puregene reagents from Gentra Systems (Qiagen; Valencia, CA, USA). 0.5 – 1.0 µg of genomic DNA was treated with sodium bisulfite as previously described (15). Methylation-specific PCR for the *CDH4* promoter was performed with primers that generate 329 bp and 325 bp amplicons from the methylated and unmethylated DNA sequences, respectively. Primer sequences were: M forward, 5'-CGG GTT TTC GGT GTC GGG TAT C-3'; U forward, 5'-GGA GTG GGT TTT TGG TGT TGG GTA TT-3'; and a shared reverse primer that does not anneal to CpGs, 5'-AAC CCC ACT CCC ACC CTA CTC C-3'. PCR was performed using ~30 ng of bisulfite modified template and Platinum Taq DNA polymerase (Invitrogen, Carlsbad, CA, USA) in 12.5 µl reaction volumes. Cycling conditions were 3 min at 94°C followed by 35 cycles of 94°C for 30 sec, 69°C for 30 sec and 72°C for 45 sec, followed by 5 min at 72°C. Amplicons were resolved on 2% agarose gels and visualized by ethidium bromide staining. Image acquisition was done using a Canon Powershot A520 digital camera and Adobe Photoshop 7.01 (Adobe Systems Inc.; San Jose, CA) for image processing, which involved conversion to greyscale, inversion of the images, and in some cases, adjusting brightness and contrast.

Quantitative bisulfite sequencing was performed by producing 698 bp amplicons using Platinum Taq DNA polymerase (Invitrogen) with forward primer 5'-TTA GGA GGG TAG AGG TTG GGT TGG TG-3' and reverse primer 5'-AAC CCC ACT CCC ACC CTA CTC C-3' and PCR conditions as follows: 94°C for 3 min followed by a stepdown protocol: 5 cycles of 94°C for 30 sec, 71°C for 30 sec and 72°C for 30 sec, 5

cycles with a 68°C annealing temperature, then 35 cycles with a 65°C annealing temperature, followed by a 5 min extension at 72°C. PCR amplicons were resolved on 2% agarose gels, excised and purified using Sigma GenElute spin columns (Sigma-Aldrich). Nucleotide sequencing used the reverse primer and the Thermosequenase Radiolabeled Dideoxy Terminator Cycle Sequencing Kit (US Biochemicals; Cleveland, OH, USA) under the following conditions: 35 cycles of 95°C for 30 sec, 62°C for 30 sec and 72 °C for 60 sec. The sequencing products were resolved on a 5% denaturing polyacrylamide gel followed by exposure to a storage phosphor screen and scanning using the GE Healthcare Storm gel and blot imaging system (Piscataway, NJ). Image analysis was performed using ImageQuant software (GE Healthcare). Percent methylation was calculated for each CpG as follows (accounting for use of a reverse sequencing primer): %mC = 100 x [G/(G+A)].

Pharmacologic inhibition of DNMT activity. Ovarian cancer cells were grown to 70% - 80% confluence and mock treated or treated with 5 μM 5-azacytidine or 2-aza-5'-deoxycytidine (Sigma-Aldrich; St. Louis, MO, USA) for 72 hours followed by purification of nucleic acids. Total cellular RNA was prepared using RNA Stat-60 (TelTest; Friendswood, TX, USA). First strand cDNA was synthesized from 2 μg RNA in a 20 μl reaction volume using Superscript II RNase H- reverse transcriptase (Invitrogen). Forward primer: 5'-GCG ACA TCG GTG ACT TCA T-3' and reverse primer 5'-ATA CAT GTC CGC CAG CTT CT-3' for *CDH4* cDNA amplification are positioned in exon 15 and 16 of *CDH4* (RefSeq NM_001794) and produce a 212 bp

product using Platinum Taq DNA polymerase (Invitrogen) in a 12.5 µl reaction volume as follows: 3 min at 94°C followed by 35 cycles of 94°C for 30 sec, 62°C for 30 sec and 72°C for 45 sec, followed by a 72°C extension for 5 min. *GAPDH* mRNA was amplified in parallel. Amplicons were visualized on 2% agarose gels by ethidium bromide staining. Image acquisition was done using a Canon Powershot A520 digital camera and Adobe Photoshop 7.01 software (Adobe Systems Inc.; San Jose, CA) was used for image processing, which involved conversion to greyscale and adjusting brightness and contrast.

CDH4 knockdown. $1x10^5$ cells/well in a 24-well plate were transfected with two independent siRNA oligos specific to *CDH4* alongside nonsilencing control siRNA oligos (5 nm each) using HiPerfect reagent (Qiagen, Valencia, CA, USA). siRNA oligo sequences were as follows: siRNA-1 target sequence in exon 13: CAC GTC CAT CAT CAA AGT CAA; siRNA-1 sense oligo: r(CGU CCA UCA UCA AAG UCA A)dTdT; siRNA-1 antisense oligo: r(UUG ACU UUG AUG AUG GAC G)dTdG; siRNA-2 target sequence in exon 7: CCA GAA TAT GTT CAC CAT CAA; siRNA-2 sense oligo: r(AGA AUA UGU UCA CCA UCA A)dTdT; siRNA-2 antisense oligo: r(UUG AUG GUG AAC AUA UUC U)dGdG. Knockdown efficiency using either *CDH4*-specific siRNA was >70% (most >90%) as compared to cells transfected with the non-silencing siRNA control oligos, measured by quantitative real time RT-PCR (TaqMan Assays on Demand). The cells were trypsinized 24 hours post-transfection and plated for proliferation and anchorage-independent growth assays. For measurement of *CDH4* influence on cell proliferation, 10^3 transfected cells/well were transferred to 96-well

plates containing 100 ul of RPMI1640 medium. Proliferation was analyzed in quadruplicate 96 hours post-transfection using CellTiter 96® AQueous One Solution Cell Proliferation Assay kit from Promega according to the protocol provided by the company. For anchorage-independent growth, 10^3 transfected cells/well were seeded into 96-well plates containing 0.5% agar/RPMI1640. The cells were cultured 7-10 days. Colonies exceeding 100 mm in diameter were counted and averaged from four transfected wells for each siRNA.

Cultured cell wound healing assays. 24 hours post-transfection with siRNA oligos as described above, cells from two wells of a 24-well plate were combined and seeded into one 3.5 cm well of a six-well plate. 72 hours later, the cells were >90% confluent. Three 'wounds' were made in the monolayer by scratching across the surface with an aerosol-resistant pipet tip (outer diameter of distal end of tip, 1.22 mm; ART 1000E, Molecular BioProducts; San Diego, CA). The cells were gently rinsed with PBS to remove the non-adherent cells and cultured in RPMI1640 medium containing 10% FBS. Assays were independently repeated with similar results. Photomicrographs were taken immediately following wound induction and at later designated time points using a Nikon Coolpix 4500 digital camera with a Nikon Eclipse TE2000-S inverted phase contrast research microscope with a 10X eyepiece lens and 10X and 20X objective lenses.

REFERENCES

1. Munkarah A, Chatterjee M, Tainsky MA. Update on ovarian cancer screening. Curr Opin Obstet Gynecol 2007;19(1):22-6.

2. Bankhead CR, Kehoe ST, Austoker J. Symptoms associated with diagnosis of ovarian cancer: a systematic review. BJOG 2005;112(7):857-65.

3. Lux MP, Fasching PA, Beckmann MW. Hereditary breast and ovarian cancer: review and future perspectives. J Mol Med 2006;84(1):16-28.

4. Baylin SB, Ohm JE. Epigenetic gene silencing in cancer - a mechanism for early oncogenic pathway addiction? Nat Rev Cancer 2006;6(2):107-16.

5. Jones PA, Baylin SB. The epigenomics of cancer. Cell 2007;128(4):683-92.

6. Tsou JA, Shen LY, Siegmund KD*, et al.* Distinct DNA methylation profiles in malignant mesothelioma, lung adenocarcinoma, and non-tumor lung. Lung Cancer 2005;47(2):193-204.

7. Costello JF, Fruhwald MC, Smiraglia DJ*, et al.* Aberrant CpG-island methylation has non-random and tumour-type-specific patterns. Nat Genet 2000;24(2):132-8.

8. Goh L, Murphy SK, Muhkerjee S, Furey TS. Genomic sweeping for hypermethylated genes. Bioinformatics 2007;23(3):281-8.

9. Berchuck A, Iversen ES, Lancaster JM*, et al.* Patterns of gene expression that characterize long-term survival in advanced stage serous ovarian cancers. Clin Cancer Res 2005;11(10):3686-96.

10. Kent WJ, Sugnet CW, Furey TS*, et al.* The human genome browser at UCSC. Genome Res 2002;12(6):996-1006.

11. Miotto E, Sabbioni S, Veronese A*, et al.* Frequent aberrant methylation of the CDH4 gene promoter in human colorectal and gastric cancer. Cancer Res 2004;64(22):8156-9.

12. Maeda M, Johnson E, Mandal SH*, et al.* Expression of inappropriate cadherins by epithelial tumor cells promotes endocytosis and degradation of E-cadherin via competition for p120(ctn). Oncogene 2006;25(33):4595-604.

13. van de Vijver MJ, He YD, van't Veer LJ*, et al.* A gene-expression signature as a predictor of survival in breast cancer. N Engl J Med 2002;347(25):1999-2009.

14. Irizarry RA, Hobbs B, Collin F*, et al.* Exploration, normalization, and summaries of high density oligonucleotide array probe level data. Biostatistics 2003;4(2):249-64.

15. Huang Z, Wen Y, Shandilya R, Marks JR, Berchuck A, Murphy SK. High throughput detection of M6P/IGF2R intronic hypermethylation and LOH in ovarian cancer. Nucleic Acids Res 2006;34(2):555-63.

ACKNOWLEDGMENTS

We gratefully acknowledge Kyoto University and Drs. John Lancaster, Jeffrey Boyd, Thomas Hamilton, Gordon Mills and Jean Hurteau for provision of cell lines used in this study. This work was supported by a grant to SKM from the DoD Ovarian Cancer Research Program, award number W81XWH-05-1-0053.

FIGURE LEGENDS

Figure 1. *Expression of CDH4 in ovarian tissues and promoter methylation in ovarian malignancies.* **(A)** Vertical scatter plot of *CDH4* transcript levels from gene expression microarrays (9) of normal ovarian surface epithelium (NOSE) and serous epithelial ovarian tumors, including borderline, stage I-II (early) and stage III-IV cancers from women living more than seven years (long) or less than 3 years (short) post-diagnosis. Horizontal bars indicate the mean for each group. **(B)** Methylation-specific PCR of the region encompassing the *CDH4* transcription start site in lymphocytes from individuals without malignancy (NL), ovarian cancer (OC) specimens, and ovarian cancer cell lines. UMD, universally methylated DNA.

Figure 2. *Influence of CDH4 promoter methylation on transcription.* Alleviation of *CDH4* promoter methylation through treatment with 5-azacytidine (AzaC) and decitabine (DAC). **(A)** Results from quantitative bisulfite sequencing of the *CDH4* promoter. Shown is the average methylation for the region sequenced. Black bars, mock treated; light grey bars, 2-aza-5'-deoxycytidine (DAC) treated; dark grey bars, 5-azacytidine (AzaC) treated. **(B)** RT-PCR detection of *CDH4* transcription. The panels are arranged in the same order as the four cell lines presented in panel **A**, with mock, DAC and AzaC shown for each. The arrows indicate samples in which transcriptional reactivation was evident. The slower migrating band for AzaC-treated SKOV4 is non-specific. *GAPDH* was also run as an endogenous control for RNA loading. **(C)** Bisulfite sequencing gel

images show a decrease in methylated cytosine with AzaC and DAC treatment. Note that sequencing was performed using a primer on the reverse strand, so methylated cytosines are represented by bands in the G lanes, while unmethylated cytosines are represented by bands in the A lanes. **(D)** *CDH4* expression (log-transformed, RMA normalized data) in 43 ovarian cell lines and promoter methylation status, assessed by MS-PCR and/or bisulfite sequencing. Black bars, methylated; white bars, unmethylated; shaded bars, undetermined.

Figure 3. *Effect of CDH4 repression on cell phenotypes in vitro.* Shown is the average for quadruplicate measurements of both cell proliferation for seven ovarian cancer cell lines **(A)** and anchorage-independent growth for four ovarian cancer cell lines **(B)** that were transfected with control non-silencing siRNA oligos or with *CDH4*-specific siRNA oligos.

Figure 4. *CDH4 affects cell-cell adhesion in ovarian cancer cell lines.* **(A)** Repression of *CDH4* expression leads to delay in return to confluency when ovarian cancer cells are disrupted by scraping with a pipet tip. Top row, OVCA429 cells transfected with a non-silencing control siRNA; bottom row, OVCA429 cells transfected with a *CDH4*-specific siRNA. Photomicrographs were taken immediately after 'wound' induction (T0), and 5, 18 and 24 hours later. 10X objective. **(B)** *CDH4* knockdown prior to 'wound' induction leads to a disorganized appearance of the leading edges of the monolayer and increases

cell scattering behavior and loss of cell-cell contacts in OVCA433 and OVCA429 ovarian cancer cell lines, shown at 22 hours post-‘wound’ induction. 20X objective.

Figure 1

A

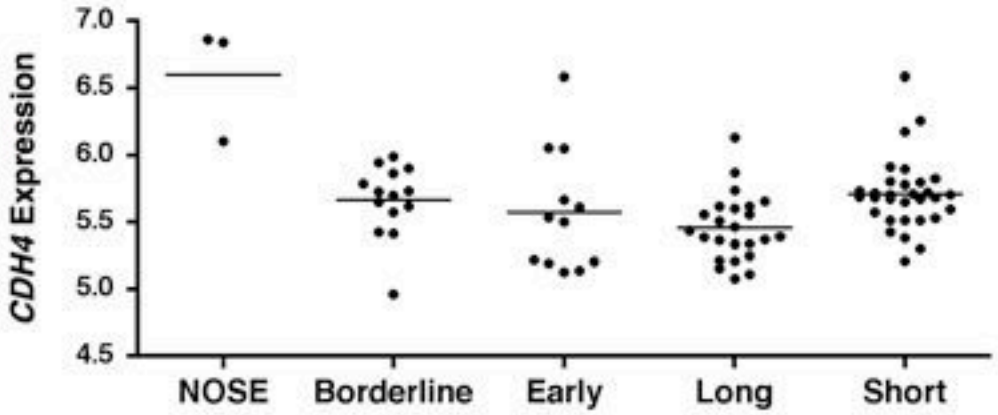
CDH4 Expression
7.0
6.5
6.0
5.5
5.0
4.5
NOSE
Borderline
Early
Long
Short

B

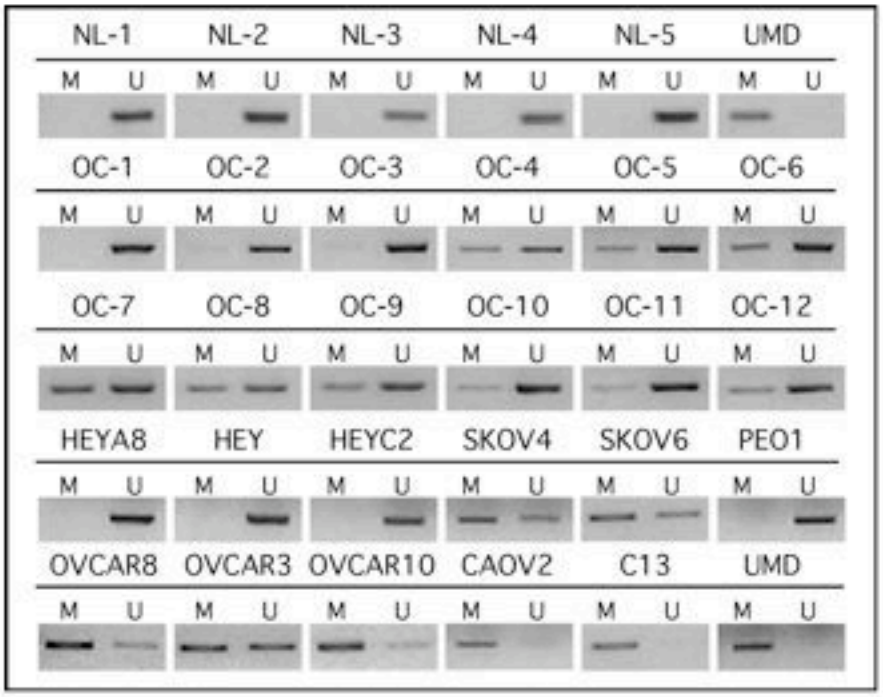
NL-1
NL-2
NL-3
NL-4
NL-5
UMD
OC-1
OC-2
OC-3
OC-4
OC-5
OC-6
OC-7
OC-8
OC-9
OC-10
OC-11
OC-12
HEYA8
HEY
HEYC2
SKOV4
SKOV6
PEO1
OVCAR8
OVCAR3
OVCAR10
CAOV2
C13
UMD
M
U

Figure 2

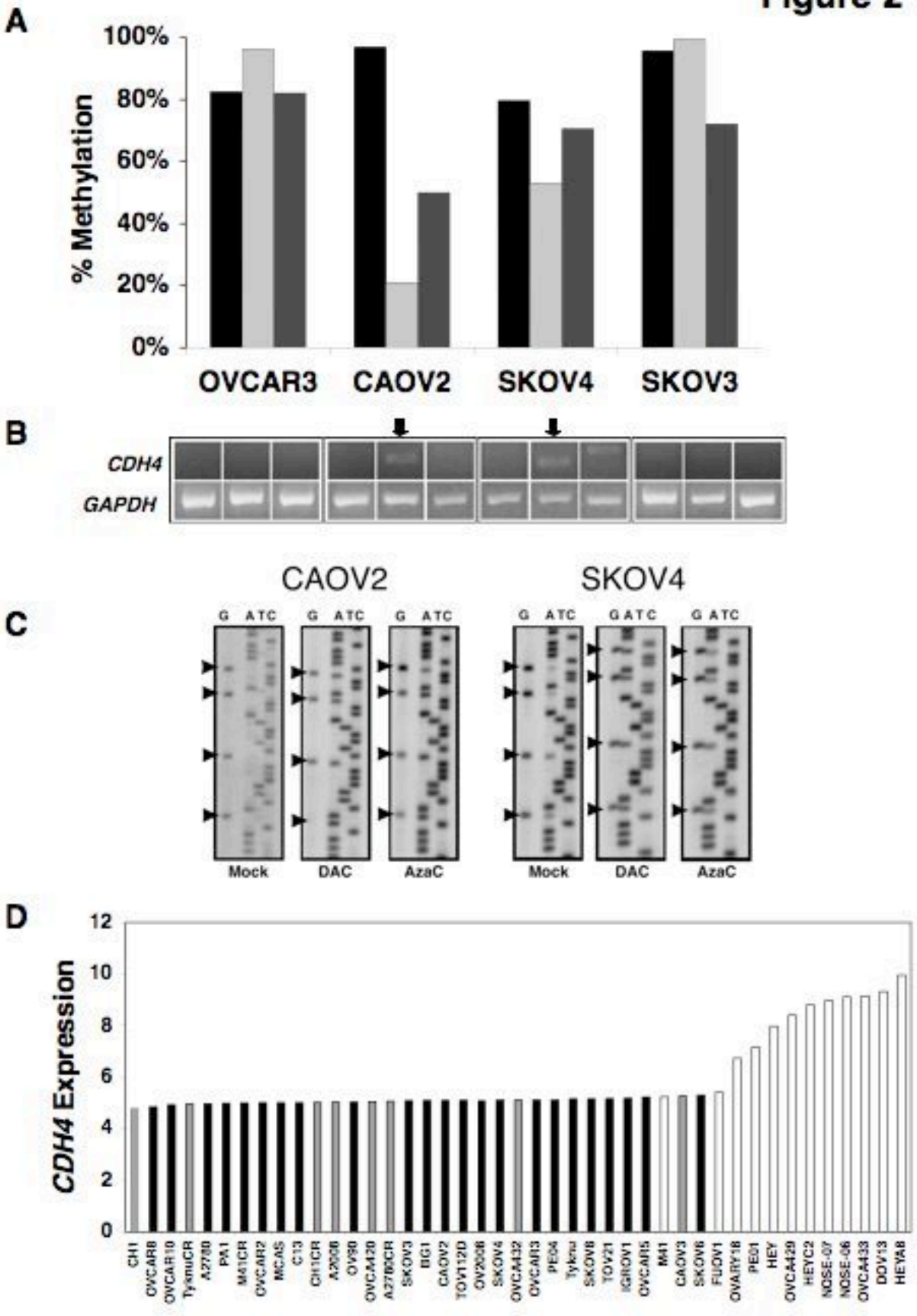
A
100%
80%
60%
40%
20%
0%
% Methylation
OVCAR3
CAOV2
SKOV4
SKOV3
B
CDH4
GAPDH
C
CAOV2
SKOV4
G ATC
Mock
DAC
AzaC
D
CDH4 Expression
12
10
8
6
4
2
0
CH1
OVCAR8
OVCAR10
TyknuCR
A2780
PA1
M41CR
OVCAR2
MCAS
C13
CH1CR
A2008
OV90
OVCA420
A2780CR
SKOV3
BG1
CAOV2
TOV112D
OV2008
SKOV4
OVCA432
OVCAR3
PE04
Tyknu
SKOV8
TOV21
IGROV1
OVCAR5
M41
CAOV3
SKOV6
FUOV1
OVARY18
PE01
HEY
OVCA429
HEYC2
NOSE-07
NOSE-06
OVCA433
DOV13
HEYA8

Figure 3

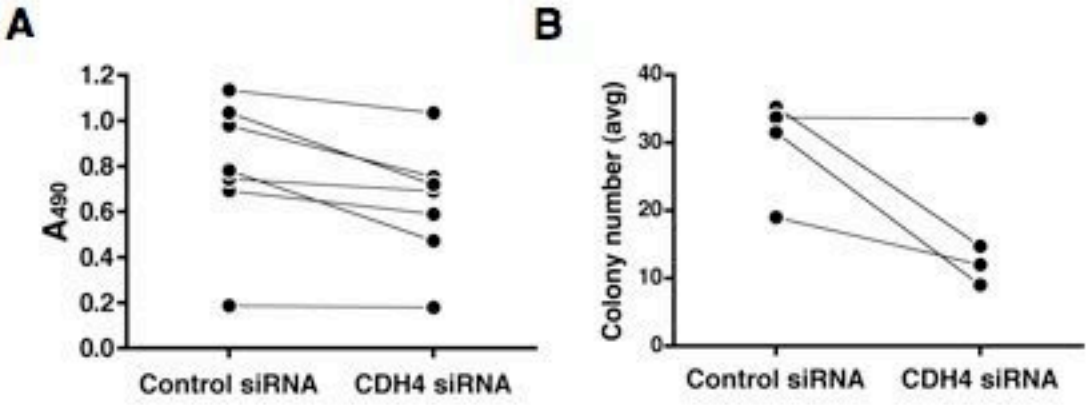
A
1.2
1.0
0.8
0.6
0.4
0.2
0.0
A490
Control siRNA
CDH4 siRNA
B
40
30
20
10
0
Colony number (avg)
Control siRNA
CDH4 siRNA

Figure 4

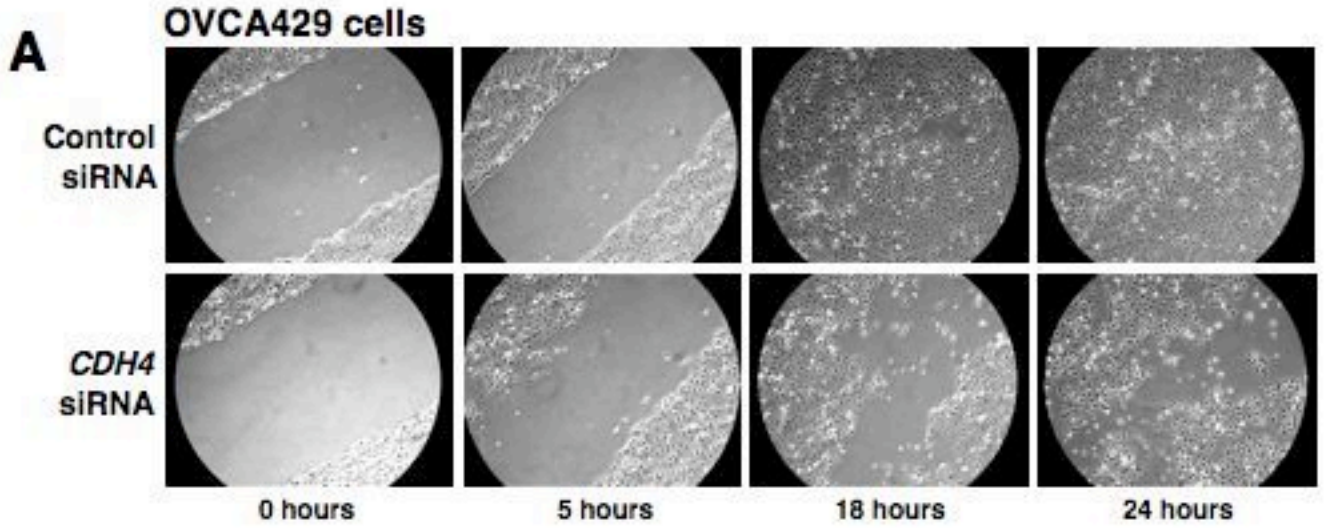
A
OVCA429 cells
Control siRNA
CDH4 siRNA
0 hours
5 hours
18 hours
24 hours

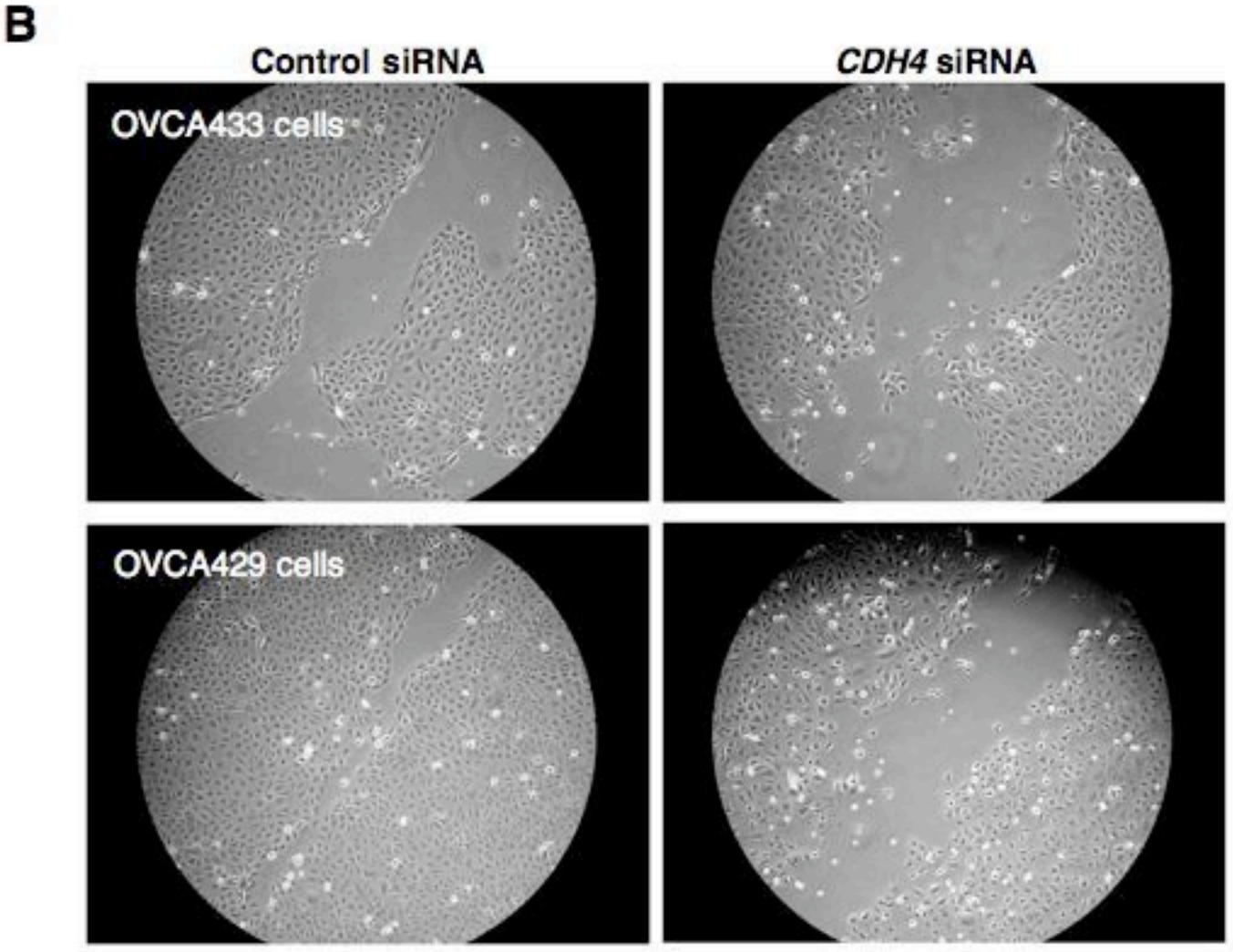
B
Control siRNA
CDH4 siRNA
OVCA433 cells
OVCA429 cells

Original
12/14/08

Transcriptome analysis reveals coordinate methylation-mediated suppression of genes associated with TGF-beta pathway activity in epithelial ovarian cancers

Noriomi Matsumura[1,2], Zhiqing Huang[1], Tiffany Perry[1], Darby Kroyer[1], Tsukasa Baba[1,2], Seiichi Mori[3], Shingo Fujii[4], Jeffrey R. Marks[5], Andrew Berchuck[1,3] and Susan K. Murphy[1,3,6 †]

(1) Gynecologic Oncology, Duke University Medical Center, Durham, NC, USA
(2) Kyoto University, Kyoto, Japan
(3) Duke Institute for Genome Sciences and Policy, Durham, NC, USA
(4) National Hospital Organization, Kyoto Medical Center, Kyoto, Japan
(5) Department of Surgery, Duke University Medical Center, Durham, NC USA
(6) Department of Pathology, Duke University Medical Center, Durham, NC USA

Key Words:
Running Title:
Word count:

† **Correspondence:**
2185 F-CIEMAS
101 Science Drive
Box 91012
Durham, NC 27708
(919) 681-3423
murph035@mc.duke.edu

INTRODUCTION

Ovarian cancer is the leading cause of death among gynecological cancers. Most patients are diagnosed at advanced stages and eventually die of persistent or recurrent disease. Understanding the process that initiates ovarian malignancy is necessary in order to develop new methods for detecting the disease at an early stage [1]. Aberrant DNA methylation is regarded as a major contributor to carcinogenesis, with increasing numbers of genes identified that are targeted by this modification, which most often leads to silencing of genes that have functions that normally deter tumor growth, invasion and/or metastasis. The repertoire of genes that are methylated within different types of cancers appears to include genes that are commonly methylated across many types of cancer (e.g., p16, RASSF1A) and genes that are specific to particular cancers based on the tissue/cell type from which the malignant cells arise. DNA methylation is a covalent modification that is faithfully replicated during cell division. Because of the relative ease of detection of this epigenetic mark, even from tumor DNA in peripheral blood specimens, aberrant methylation may provide a promising means to enhance early detection of ovarian cancer [2].

In this study, we used gene expression microarray transcriptome profiling to identify candidate aberrantly methylated genes in epithelial ovarian cancer. We treated 43 established ovarian cell lines and 17 primary ovarian culture specimens (from normal ovarian surface epithelium and ovarian cancer) with demethylating agents and followed this by expression microarray analysis. This relatively large number of samples enabled the identification of candidate methylated genes using a step-wise rationale approach based on several criteria. We first found that the gene set exhibiting maximal higher fold-induction by the demethylating agents was enriched in genes already already known to be methylated in cancer. We next found that among untreated specimens, genes that exhibit a larger variance in expression also were enriched for genes already known to be methylated in cancers. Using these two parameters, we identified 360 candidate methylated genes, among which all of those analyzed exhibited evidence of methylation in ovarian cancers.

Next, we turned to the relationship between methylation and the TGF-beta pathway because gene ontology terms related to TGF-beta signaling were enriched among the predicted set of 360 candidate genes. TGF-beta signaling has various cellular functions including roles in angiogenesis, induction of apoptosis, growth suppression, and suppression of the immune response. Though secretion of TGF-beta is often increased from tumor cells, the TGF-beta signaling pathway inside tumor cells is inhibited [3]. Reports of epigenetic inactivation of specific genes that participate in TGF-beta pathway signaling have implicated epigenetic deregulation as a mechanism explaining pathway repression [4-6]. In this study, we analyzed the association between TGF-beta pathway activity and methylation of pathway genes. We show herein that 14 TGF-beta pathway genes are methylated in ovarian cancers. Furthermore, treatment of ovarian cancer cells with 5Aza-dC upregulated TGF-beta activity, indicating that the net effect of pathway gene methylation is the downregulation of TGF-beta activity in these cells.

Recent findings indicate that the biological and clinical characteristics of cancers are associated with coordinated methylation of several genes, which has been referred to as the "CpG island methylator phenotype" (CIMP) [7]. Though the CIMP has been studied in colorectal cancers, the existence of the CIMP has only been investigated in ovarian cancers using a small number of marker genes [8]. We found that hierarchical clustering based on expression of the 360 genes generated a defined gene cluster in ovarian cancer tissue samples, suggesting the existing of the CIMP in ovarian cancer. Lower expression of the gene cluster was associated with increased age and lower TGF-beta activity, suggesting that age-related coordinate accumulation of methylation contributes to downregulation of TGF-beta activity. We suggest that the age-related and coordinated accumulation of epigenetic gene silencing contributes to the ovarian carcinogenic process by suppressing TGF-beta signaling. These data reveal a fundamental mechanism underlying the development of ovarian cancer.

MATERIALS AND METHODS

Cell lines

Forty three established ovarian cell lines, including 41 cancer cell lines and two immortalized normal ovarian surface epithelium cell lines were collected and used in this study. A detailed description of these cell lines was previously reported [9]. All cells were grown in RPMI 1640 supplemented with 10% fetal bovine serum and penicillin-streptomycin (GIBCO). For microarray analysis cells were grown to ~60% - 70% confluence and then treated with 5 μM 5Aza-dC (Sigma-Aldrich; St. Louis, MO) or mock-treated for 72 hours.

Primary culture

All patient specimens were obtained with informed consent and used under a protocol approved by the Duke University Institutional Review Board. For microarray analysis, tumor specimens or intraoperatively scraped ovarian surface epithelium (OSE) were obtained at the time of surgery from patients under the care of the Division of Gynecologic Oncology at Duke University Medical Center. Confirmation of histology was obtained through Board Certified Pathologists at Duke University Medical Center. Thirteen epithelial ovarian cancer (12 serous and 1 endometrioid ovarian cancers) and two serous borderline tumors (Table S4) were gently dissociated using scalpel blades and cultured in 119 and 105 medium (1:1) (GIBCO) supplemented with 15 % serum and penicillin-streptomycin, as previously reported [10]. Following establishment of a monolayer, the cells were briefly trypsinized and washed with PBS to remove fibroblasts. The cells were then exosed to additional trypsin/EDTA to allow passage into three 10 cm dishes. Once these monolayer cultures reached ~60% - 70% confluence, one dish was treated with 5 μM 5Aza-C, one dish was mock treated with carrier, and the remaining dish was untreated. Cells were harvested 72 hours following initiation of treatment. Ovarian surface epithelium samples were collected from patients undergoing oophorectomy for reasons other than malignancy. OSE was also similarly divided into three 6 cm dishes for mock/5Aza-C/no treatment. Due to limited cell numbers, OSE specimens were pooled from five patients for each of two independent microarray hybridizations (N=10 patients). Prior to analysis, the epithelial content of the cells was confirmed to be >90% by cytokeratin immunostaining as previously described [11].

Tumor specimens used for methylation analysis were derived from the Duke Gynecologic Oncology Tumor bank and were comprised of stage III and IV serous epithelial ovarian cancers.

Methylation analyses.

DNA was bisulfite modified using our high throughput protocol as described, using 300-500 ng of genomic DNA [12]. Methylation analysis was performed using MS-PCR and/or Pyrosequencing. MS-PCR primers used in this study were from Sigma-Genosys (St. Louis, MO) and are provided in Supplementary Materials. Primers were designed to be specific to the methylated or unmethylated versions of the sequence following bisulfite modification, and were optimized using control DNA specimens including bisulfite modified universally methylated genomic DNA and normal human genomic DNA in addition to human genomic DNA that had not been bisulfite modified in order to demonstrate specificity of the primers for the bisulfite modified sequence. Amplicons were resolved by agarose gel electrophoresis. Although MS-PCR provides qualitative data, we classified the results of these assays based on ethidium bromide staining and visualization as either 1) >50% methylated (amplicon produced by methylated primer set was greater in intensity than that produced by the unmethylated primer set); <50% methylated (amplicon produced by methylated primer set was lesser in intensity than that of the amplicon produced by the unmethylated primer set) or as unmethylated (absence of an amplicon from the methylated primer set).

Pyrosequencing was carried out using a Pyromark MD instrument (Biotage; Uppsala, Sweden). Assay design was performed using the manufacturer's provided software. Primers were first optimized for PCR and then for Pyrosequencing by generating standard curves using mixtures of unmethylated and universally methylated DNA in defined ratios. Data analysis was performed using Biotage PyroQ-CpG software, which checks conversion efficiency of the bisulfite treatment by measuring signal produced for cytosine and thymidine at specified non-CpG cytosines and provides a quantitative measure of the proportion of methylation present at each CpG cytosine within the sequenced region. Data was analyzed for each of the CpG sites individually and as an average of all CpG sites measured for each gene.

Western blotting

Under construction.

Luciferase assay

Under construction.

Microarray

RNA was isolated from tissues using RNA Stat-60 (Telest; Friendswood, TX) and assessed using an Agilent Bioanalyzer for RNA quality and integrity, prior to microarray processing and hybridization onto Affymetrix HT-U133A (cell lines) or U133 plus 2 (primary culture) genes chips at the Duke DNA Microarray Facility.

Published datasets

Microarray datasets obtained from the Gene Expression Omnibus website (http://www.ncbi.nlm.nih.gov/sites/entrez) were GSE4717, GSE5230, GSE5816, GSE1724, GSE6653, GSE5457, GSE7144, GSE3149, and GSE2109. Unpublished microarray datasets used in previously published papers were kindly provided by Dr. Ushijima [13], Dr. Suzuki [14], and Dr. Keen [15]. A list of genes known to be methylated in cancers was obtained from http://www.mdanderson.org/departments/methylation/. Gene lists detected as methylated by methylation microarray were obtained from tables in published papers (references).

Data mining of microarray datasets

Graphs for the frequency of the M.D. Anderson probes in the neighboring 100 probes (Figure 1A, 1B, 2A, 2B) were prepared using Microsoft Excel. Other software used for these analyses were obtained from: R, http://www.r-project.org; Java TreeView version 1.1.2, http://jtreeview.sourceforge.net; Cluster 3.0, http://rana.lbl.gov/EisenSoftware.htm; Binary regression, http://data.genome.duke.edu/oncogene.php. In order to analyze the enrichment of gene ontology terms or KEGG pathway terms, GATHER (http://gather.genome.duke.edu/) web-based software was used [16]. Blue-yellow-red heatmaps were drawn using R and the other heatmaps were drawn using Java TreeView. For hierarchical clustering, average linkage hierarchical clustering was conducted with mean centered and normalized gene expression.

Statistical analysis was performed using GraphPad Prism Version 4.0b. Binary regression was conducted using Mas5 normalized values. All other microarray datasets were analyzed using RMA normalized $\log_2$ values. In analyzing U133 Plus 2.0 probesets, only the 22,215 probes that match with the U133A probeset were used. U95A Plus 2 gene chips were merged with U133A probes using the "bestmatch" annotations available from the Affymetrix website (http://www.affymetrix.com/index.affx).

RESULTS

Comparison of fold change following 5Aza-dC treatment in cancer cells

We conducted microarray analysis for 43 ovarian cell lines that were treated with 5Aza-dC or mock treated. These cell lines include 41 ovarian cancer cell lines and two spontaneously immortalized OSE cell lines. First, we performed an unsupervised hierarchical clustering using all 86 samples (Figure S1). Chemo-resistant derivatives cell lines tended to cluster with their respective parental cell lines as did 5Aza-dC-treated cells and their corresponding mock treated counterparts. This analysis indicates that the 5Aza-dC treatment did not cause non-specific genome-wide changes in gene expression.

Next, we calculated the fold change in gene expression resulting from 5Aza-dC treatment for all U133A probes in all 43 ovarian cell lines. The average fold change of individual probes in the 43 ovarian cell lines was then compared with other types of cancers (Table S1, Figure S2). Regardless of the original organs from which the cells were derived, the pattern of fold change by 5Aza-dC was strikingly similar to that in ovarian cell lines.

Analysis using genes already established as methylated in cancer

A list of known methylated genes in various types of cancers was obtained from M.D. Anderson Cancer Center (M.D. Anderson genes, Table S2). Because genes methylated in other types of cancers are more likely to be methylated in ovarian cancer than other randomly selected genes throughout the genome, we searched for parameters that enrich the M.D. Anderson gene list in our microarray data in order to find the criteria to use for prediction of other novel candidate methylated genes in ovarian cancer.

When all microarray probes were sorted by the maximal fold change (MaxFC) occurring among the 43 cell lines, the M. D. Anderson genes were effectively enriched. The frequency of inclusion of the M. D. Anderson genes was drastically elevated at the point where the MaxFC was > 2.9 (Figure 1A).

Another parameter that enriched for the M. D. Anderson genes was the standard deviation (SD) of gene expression of untreated cell lines. That is, when the variation of gene expression is large, the M.D. Anderson genes were enriched. The frequency of the M. D. Anderson genes was markedly elevated at the point where the SD was > 1.7 (Figure 1B). Furthermore, the combination of these two parameters, Max FC and SD, enriched for the M. D. Anderson list genes more efficiently than either of the two parameters alone (Figure 1C).

Methylation microarrays have been used to detect genome-wide methylation directly using methylation-sensitive restriction enzymes or by selective hybridization of DNA fragments bound by methyl-DNA binding proteins, generating relatively unbiased lists of methylated genes. We analyzed published gene lists from methylation microarrays (Table S3) to determine the applicability of our threshold values for MaxFC and SD in the enrichment of genes from these unbiased lists. Like the M.D. Anderson list, the cut off values of MaxFC > 2.9 and SD > 1.7 enriched genes from the methylation microarray gene list (Table 1). These two cut-off values selected a set of 359 probes (293 genes), which are expected to enrich authentically methylated genes in ovarian cancer.

The SD values of individual genes can be calculated from any microarray dataset including those generated from clinical samples. We therefore analyzed two available ovarian cancer tissue microarray datasets (GSE3149 and GSE2109) in terms of enrichment of the M.D. Anderson genes by SD values. Similar to the ovarian cell lines, the M.D. Anderson genes were enriched by selection based on high SD values in these primary ovarian cancer tissue datasets (Figure S3).

Comparison of cell lines and primary culture

In addition to our analysis of the ovarian cell lines, computational analysis for prediction of candidate methylated genes was performed independently using ovarian tumor and OSE primary culture specimens. Microarray analysis was conducted for both 5AzaC-treated and mock-treated primary culture specimens. We used 17 total specimens, including 13 ovarian cancers, two ovarian borderline tumors and two independent pooled OSE specimens (N=5

samples in each pool; Table S4). Like the cell lines, a high MaxFC induced by treatment with 5AzaC and a high SD of expression among untreated samples enriched for genes in the M.D. Anderson list. A MaxFC > 1.5 and SD > 1.6 were determined as cut-off values in this analysis (Figure 2), which identified 108 candidate methylated genes (128 probes). These two cut-off values again enriched for methylated genes from the unbiased methylation microarray gene list (Table 2).

The cell line dataset and the primary culture dataset were compared with regard to the selected candidate methylated genes. The 128 probes selected from the primary culture analysis showed apparent high MaxFC and high SD in the cell line dataset (Figure 3A). Similarly, the 359 probes selected from the cell lines showed apparent high MaxFC and high SD in the primary culture dataset (Figure 3B). The reproducible patterns for the two parameters indicates that methylation target genes are not substantially different between cell lines and primary culture in ovarian cancer.

In summary, we predicted 293 genes (359 probes) from the cell line dataset and 108 genes (128 probes) from the primary culture dataset as methylated in ovarian cancer. There was a 41 gene overlap between these datasets, and in total, 360 genes (436 probes) were predicted as methylated in ovarian cancer (Table S5).

Verification of methylation for the predicted genes

Among the 360 genes predicted as subject to methylation in ovarian cancer, 128 genes (36%) have been reported as methylated in other types of cells. In order to verify the prediction, we analyzed methylation for 20 genes, including one gene that had been reported as methylated in ovarian cancer, 11 genes that have been reported as methylated in other types of cancers, and 8 genes that have not been reported as methylated. We found that all 20 genes (100%) were methylated in at least one or more of the ovarian cell lines (Table 3). Furthermore, we found methylation for 12 additional genes, selected mainly by either high MaxFC or high SD in cell lines or primary culture. Among the 32 total genes that exhibited methylation in the ovarian cell

lines, 16 genes were also analyzed in ovarian cancer tissues and all 16 were found to exhibit methylation in more than 15% of the tumors analyzed (Table 4).

Because a close relationship between methylation and the TGF-beta signaling pathway was strongly suggested by the results to be presented later, we extensively analyzed methylation for genes that belong to the TGF-beta signaling pathway (KEGG; Kyoto Encyclopedia of Genes and Genomes: http://www.genome.ad.jp/kegg/). The 32 total tested genes contained 14 TGF-beta signaling pathway genes, including *BMP2, BMP4, BMP7, FST, ID1, ID2, ID4, INHBB, SMAD5, SMAD7, SMURF2, TGFB2, TGFBR2,* and *THBS1*. None of these genes have been reported as methylated in ovarian cancer and six have not previously been reported as methylated in any type of cells (Table 4).

Correlation of methylation and expression.

As MS-PCR was conducted using primers that detect either "methylated" or "unmethylated" loci near the annotated transcription start sites of the genes anlayzed, we were able to assign a subjective methylation status to genes in individual samples by comparing the intensity of the amplicons produced following separation by agarose gel electrophoresis and ethidium bromide staining. Genes status was assigned as either >50% methylated, <50% methylated, or unmethylated (as described in Materials and Methods). Expression of genes with methylation >50% was significantly lower than that of genes with methylation <50% or unmethylated genes. The difference in expression between genes with methylation <50% and unmethylated genes was very small (Figure 4A). Results for four representative genes (*BMP7*, *CCNA1*, *ID4*, and *TGFBI*) are shown in Figure 4B. The relationship between expression and methylation was also analyzed using Pyrosequencing following bisulfite modification. Gene expression negatively correlated with methylation at CpG sites in the promoter regions for both *TGFBR2* (Figure 4C) and *THBS1* (Figure 4D).

The relationship between fold change following treatment with 5Aza-dC and methylation status was also analyzed. Fold change in expression of genes with methylation >50% was higher than the other genes (Figure S4A). However, many of the methylated genes remain recalcitrant

to reactivation by 5Aza-dC treatment. Other epigenetic factors such as histone modifications may be involved in repressing these genes (Figure S4B).

Gene ontology terms of the predicted methylation genes

In order to determine the biological relevance of methylation in ovarian cancer, Gene Ontology terms for the 360 predicted methylation target genes was analyzed using GATHER [17] (Table 5). A close relationship between methylation and TGF-beta pathway signaling was suggested by the enrichment of relevant terms, such as "development", "negative regulation of cell proliferation", "apoptosis", "adhesion", "angiogenesis", and "immune response" [18]. Furthermore, we assessed potential associations with KEGG pathways using GATHER and found that the "TGF-beta signaling pathway" was enriched compared to the genome ($p=0.007$, data not shown).

Activation of TGFb signaling pathway by 5Aza-dC treatment in ovarian cancer cell lines

The results described above, i.e., methylation of as many as 14 known TGF-beta pathway genes (Table 4), and enrichment of gene ontology terms relevant to the TGF-beta pathway (Table 5), suggested that there is pathway specific modification by methylation in ovarian cancer. We therefore next examined if the TGF-beta signaling pathway is modified by 5Aza-dC treatment in the ovarian cancer cell lines. We found 5Aza-dC activated TGF-beta activity in several ovarian cancer cell lines by Western blotting experiments using antibodies against p-SMAD2/3. Interestingly, the activation by 5Aza-dC was often stronger than the treatment by TGFb1 alone (Figure 5A). This trend was reproduced using SMAD3-reporter plasmids in luciferase assays (Figure 5B).

In order to further confirm the activation of TGF-beta pathway activity by 5Aza-dC, we conducted computational analysis. We developed a TGF-beta signature using Binary Regression [19] comprising the top 300 genes that best discriminate untreated from TGFb1-treated human cultured fibroblasts (GSEA1724; Figure 6A). Leave-one-out cross validation indicated the TGF-beta signature predicted the TGFb1 treatment with 100% accuracy in the training dataset (Figure 6B). This TGF-beta signature also clearly predicted TGFb1 treatment in 4 external datasets, including that of immortalized OSE (Figure 6C). This TGF-beta gene signature was used to

analyze the 43 ovarian cell lines with or without 5Aza-dC treatment. Similar to the results obtained from Western blotting and the luciferase assays, this computational analysis indicated that 5Aza-dC treatment significantly upregulated the TGF-beta signature probability, i.e., TGF-beta pathway activity (Figure 6D).

Coordinated expression of the methylation target genes in ovarian cancer

The CpG island methylator phenotype (CIMP) is identified by the coordinated methylation of marker genes in clinical samples [7]. Coordinated methylation is expected to be associated with the coordinated expression of genes targeted by DNA methylation. Hence, we employed a hierarchical clustering of ovarian cancer datasets using the 360 predicted methylated genes. We first analyzed the ovarian cancer dataset that we previously published ([20], GSE 3149). This dataset contains only advanced (stage III/IV) serous ovarian cancer tissues (n=146). One gene cluster, which we named "CIMP" genes, divided the ovarian cancer data into two groups (Figure 7A). Survival of patients was not significantly different based on grouping with respect to the CIMP genes (data not shown). Interestingly, the patient's age at diagnosis was higher in the tumor group in which the expression of the CIMP genes was suppressed. The frequency of patients older than 60 years was significantly different between the two tumor groups (Figure 7A).

The CIMP genes defined by the GSE3149 dataset were used to conduct hierarchical clustering in an independent ovarian tumor dataset (GSE2109, n=77). This dataset contains only serous ovarian tumors, but contains borderline tumors, stage I/II tumors, and stage III/IV tumors. The CIMP genes again formed one gene cluster and divided the ovarian cancers into two groups (Figure 7B). The distribution of borderline and early stage tumors was not deviated between the two clusters (data not shown). However, like the GSE3149 dataset, the frequency of patients older than 60 years was higher in the 'CIMP low' tumor group (Figure 7B). These data indicate that expression of a subset of methylation target genes reproducibly generates a gene cluster dividing younger from older patients with serous epithelial ovarian tumors.

Correlation of the "CIMP" gene expression and the TGF-beta signature probability in ovarian cancer

Because the 5Aza-dC experiments indicated that inhibition of DNA methyltransferase activity led to increased activity of the TGF-beta pathway in ovarian cancer cells (Figure 5 and 6), we next analyzed the relationship between expression of the CIMP genes and the TGF-beta signature probability. In the two ovarian cancer tissue datasets (GSE3149 and GSE2109), the average expression of the CIMP genes showed a very strong positive correlation with the TGF-beta signature probability (Figure 8A, 8B, $p<0.0001$, respectively).

Similarly, the average expression of the CIMP genes showed strong positive correlation with the TGF-beta signature probability in both cell lines and primary culture specimens (Figure 8C, 8D, $p<0.0001$, respectively). The two immortalized normal OSE cell lines showed high expression of the CIMP genes and high TGF-beta signature probability (Figure 8C). And the two pooled primary normal OSE specimens also showed high expression of the CIMP genes and high TGF-beta signature probability in the primary culture dataset (Figure 8D). The distribution of the two borderline tumor specimens did not show any specific deviation (data not shown).

DISCUSSION

DNA methylation determines cell fate in physiological situations. Accumulation of aberrant DNA methylation at the promoter regions of genes is believed to contribute to the carcinogenic process of human cells by silencing expression of tumor suppressor genes. Research has been conducted in order to identify methylated genes in ovarian cancer because DNA methylation is regarded as a promising biomarker for the early detection of this disease [2].

Inhibitors of DNA methyltransferase activity, such as 5Aza-dC or 5AzaC that reactivate transcription of silenced genes, have been used to detect genome-wide methylation changes in combination with expression microarray analysis. This method's strength lies in the fact that genome-wide methylation relevant to gene expression can be identified, but a weakness is that this method can only be used for cultured cells [21]. Other published microarray datasets used to analyze the response to 5Aza-dC examined at most only ten cell lines [22]. It is possible that this small sample size may substantially limit detection of methylated genes due to the highly variable natures of cancer cells. We tried to overcome this potential limitation by performing analyses on 43 ovarian cell lines, including 41 ovarian cancer cell lines and two spontaneously immortalized normal OSE cell lines, and analyzed their response to treatment with DNA methyltransferase inhibitors using gene expression microarrays.

Most of the known methylated genes in ovarian cancer are also known to be methylated in other types of cancers, though the frequency of methylated genes is different in other types of cancers [2]. The average response of the 43 cell lines treated with 5Aza-dC was very similar to the responses in different organ-derived cell lines (Figure S2). Although the transcriptional changes assessed on a genome-wide scale also must include indirect effects on non-methylated genes, the biological effect of 5Aza-dC is thought to be very similar, probably because there are a significant number of commonly methylated genes in cancers.

Many prior studies that analyzed the response to 5Aza-dC or 5Aza-C reported arbitrary cut-off values for fold induction used to select candidate methylated genes [21]. Even with as many as 43 cell lines, rational threshold values are necessary in order to select the maximal

number of candidate methylated genes. We used an external list of well-known methylated genes in various types of cancers (M.D. Anderson list genes) because we speculated that truly methylated genes in ovarian cancer should also be methylated in various types of cancers compared to other randomly selected genes throughout the genome.

At first, we calculated the maximal fold change in the 43 cell lines and tested if this value could be used as a parameter to enrich for methylation target genes and indeed found that maximal fold change following 5Aza-dC treatment in the 43 cell lines enriches for genes on the M.D. Anderson list (Figure 1A). This is consistent with a previous report that identified methylated genes by a high fold induction [22]. In the present study, an apparent threshold value was identified based on the observation that the M.D. Anderson list genes suddenly increased above this value (Figure 1A). Because the frequency of methylated genes in ovarian cancer is thought to at least partially mimic that found in other types of cancers, we predicted that the this cut-off would discriminate between methylated and unmethylated genes in the ovarian cell line dataset.

The response to 5Aza-dC alone may not predict truly methylated genes because this method is an indirect method, which can cause secondary changes influencing gene expression. Therefore, we looked for another parameter that could independently enrich for selection of the M.D. Anderson list genes. We found that a high standard deviation (SD) of gene expression among the untreated samples indeed also enriches genes from the list of known methylated genes. The frequency of M.D. Anderson gene identification was increased above a certain threshold for the gene expression SD, which again enabled us to use a rational approach to generate a list of candidate methylated genes. This was an unexpected result since the association between methylation and wide variability in gene expression has not, to our knowledge, been used previously to identify potentially methylated target genes. This data indicates that substantial differences in gene expression may be attributable to methylation mediated regulation. Furthermore, we found high SD values enrich for the M.D. Anderson list genes in microarray datasets of ovarian cancer tissues (Figure S3). Furthermore, combining the two parameters, MaxFC and SD, enriched for the M.D. Anderson list genes and generated a list of 293 methylated genes (Figure 1C). These data suggest that methylated genes can be predicted by

analyzing virtually any microarray data for clinical samples. This result may facilitate research aimed at analyzing DNA methylation in cancer.

Because research focused on identification of methylated genes in cancer has been conducted based on the premise that methylation targets tumor suppressor genes, it was possible that the enrichment of M.D. Anderson list genes in the ovarian datasets might only represent the enrichment of genes with a specific biological phenotype, but not necessarily methylated genes. There are several other methods to detect genome-wide methylation in an unbiased manner. Methylation microarrays aim to detect methylated loci directly by using methylation-sensitive restriction enzymes or immunoprecipitation for methyl DNA binding protein [23, 24]. Aside from the accuracy of the assays, the methylation microarray methods have a weak point in that the results of methylation data do not necessarily correlate with the gene expression (####). However, these assays generate independent unbiased methylation gene lists from the genome, and we used them statistically to verify our prediction of methylated genes. We found that the methylation microarray gene list was also enriched by the cut-off values determined by the M.D. Anderson list genes (Table 1). Therefore, we considered the cut-off values to be truly useful in the detection of methylated genes in the ovarian cell lines.

Patterns of DNA methylation in cells can change as a result of cell culture (ref). However, previous reports have demonstrated that many genes exhibiting methylation in established cell lines are also subject to methylation *in vivo* (ref). Cell culture-mediated changes in methylation may affect genes that are likely to be methylated due to an inherent vulnerability to such events *in vivo* or *in vitro*, or as a consequence of gene function. In order to compare the candidate methylated gene list developed from analysis of ovarian cancer cell lines to primary ovarian cancers, we developed a primary culture dataset independently, which is comprised of 13 ovarian cancers, two borderline tumors, and two pooled normal OSE samples. Just as we found for the cell lines, both parameters, MaxFC induced by 5AzaC treatment and high SD of gene expression of untreated samples enriched for genes on the M. D. Anderson list genes. These genes drastically increased over certain cut-off values, which identified 108 candidate methylated genes (Figure 2 A, 2B, 2C). Furthermore, high MaxFC and high SD in cell lines clearly enriched the genes selected from the primary culture and vice versa (Figure 3A, 3B).

These data suggest that genes targeted by DNA methylation are not substantially different between cell lines and clinical samples in ovarian cancer, which is consistent with previous reports (refs). Compared to the large number of genes selected from cell lines (359 probes, 293 genes), only 128 probes (108 genes) were selected from the primary culture, probably due to the smaller sample size. Nevertheless, given the high reproducibility between the cell line and primary culture dataset, both gene lists comprised plausible candidates, and in total, 360 genes (436 probes) were selected as candidate methylated genes in ovarian cancer.

The reliability of the list of the 360 candidate methylation genes was suggested from literature reports, because as many as 127 genes (35%) had been reported as methylated in other studies (Table 3). We tested methylation of 20 genes among these 360 genes and found methylation for all 20 genes, including nine genes that have never been reported as subject to DNA methylation (Table 3, 4). These data suggest that many of the predicted genes, if not all, are actually the target of methylation. As expected, a negative correlation between gene expression and DNA methylation at the promoter regions was detected by MS-PCR (Figure 4A, 4B) or Pyrosequencing analysis (Figure 4C, 4D) in the cell lines, which indicates that methylation contributes directly to regulation of expression of these predicted genes. Though the responses to 5Aza-dC treatment of densely methylated genes were significantly higher than the other genes, many genes remain unchanged by the treatment (Figure S4A, B). This may suggest that histone modifications coexist at the methylated genes, a common feature among epigenetically regulated genes (refs). The inability to reactivate a larger number of the suppressed genes through DNA methyltransferase inhibition indicates the importance of testing a larger sample size to maximize the ability to identify methylated genes. The 16 genes tested in both cell lines and cancer tissues were found to exhibit methylation in both specimen types, which again indicates the reproducibility between cell lines and clinical samples (Table 4).

We next analyzed gene ontology terms of the 360 candidate methylated genes (Table 5). Many gene ontology terms were enriched among the set of candidate methylated genes as compared to the genome. Gene ontology terms for “tumor suppressor genes”, such as “negative regulation of cell proliferation” and “apoptosis” were included. This result is consistent with the well-supported notion that methylation causes silencing of tumor suppressor genes [25]. Other

gene ontology terms, such as “development” and “morphogenesis” also seem to be consistent with previous reports that DNA methylation is essential in the physiological process of development [26]. In addition to the above gene ontology terms, “adhesion”, “angiogenesis”, and “immune response” directed our attention toward the TGF-beta signaling pathway [18] as did the finding from GATHER analysis that the “TGF-beta signaling pathway” was enriched among our selected candidate genes among the KEGG pathways as compared to the genome ($p=0.007$, data not shown). Therefore, we surmised that the TGF-beta signaling pathway may be one of the major pathways targeted by methylation-mediated repression in ovarian cancer. Hypermethylation of genes comprising the KEGG TGF-beta signaling pathway have been previously reported [13, 27-32], but the relationship between TGF-beta pathway activity and the pattern of genome-wide methylation has never been examined. We conducted methylation analysis for the KEGG TGF-beta pathway genes extensively and found methylation of as many as 14 genes in ovarian cancer (Table 4), all of which have not been reported as methylated in ovarian cancer. These results suggest a close relationship between DNA methylation and TGF-beta pathway activity in ovarian cancer. Since not only pathway stimulatory genes, but also pathway inhibitory genes, such as SMAD7 and SMURF2, were methylated (Table 4), we next focused on the net effect of methylation on TGF-beta pathway activity.

TGF-beta acts to inhibit proliferation of normal OSE and early stage ovarian carcinomas. Conversely, in later stage ovarian cancer the inhibitory actions of TGF-beta on epithelial proliferation are overcome through the modified internal signaling [33]. In order to examine the net effect of DNA methylation on the TGF-beta signaling pathway, we added 5Aza-dC to ovarian cancer cell lines, followed by Western blotting or luciferase assays to detect pathway activity. Upregulation of TGF-beta pathway activity was observed following treatment in ovarian cancer cell lines, indicating that DNA methylation suppresses TGF-beta pathway activity (Figure 5A, 5B). Interestingly, 5Aza-dC treatment activated TGF-beta pathway more efficiently than TGFb1 in ovarian cancer cell lines. This further suggests the modification of TGF-beta pathway signaling in ovarian cancer cells is largely mediated by DNA methylation. We next conducted a computational analysis to analyze TGF-beta signaling pathway activity using binary regression. This method identifies a signature of genes based on phenotype that can be applied to external datasets to estimate the likelihood that the phenotype is in common, including the activity of

pathways [20, 34, 35]. The signature of genes, developed by the change in transcription in cultured human fibroblasts treated with TGFb1, clearly identified various type of cells including immortalized OSE that were treated with TGFb1 versus their mock-treated counterparts, (Figure 6A, 6B, 6C), indicating the accuracy of the gene signature in predicting TGF-beta pathway activity. Consistent with the results shown in Figure 5, the probability of having the TGF-beta pathway signature was increased in ovarian cell lines following 5Aza-dC treatment (Figure 6D).

Recent studies of methylation in cancer have revealed that there is coordinate methylation of a number of genes in a subset of colon cancers, which is referred to as the CpG island methylator phenotye (CIMP) [7]. Revealing CIMP in cancers is expected not only to identify clinically and biologically distinct cancers, but also to clarify the mechanism of aberrant DNA methylation in cancers. CIMP markers will largely reflect cell type-specific or organ type-specific changes in methylation patterns and thus should be determined in individual cancer types [7]. However, as there are few reports that analyzed genome-wide DNA methylation in ovarian cancer, the existence of CIMP in ovarian cancer has not been fully elucidated. In the present study, we examined the potential for CIMP in ovarian cancer through the coordinated expression of the candidate methylated genes. Because expression of methylated genes is expected to inversely correlate with their methylation, the coordinate downregulation of expression in a subset of tumors suggests that these genes may be coordinately methylated (Figure 4). First, hierarchical clustering was conducted for the 146 advanced ovarian cancers of serous histology and one gene cluster was generated (Figure 7A). The genes in this cluster reproducibly formed a similar gene cluster in an external dataset of serous ovarian tumors (Figure 7B). Interestingly, coordinate suppression of these genes in both datasets was associated with higher patient age at diagnosis. In colon cancers, the CIMP is observed in elderly patients probably due to the carcinogenic process caused by age-related accumulation of methylation changes [7]. This process may also be true in ovarian cancer, which is a disease most often affecting postmenopausal women.

Given the negative correlation between expression and DNA methylation, the average expression of coordinately expressed CIMP genes should negatively correlate with the probability of exhibiting the CIMP. The average expression of the “CIMP” genes positively

correlated with the TGF-beta signature probability in ovarian cancer samples (Figure 8A, 8B, 8C, 8D). These results, and the upregulation of TGF-beta pathway activity following treatment with 5Aza-dC (Figure 5A, 5B, 6D) indicate that TGF-beta pathway activity is downregulated through genome-wide accumulation of DNA methylation in ovarian cancer. Because high expression of the "CIMP" genes and high TGF-beta signature probability were observed in the two immortalized normal OSE cell lines (Figure 8C) and the two pooled primary culture OSE specimens (Figure 8D), genome-wide accumulation of DNA methylation may be carcinogenic through suppression of TGF-beta pathway activity.

In conclusion, using 43 ovarian cell lines and 17 ovarian primary culture specimens, we identified 360 candidate methylated genes in ovarian cancer. Analysis of those genes strongly suggests that age-related coordinated accumulation of DNA methylation contributes to ovarian carcinogenesis by suppressing the TGF-beta signaling pathway. These results deepen our understanding how epigenetics changes play a fundamental role in the etiology of ovarian cancer and should facilitate our ability to exploit this information for diagnostic and therapeutic benefit.

ACKNOWLEDGMENTS

This work was supported by a grant to SKM from the Department of Defense Ovarian Cancer Research Program, W81XWH-05-1-0053.

REFERENCES

1. Badgwell, D. and R.C. Bast, Jr., *Early detection of ovarian cancer.* Dis Markers, 2007. **23**(5-6): p. 397-410.
2. Barton, C.A., et al., *DNA methylation changes in ovarian cancer: implications for early diagnosis, prognosis and treatment.* Gynecol Oncol, 2008. **109**(1): p. 129-39.
3. Siegel, P.M. and J. Massague, *Cytostatic and apoptotic actions of TGF-beta in homeostasis and cancer.* Nat Rev Cancer, 2003. **3**(11): p. 807-21.
4. Chen, G., et al., *Resistance to TGF-beta 1 correlates with aberrant expression of TGF-beta receptor II in human B-cell lymphoma cell lines.* Blood, 2007. **109**(12): p. 5301-7.
5. Onwuegbusi, B.A., et al., *Impaired transforming growth factor beta signalling in Barrett's carcinogenesis due to frequent SMAD4 inactivation.* Gut, 2006. **55**(6): p. 764-74.
6. Varga, A.E., et al., *Silencing of the Tropomyosin-1 gene by DNA methylation alters tumor suppressor function of TGF-beta.* Oncogene, 2005. **24**(32): p. 5043-52.
7. Issa, J.P., *CpG island methylator phenotype in cancer.* Nat Rev Cancer, 2004. **4**(12): p. 988-93.
8. Strathdee, G., et al., *Primary ovarian carcinomas display multiple methylator phenotypes involving known tumor suppressor genes.* Am J Pathol, 2001. **158**(3): p. 1121-7.
9. Baba, T., et al., *Epigenetic regulation of CD133 and tumorigenicity of CD133+ ovarian cancer cells.* Oncogene, 2008.
10. Lounis, H., et al., *Primary cultures of normal and tumoral human ovarian epithelium: a powerful tool for basic molecular studies.* Exp Cell Res, 1994. **215**(2): p. 303-9.
11. Rodriguez, G.C., et al., *Epidermal growth factor receptor expression in normal ovarian epithelium and ovarian cancer. II. Relationship between receptor expression and response to epidermal growth factor.* Am J Obstet Gynecol, 1991. **164**(3): p. 745-50.
12. Huang, Z., et al., *High throughput detection of M6P/IGF2R intronic hypermethylation and LOH in ovarian cancer.* Nucleic Acids Res, 2006. **34**(2): p. 555-63.
13. Yamashita, S., et al., *Chemical genomic screening for methylation-silenced genes in gastric cancer cell lines using 5-aza-2'-deoxycytidine treatment and oligonucleotide microarray.* Cancer Sci, 2006. **97**(1): p. 64-71.
14. Suzuki, H., et al., *A genomic screen for genes upregulated by demethylation and histone deacetylase inhibition in human colorectal cancer.* Nat Genet, 2002. **31**(2): p. 141-9.
15. Keen, J.C., et al., *Epigenetic regulation of protein phosphatase 2A (PP2A), lymphotactin (XCL1) and estrogen receptor alpha (ER) expression in human breast cancer cells.* Cancer Biol Ther, 2004. **3**(12): p. 1304-12.
16. Chang, J.T. and J.R. Nevins, *GATHER: a systems approach to interpreting genomic signatures.* Bioinformatics, 2006. **22**(23): p. 2926-33.
17. Chang, J. and J. Nevins, *GATHER: A Systems Approach to Interpreting Genomic Signatures.* Bioinformatics, 2006: p. Accepted for Publication.
18. Jakowlew, S.B., *Transforming growth factor-beta in cancer and metastasis.* Cancer Metastasis Rev, 2006. **25**(3): p. 435-57.
19. West, M., et al., *Predicting the clinical status of human breast cancer by using gene expression profiles.* Proc Natl Acad Sci U S A, 2001. **98**(20): p. 11462-7.

20. Bild, A.H., et al., *Oncogenic pathway signatures in human cancers as a guide to targeted therapies.* Nature, 2006. **439**(7074): p. 353-7.
21. Karpf, A.R., *Epigenomic reactivation screening to identify genes silenced by DNA hypermethylation in human cancer.* Curr Opin Mol Ther, 2007. **9**(3): p. 231-41.
22. Shames, D.S., et al., *A genome-wide screen for promoter methylation in lung cancer identifies novel methylation markers for multiple malignancies.* PLoS Med, 2006. **3**(12): p. e486.
23. Mohn, F., et al., *Methylated DNA Immunoprecipitation (MeDIP).* Methods Mol Biol, 2009. **507**: p. 55-64.
24. Yan, P.S., et al., *Differential methylation hybridization: profiling DNA methylation with a high-density CpG island microarray.* Methods Mol Biol, 2009. **507**: p. 89-106.
25. Esteller, M., *Epigenetics in cancer.* N Engl J Med, 2008. **358**(11): p. 1148-59.
26. Razin, A. and R. Shemer, *DNA methylation in early development.* Hum Mol Genet, 1995. **4 Spec No**: p. 1751-5.
27. Furuta, J., et al., *Silencing of Peroxiredoxin 2 and aberrant methylation of 33 CpG islands in putative promoter regions in human malignant melanomas.* Cancer Res, 2006. **66**(12): p. 6080-6.
28. Hall, I.H., et al., *DNA interaction with metal complexes and salts of substituted boranes and hydroborates in murine and human tumor cell lines.* Anticancer Drugs, 1991. **2**(4): p. 389-99.
29. Li, Q., et al., *Methylation and silencing of the Thrombospondin-1 promoter in human cancer.* Oncogene, 1999. **18**(21): p. 3284-9.
30. Umetani, N., et al., *Aberrant hypermethylation of ID4 gene promoter region increases risk of lymph node metastasis in T1 breast cancer.* Oncogene, 2005. **24**(29): p. 4721-7.
31. Wen, X.Z., et al., *Frequent epigenetic silencing of the bone morphogenetic protein 2 gene through methylation in gastric carcinomas.* Oncogene, 2006. **25**(18): p. 2666-73.
32. Zhao, H., et al., *CpG methylation at promoter site -140 inactivates TGFbeta2 receptor gene in prostate cancer.* Cancer, 2005. **104**(1): p. 44-52.
33. Nilsson, E.E. and M.K. Skinner, *Role of transforming growth factor beta in ovarian surface epithelium biology and ovarian cancer.* Reprod Biomed Online, 2002. **5**(3): p. 254-8.
34. Dressman, H.K., et al., *An integrated genomic-based approach to individualized treatment of patients with advanced-stage ovarian cancer.* J Clin Oncol, 2007. **25**(5): p. 517-25.
35. Potti, A., et al., *Genomic signatures to guide the use of chemotherapeutics.* Nat Med, 2006. **12**(11): p. 1294-300.

FIGURE LEGENDS

Figure S1. ***Unbiased hierarchical clustering of all the cell line samples.***

Microarray analysis was conducted using the 43 ovarian cell lines with or without 5Aza-dC. All the 86 samples were analyzed by an unbiased hierarchical clustering using 15218 U133A probes with RMA expression >7 in at least one sample. In general, 5Aza-dC treated cells made cluster with their untreated cells. Chemo-resistant derivatives tended make close clusters with their parental cells.

Table S1. ***Published U133 microarray datasets that were used in Figure S2.***

List of published U133A or U133 plus 2 microarray datasets that analyzed response to 5Aza-dC in various types of cancers used in Figure S2 is shown. When U133 plus 2 datasets were analyzed, matched 22215 probes with U133A gene chip were used.

Figure S2. ***Similar pattern of fold change of gene expression by 5Aza-dC in various organ-derived cancer cells.***

Fold change by 5Aza-dC based on the RMA log2 expression was calculated as (5Aza-dC expression) – (untreated expression). All the U133A probes were arranged in the order of the average fold change by 5Aza-dC in the 43 ovarian cell lines. Top 1000 (right) and bottom 1000 (left) probes are shown in the figure. Responses to 5Aza-dC in various types of cancer cells in the published microarray datasets (Table S1) were compared with the average response in the 43 ovarian cells by placing the same probes at the same raw.

Regardless of the organs from which the cells are derived from, the pattern of fold change by 5Aza-dC was quite similar to that of the ovarian cell lines.

Table S2. ***Well-known methylated genes in cancers listed by M. D. Anderson Cancer Center.***

M. D. Anderson Cancer Center publishes a list of well-known methylated genes in the web site (M.D.Anderson list genes). (http://www.mdanderson.org/departments/methylation/).

Figure 1. ***Cut-off values that enrich the M.D.Anderson list genes in the ovarian cell line dataset.***

A) Maximal fold change by 5Aza-dC (MaxFC) in the 43 cell lines enriched the M.D. Anderson list genes. All the U133A probes are sorted by MaxFC: left; low and right; high. Red bars (M.D. Anderson list genes) are collected in the right. The graph shows number of genes for M.D. Anderson list probes per neighboring 100 probes. M.D.Anderson list probes were enriched when MaxFC is over 2.9.

B) Standard deviation of expression (SD) in the untreated 43 cell lines enriched the M.D. Anderson list genes. All the U133A probes are sorted by SD: left; low and right; high. M.D.Anderson list probes were enriched when SD is over 1.7.

C) Combination of the two parameters, MaxFC and SD, enriched the M.D. Anderson list genes more efficiently. All the U133A probes are plotted in the 2D map; the X axis is sorted by SD and the Y axis by MaxFC. Combination of the two cut-off values enriched M.D. Anderson list genes efficiently. 293 genes (359 probes) were selected as the candidate methylation genes in the cell line dataset.

Table S3. ***Published list of "methylated genes" by methylation microarray.***

7 published lists by methylation microarray analysis were used to generate unbiased list of methylated genes in cancer. In total, 1772 probes were annotated as “methylated genes”.

Table 1. ***MaxFC and SD in the cell line dataset enriched the unbiased methylation list genes.***

The “methylated genes” detected by published methylation microarray analysis was used as the unbiased methylation gene set (Table S3). Combination of the two cut-off values of MaxFC>2.9 and SD>1.7 enriched the “methylated genes”. The distribution was statistically significant ($p<0.0001$, Chi-square test.)

Table S3. ***List of the primary culture samples.***

Primary culture for 13 ovarian cancers, 2 ovarian borderline tumors, and 10 ovarian surface epithelium (OSE) samples were conducted. These primary culture samples were divided into two to collect samples with or without 5AzaC treatment. U133 plus 2 gene chips were used for the microarray analysis though we used only the matched U133A probes in this research. In order to collect enough RNA for microarray analysis, OSE samples from 5 individuals were mixed, so there are two microarray data for OSE.

Figure 2. ***Cut-off values that enrich the M.D.Anderson list genes in the ovarian primary culture dataset.***

Just like cell lines, the ovarian primary culture dataset enriched M.D. Anderson list genes using the two parameters; maximal fold change by 5AzaC (MaxFC) (A) and standard deviation of expression of untreated samples (SD) (B). Combination of the two parameters enriched the list

genes efficiently (C). 108 genes (128 probes) were selected as the candidate methylation target genes by the cut-off values of MaxFC>1.5 and SD>1.6.

Table 2. ***MaxFC and SD in the primary culture dataset enriched the unbiased methylation list genes.***

The "methylated" genes by methylation microarray (Table S3, Table 1) were again used. Combination of the two cut-off values of MaxFC>1.5 and SD>1.6 in the primary culture dataset enriched the "methylated genes". The distribution was statistically significant ($p<0.0001$, Chi-square test.)

Figure 3. ***Similar patterns of the selected candidate methylation genes between cell lines and primary culture.***

A) The 128 probes for the candidate methylation genes selected from primary culture show the pattern of high MaxFC and high SD in the cell line dataset.

B) The 359 probes for the candidate methylation genes selected from cell lines show the pattern of high MaxFC and high SD in the primary culture dataset.

Table 3. ***Summary of the predicted methylation target genes.***

293 genes (359 probes) were selected from cell lines and 108 genes (128 probes) were selected from primary culture as candidate methylation genes. Because 41 genes were overlapped, total 360 genes were selected as methylation candidate genes in ovarian cancer. Among the 360 genes, 127 genes (35%) have been reported as methylated in any types of cells.

20 genes, including 9 genes with no report for methylation, were tested by MS-PCR and all the 20 genes (100%) were methylated in ovarian cancer.

Table 4. ***Summary of methylation results by MS-PCR assay.***

20 genes are among the predicted genes. 10 other genes with high MaxFC or high SD in the cell line dataset or primary culture dataset were methylated. 3 other genes that belong to KEGG TGFb pathway were also methylated. In total, 33 genes were methylated. Among the 33 genes, one gene was reported as methylated in ovarian cancer, 14 genes were reported as methylated in other types of cancer, and 18 genes have never been reported as methylated.

Red colored gene symbols; KEGG TGF-beta signaling pathway genes.

−; not tested

#; We are going to report methylation of PROM1, MAL, and CDH4 elsewhere. Results for these three genes are excluded from the following analysis in this manuscript.

Red numbers; Values that exceeded the cut-offs determined in Figure 1 and Figure 2.

Figure 4. ***Relationship between the microarray expression and methylation data in the cell lines.***

A) Microarray expression data of the 30 genes in the untreated samples which MS-PCR analysis was conducted are plotted. % methylation was determined by comparing the “methylated” and the “unmethylated” bands.

B) Fold change by 5Aza-dC of the 30 genes in samples which MS-PCR analysis was conducted are plotted.

C) 2D plot by the expression and the fold change. X-axis; expression of untreated samples, Y-axis; fold change by 5Aza-dC.

D) Representative 4 genes that expression negatively correlated with the methylation status detected by MS-PCR.

E) Quantitative methylation assay for TGFBR2 by pyrosequencing. Ovarian cell lines are arranged in the order of TGFBR2 expression from low (left; green) to high (right; red). % methylation of 8 CpG sites at the promoter region is shown as the white-black heatmap. Pearson's correlation coefficients between expression and % methylation were calculated independently.

F) Quantitative methylation assay for THBS1 by pyrosequencing.

Note that the two immortalized OSE cell lines (NOSE06 and NOSE07) have high expression and unmethylated CpG for both TGFBR2 and THBS1.

M (>50%); methylated band was equal or stronger than unmethylated band. M (<50%); methylated band was weaker than unmethylated band. U; unmethylated.

***; $p<0.001$, **; $p<0.01$, *; $p<0.05$.

Table 5. ***Gene Ontology terms enriched in the predicted methylation genes***

Enrichment of Gene Ontology terms was analyzed by GATHER (http://gather.genome.duke.edu/). Representative gene ontology terms enriched compared to genome ($p<0.01$) in the 360 predicted methylation genes are listed. Complete list of enriched Gene Ontology terms is shown in the Table S###.

Figure 5. ***Activation of TGFb pathway by 5Aza-dC treatment.***

A) Western blotting analysis using p-SMAD2/3 antibody was conducted. 5Aza-dC increased p-SMAD2/3 in ovarian cancer cell lines.

B) Luciferase assay using the SMAD3-reporter was conducted. 5Aza-dC treatment significantly increased the relative luciferase activity in ovarian cancer cell lines.

*; $p<0.05$, **; $p<0.01$, ***; $p<0.001$

Figure 6. ***Development and validation of gene signature for the TGF- beta pathway.***

A) Web-based dataset (GSE1724) for cultured human fibroblast with or without addition of TGF-beta 1 (n=9 each) was used to develop the gene signature for the TGF-beta pathway. Top 300 probes that discriminate TGF-beta 1 treated samples from control samples are shown. B) Leave-one-out cross validation indicates both sensitivity and specificity of the prediction by the signature are 100%. Blue; control samples. Red; TGF-beta 1 treated samples. C) External validation was conducted using web-based datasets. The TGF-beta signature predicts TGF-beta1 treated samples in the datasets of immortalized OSE cells (GSE6653), A549 cells (GSE5457), AAKata cells (GSE5457), and trabecular meshwork (TM) cells (GSE7144).

D) 5Aza-dC treatment significantly upregulated the TGFb signature probability in the 43 ovarian cell lines ($p<0.0001$).

Figure 7. ***Development of "CIMP" genes based on the expression microarray in ovarian cancer.***

A) Web-based microarray dataset (GSE3149) that comprises of 146 advanced (stage3-4) serous ovarian cancers was used. Hierarchical clustering by the 360 candidate methylation genes (436

probes) divided the ovarian cancer tissue samples into two clusters by a definite gene cluster ("CIMP" genes). The tumor clusters were significantly different for patient's age (p=0.0015). Age; patient's age at diagnosis.

B) Hierarchical clustering by the same "CIMP" genes in the external ovarian tumor dataset. Web-based dataset (GSE2109) was used. This data set contains 77 serous ovarian tumors, including borderline tumors (n=6), stage 1-2 tumors (n=14), stage 3-4 tumors (n=47), and tumors with no annotation for staging (n=10). The "CIMP" genes again formed one gene cluster.

Figure 8. ***Relationship between the expression of the "CIMP" genes and TGFb signature probability in ovarian cancer.***

A) Average expression of the "CIMP" genes (Figure 7) positively correlated with the TGFb signature probability in the serous advanced ovarian cancers (GSE3149).

B) Average expression of the "CIMP" genes positively correlated with the TGFb signature probability in the serous ovarian tumors (GSE2109).

C) Average expression of the "CIMP" genes positively correlated with the TGFb signature probability in the 43 ovarian cancer cell lines. The two immortalized OSE cell lines showed high expression of the "CIMP" genes and high TGFb signature probability (blue dots).

D) Average expression of the "CIMP" genes positively correlated with the TGFb signature probability in the 17 primary culture samples. The two OSE samples showed high expression of the "CIMP" genes and high TGFb signature probability (blue dots).

Figure 1

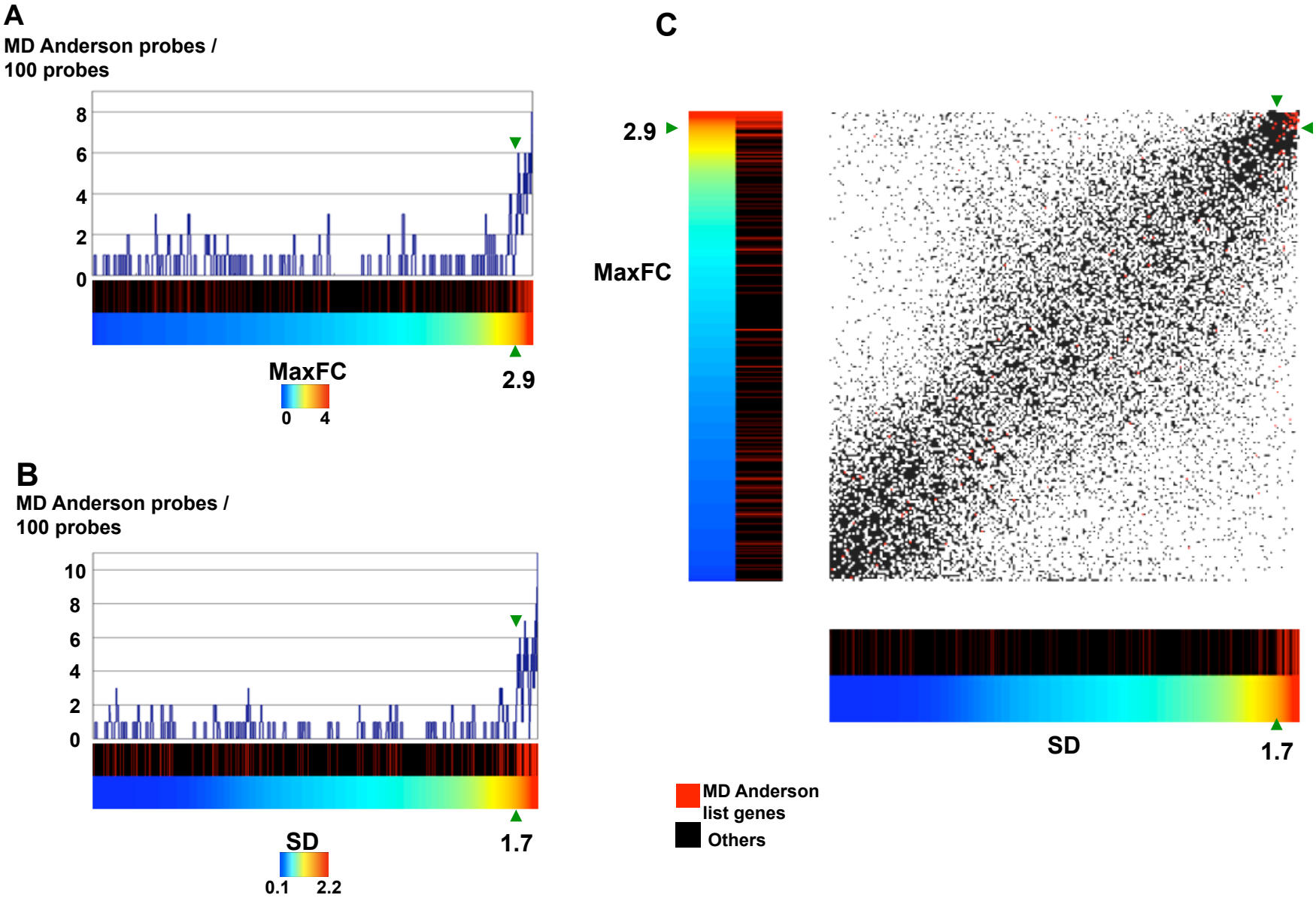
A
MD Anderson probes /
100 probes
8
6
4
2
0
MaxFC
0
4
2.9
B
MD Anderson probes /
100 probes
10
8
6
4
2
0
SD
0.1
2.2
1.7
C
2.9
MaxFC
SD
1.7
MD Anderson
list genes
Others

Figure 2

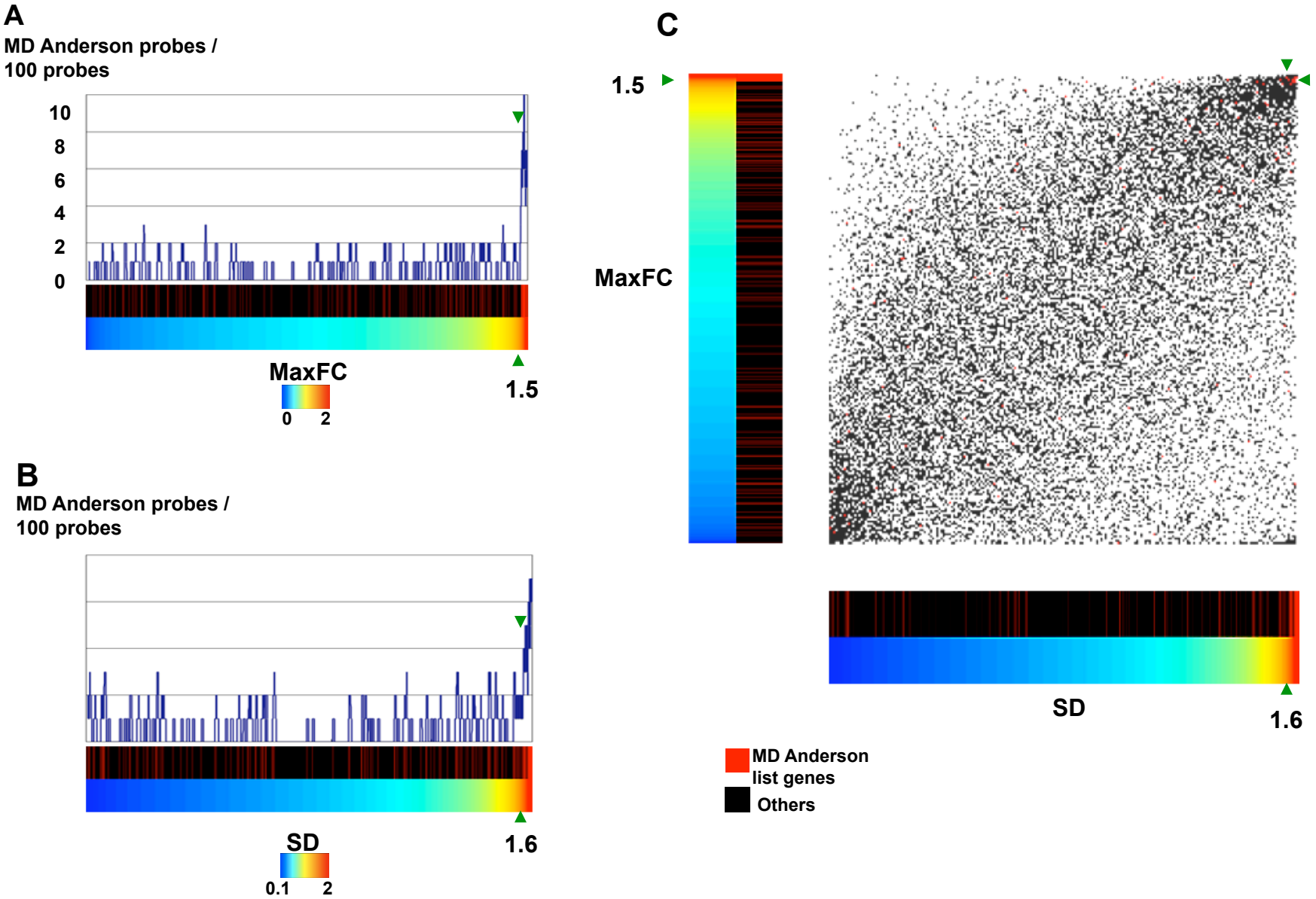
A
MD Anderson probes /
100 probes
10
8
6
4
2
0
MaxFC
0
2
1.5
B
MD Anderson probes /
100 probes
SD
0.1
2
1.6
C
1.5
MaxFC
SD
1.6
MD Anderson
list genes
Others

Figure 3

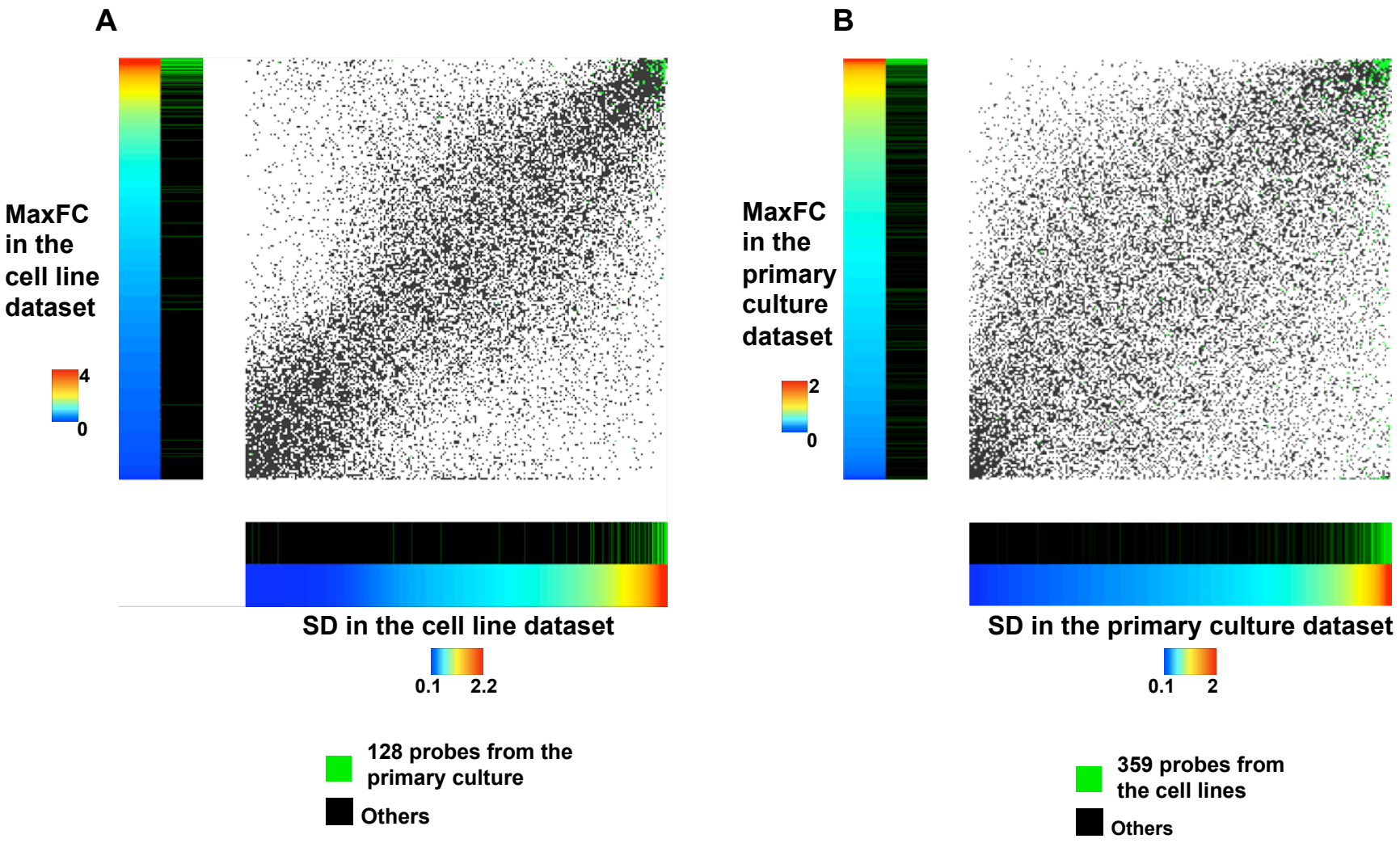
A
MaxFC in the cell line dataset
4
0
SD in the cell line dataset
0.1
2.2
128 probes from the primary culture
Others
B
MaxFC in the primary culture dataset
2
0
SD in the primary culture dataset
0.1
2
359 probes from the cell lines
Others

Figure 4

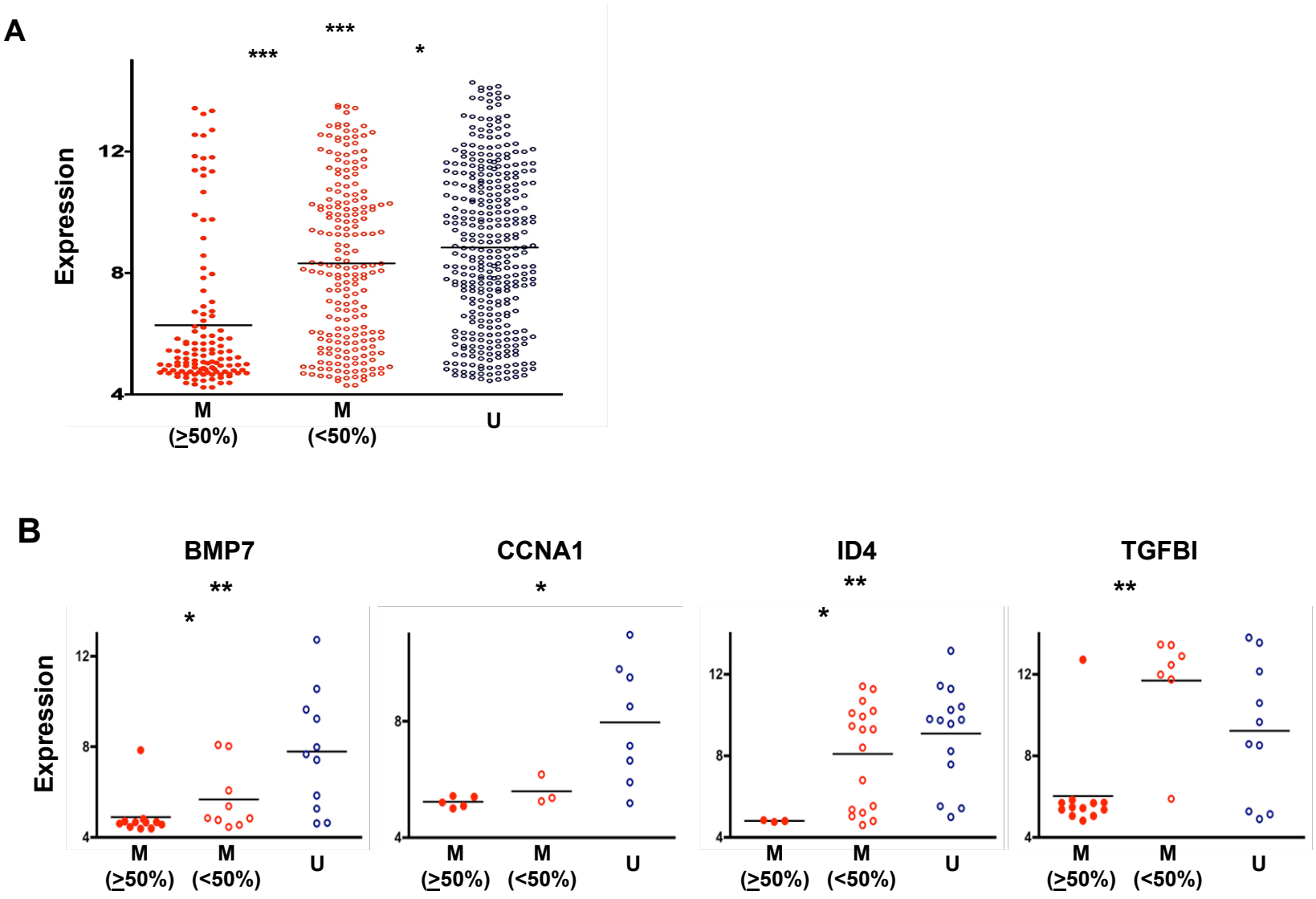
A
***
***
*
Expression
12
8
4
M
(≥50%)
M
(<50%)
U
B
BMP7
**
*
CCNA1
*
ID4
**
*
TGFBI
**
Expression
12
8
4
M
(≥50%)
M
(<50%)
U

Figure 4

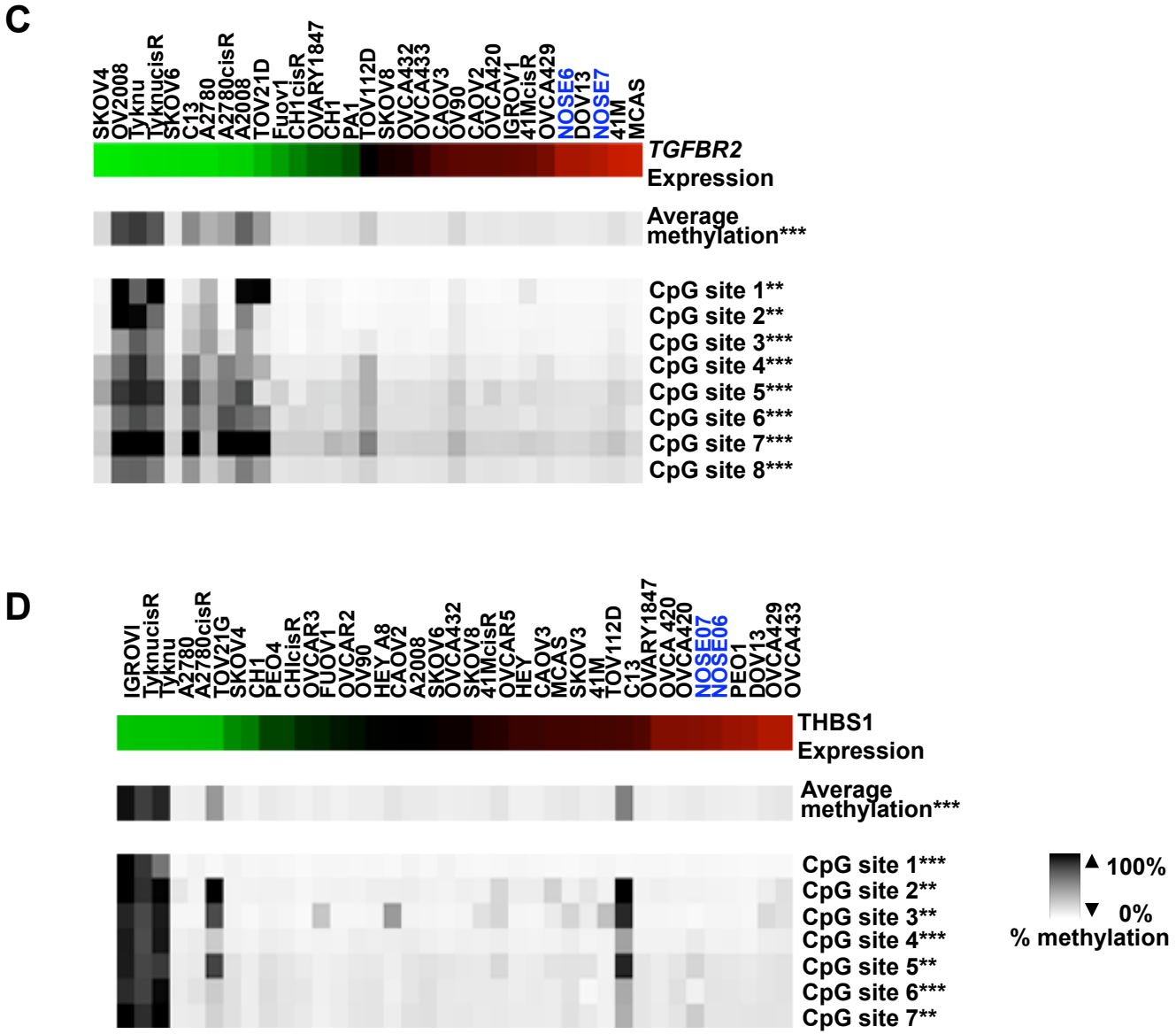
C
SKOV4
OV2008
Tyknu
TyknucisR
SKOV6
C13
A2780
A2780cisR
A2008
TOV21D
Fuov1
CH1cisR
OVARY1847
CH1
PA1
TOV112D
SKOV8
OVCA432
OVCA433
CAOV3
OV90
CAOV2
OVCA420
IGROV1
41McisR
OVCA429
NOSE6
DOV13
NOSE7
41M
MCAS
TGFBR2
Expression
Average
methylation***
CpG site 1**
CpG site 2**
CpG site 3***
CpG site 4***
CpG site 5***
CpG site 6***
CpG site 7***
CpG site 8***
D
IGROVI
TyknucisR
Tyknu
A2780
A2780cisR
TOV21G
SKOV4
CH1
PEO4
CHIcisR
OVCAR3
FUOV1
OVCAR2
OV90
HEYA8
CAOV2
A2008
SKOV6
OVCA432
SKOV8
41McisR
OVCAR5
HEY
CAOV3
MCAS
SKOV3
41M
TOV112D
C13
OVARY1847
OVCA 420
OVCA420
NOSE07
NOSE06
PEO1
DOV13
OVCA429
OVCA433
THBS1
Expression
Average
methylation***
CpG site 1***
CpG site 2**
CpG site 3**
CpG site 4***
CpG site 5**
CpG site 6***
CpG site 7**
100%
0%
% methylation

Figure 5

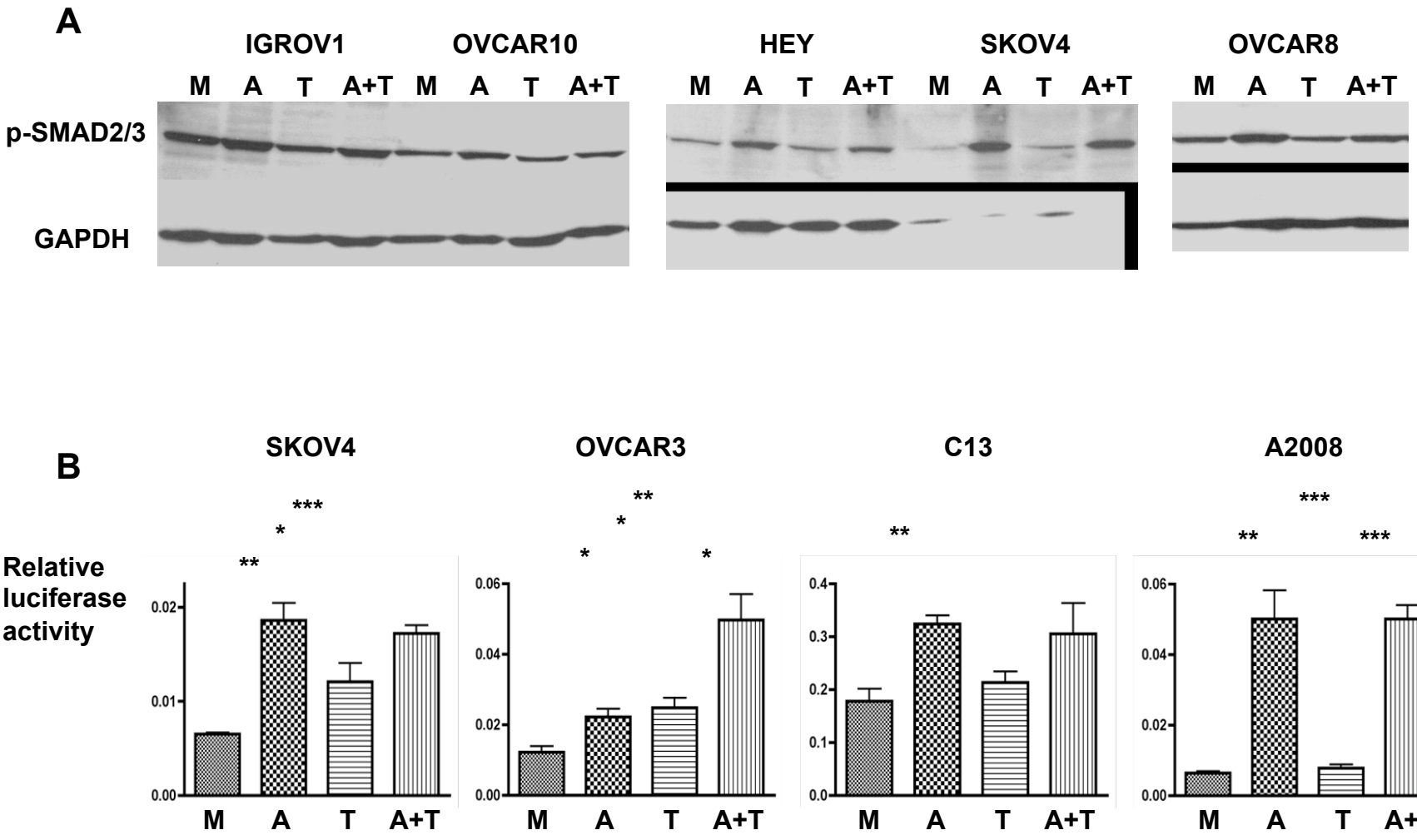
A
IGROV1
OVCAR10
HEY
SKOV4
OVCAR8
M A T A+T M A T A+T
M A T A+T M A T A+T
M A T A+T
p-SMAD2/3
GAPDH
B
SKOV4
OVCAR3
C13
A2008
Relative luciferase activity
M A T A+T

Figure 6

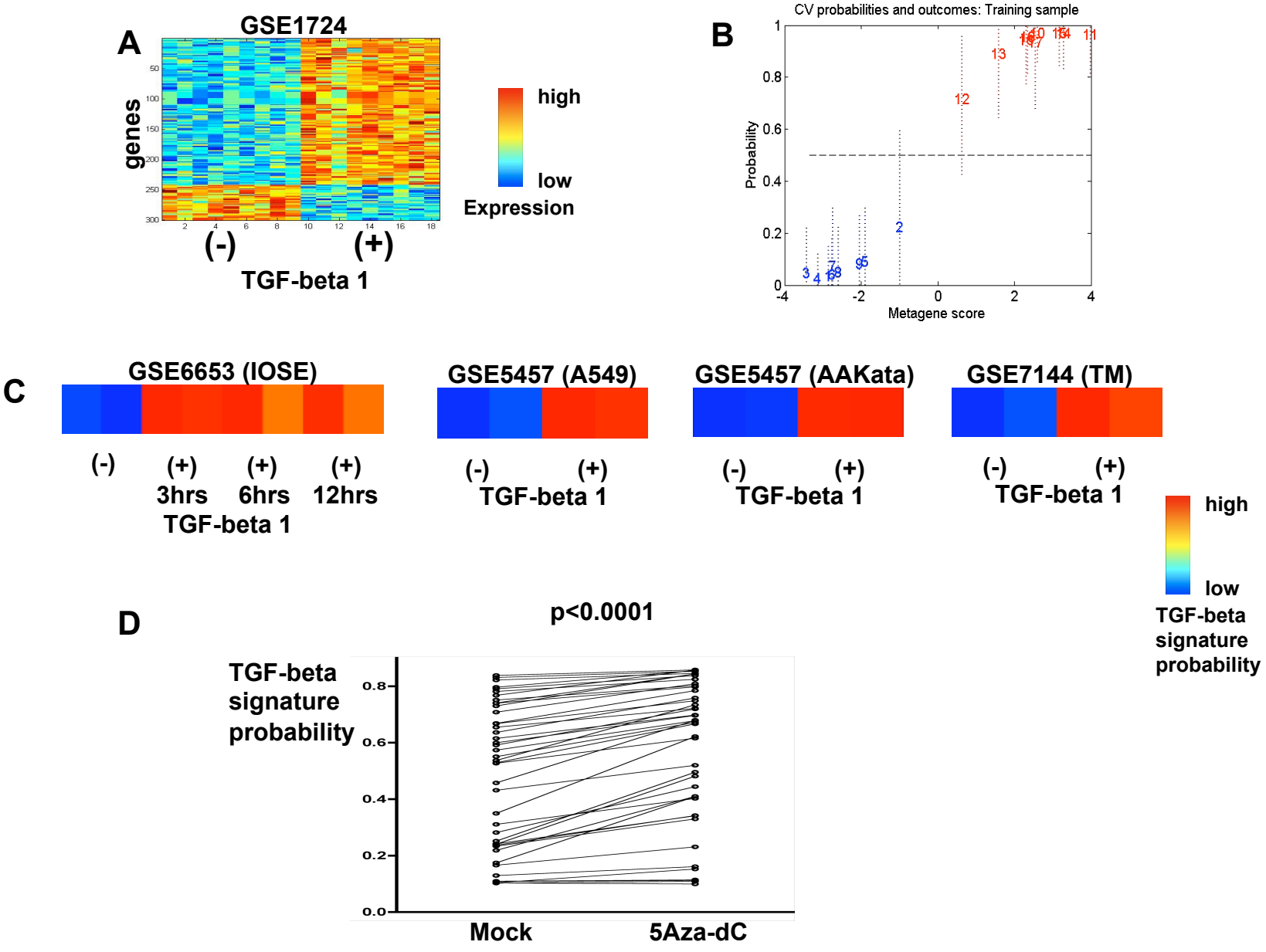
A
GSE1724
genes
(-)
(+)
TGF-beta 1
high
low
Expression
B
CV probabilities and outcomes: Training sample
Probability
Metagene score
C
GSE6653 (IOSE)
(-)
(+) 3hrs
(+) 6hrs
(+) 12hrs
TGF-beta 1
GSE5457 (A549)
GSE5457 (AAKata)
GSE7144 (TM)
high
low
TGF-beta signature probability
D
p<0.0001
TGF-beta signature probability
Mock
5Aza-dC

Figure 7

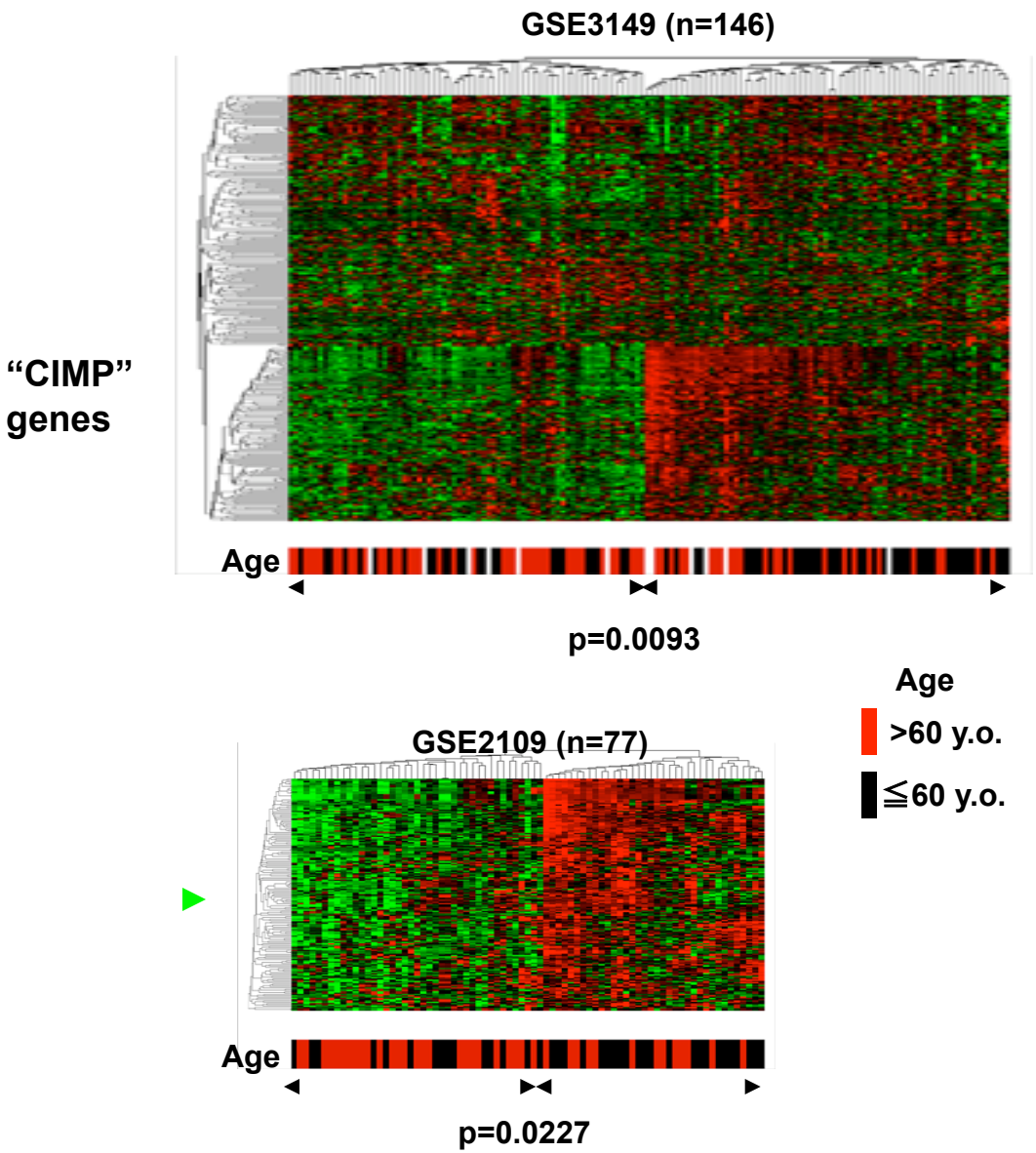
A
GSE3149 (n=146)
"CIMP" genes
Age
p=0.0093
Age
>60 y.o.
≦60 y.o.
B
GSE2109 (n=77)
Age
p=0.0227

Figure 8

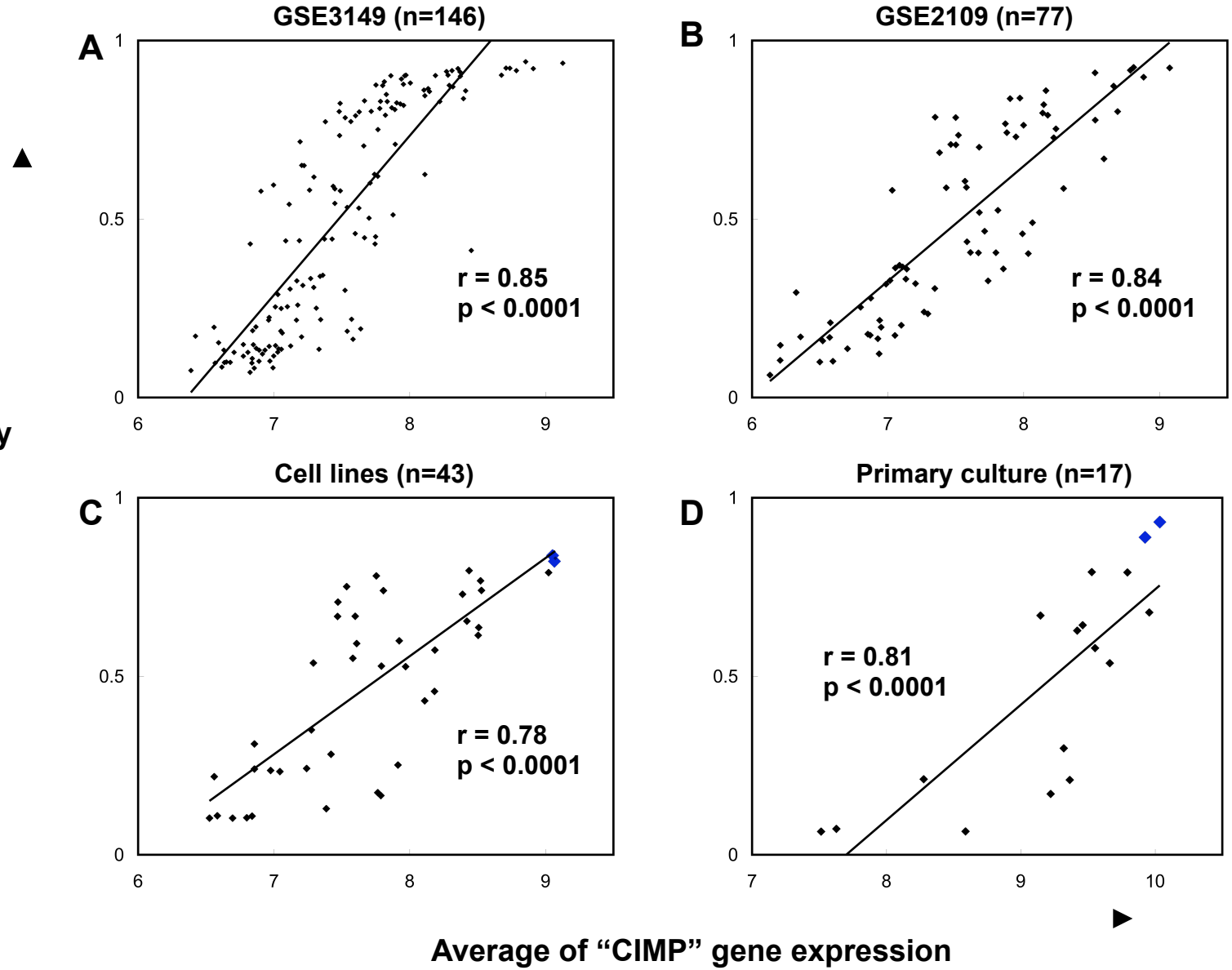
A
GSE3149 (n=146)
r = 0.85
p < 0.0001
B
GSE2109 (n=77)
r = 0.84
p < 0.0001
C
Cell lines (n=43)
r = 0.78
p < 0.0001
D
Primary culture (n=17)
r = 0.81
p < 0.0001
TGF-beta signature probability
Average of "CIMP" gene expression

Figure S1

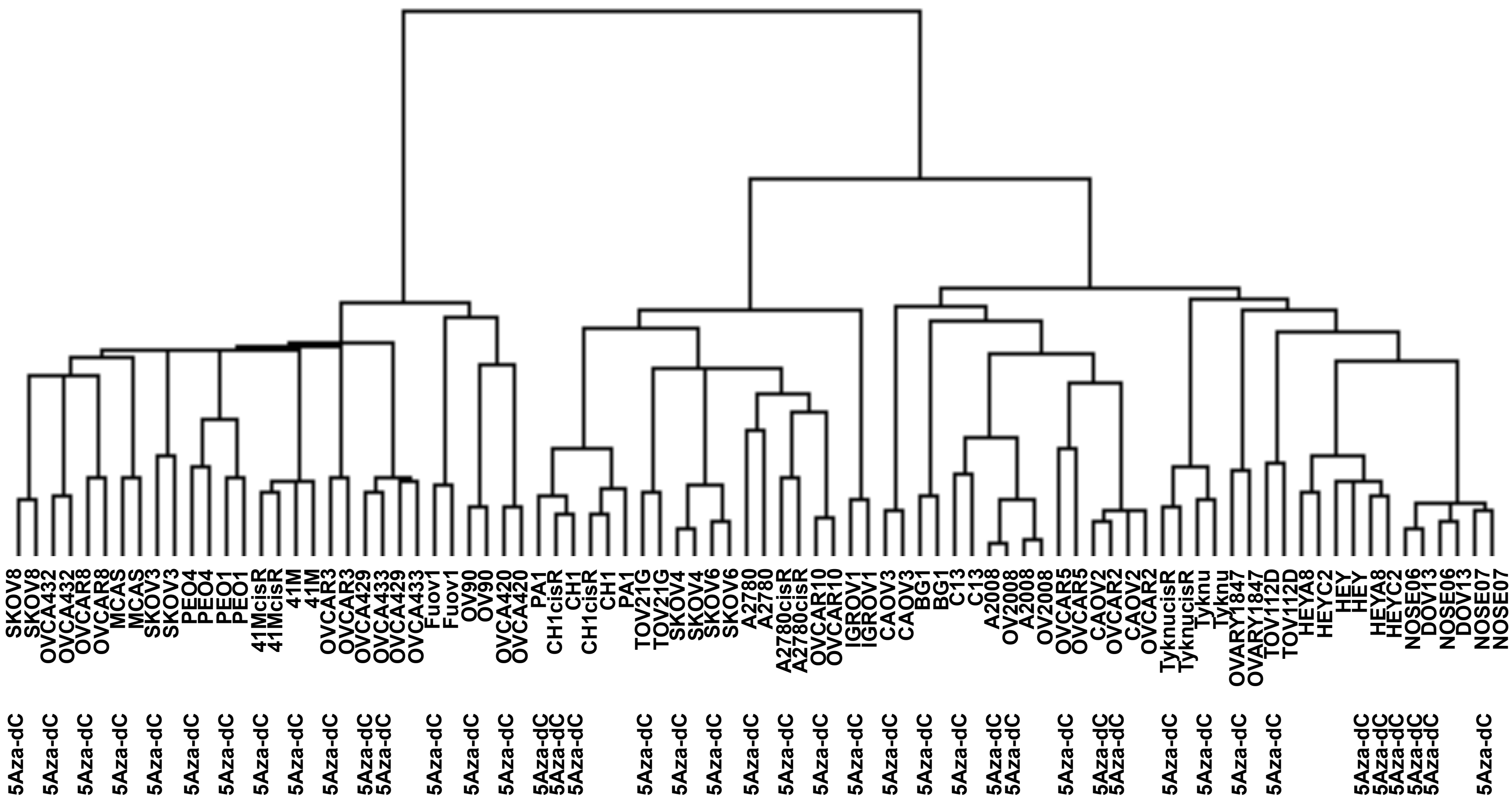
SKOV8
SKOV8
OVCA432
OVCA432
OVCAR8
OVCAR8
MCAS
MCAS
SKOV3
SKOV3
PEO4
PEO4
PEO1
PEO1
41McisR
41McisR
41M
41M
OVCAR3
OVCAR3
OVCA429
OVCA433
OVCA429
OVCA433
Fuov1
Fuov1
OV90
OV90
OVCA420
OVCA420
PA1
CH1cisR
CH1
CH1cisR
CH1
PA1
TOV21G
TOV21G
SKOV4
SKOV4
SKOV6
SKOV6
A2780
A2780
A2780cisR
A2780cisR
OVCAR10
OVCAR10
IGROV1
IGROV1
CAOV3
CAOV3
BG1
BG1
C13
C13
A2008
OV2008
A2008
OV2008
OVCAR5
OVCAR5
CAOV2
OVCAR2
CAOV2
OVCAR2
TyknucisR
TyknucisR
Tyknu
Tyknu
OVARY1847
OVARY1847
TOV112D
TOV112D
HEYA8
HEYC2
HEY
HEY
HEYA8
HEYC2
NOSE06
DOV13
NOSE06
DOV13
NOSE07
NOSE07

Figure S2

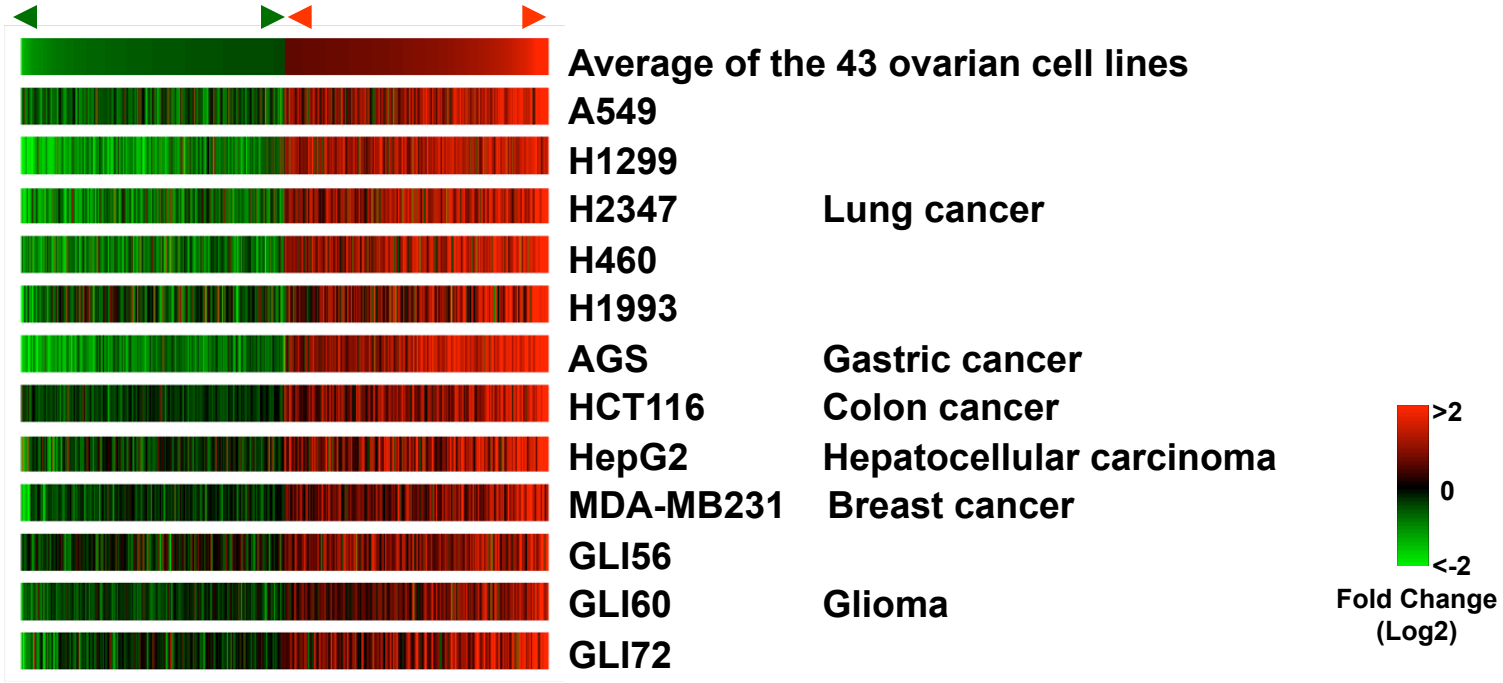
Average of the 43 ovarian cell lines
A549
H1299
H2347
H460
H1993
AGS
HCT116
HepG2
MDA-MB231
GLI56
GLI60
GLI72
Lung cancer
Gastric cancer
Colon cancer
Hepatocellular carcinoma
Breast cancer
Glioma
>2
0
<-2
Fold Change
(Log2)

Figure S3

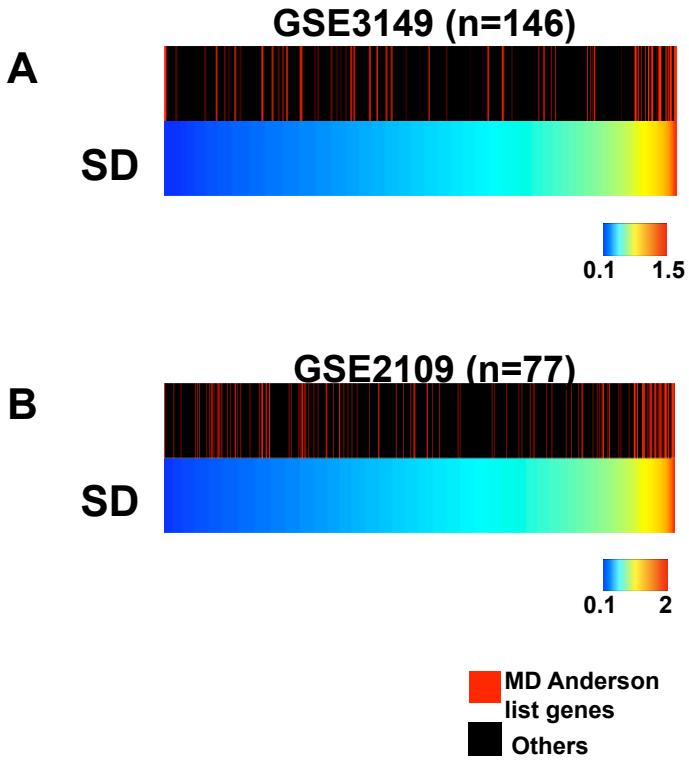
GSE3149 (n=146)
A
SD
0.1
1.5
GSE2109 (n=77)
B
SD
0.1
2
MD Anderson list genes
Others

Figure S4

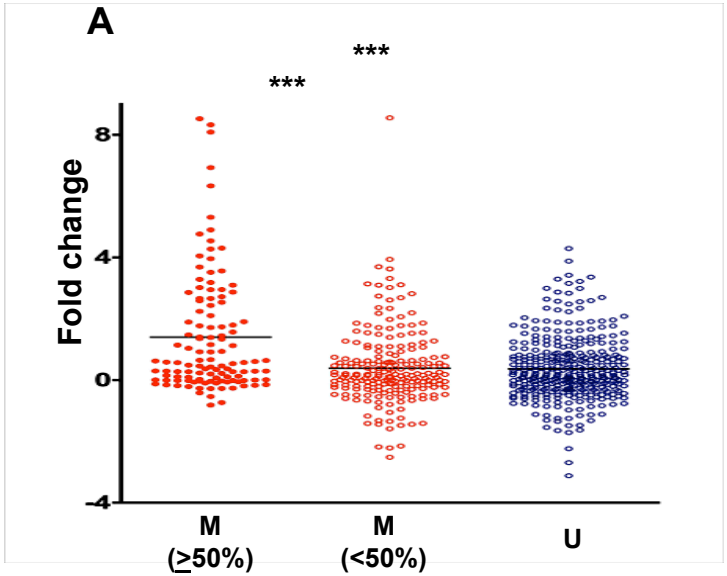
A
***
***
Fold change
8
4
0
-4
M
(≥50%)
M
(<50%)
U

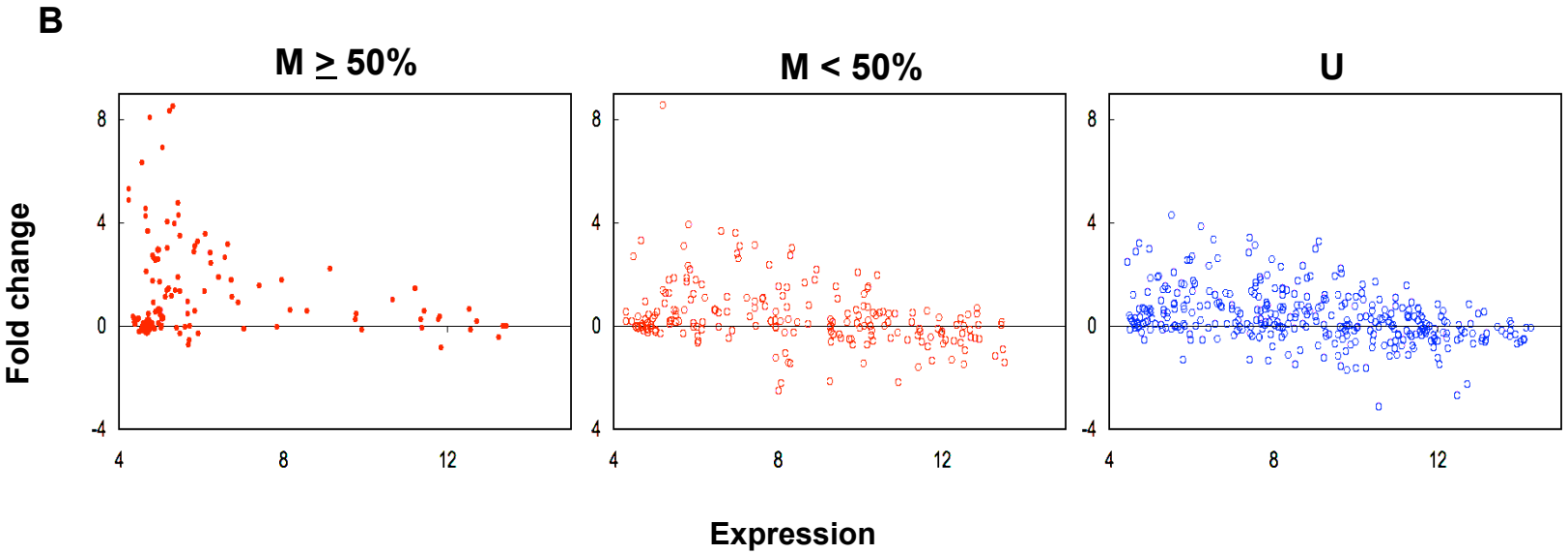
B
M ≥ 50%
M < 50%
U
Fold change
8
4
0
-4
4
8
12
Expression

Table1

	SD>1.7	SD<1.7	total
MaxFC>2.9	17.0% (61/359)	14.1% (62/441)	15.4% (123/800)
MaxFC<2.9	11.6% (58/499)	7.6% (1591/20916)	7.7% (1652/21437)
total	13.9% (119/858)	7.7% (1653/21357)	8.0% (1772/22215)

Table 2

	SD>1.6	SD<1.6	total
MaxFC>1.5	17.2% (22/128)	13.3% (39/293)	14.5% (61/421)
MaxFC<1.5	13.4% (46/343)	7.8% (1665/21451)	7.9% (1771/21794)
total	14.4% (68/471)	7.8% (1704/21744)	8.0% (1772/22215)

Table 3

Published data (～Jun 2008)	Number of genes	Methylated/ Analyzed
Methylated in ovarian cancer	13	1/1
Methylated in other types of cancer	101	10/10
Methylated in non cancerous cells	8	
Imprinted	5	
No report for methylation	233	9/9
Total	360	20/20 (100%)

Table 4

Gene Symbol	Ovarian cell lines	Ovarian cancer tissues	Representative U133A probe	Cell lines (n=43)		Primry culture (n=17)		Methylated in Ovarian cancer (PubMed ID)	Methylated in Cancer (PubMed ID)
				MaxFC	SD	MaxFC	SD		
BMP2	10/30 (33%)	13/34 (38%)	205290_s_at	3.22	1.56	0.53	1.79		16314833
BMP4	24/31 (77%)	20/35 (57%)	211518_s_at	3.88	1.85	0.12	0.86		17696196
BMP7	20/31 (65%)	34/40 (85%)	209591_s_at	0.28	2.28	0.46	0.57		16367923
CCNA1	8/16 (50%)	15/40 (38%)	205899_at	5.19	1.92	1.66	2.19		15342377
CDH1	16/43 (37%)	-	201131_s_at	3.56	3.42	2.40	2.39	16061849	
CDH4	#		220227_at	0.46	1.85	1.11	1.03		15548679
EPM2AIP1	6/8 (75%)	-	202909_at	2.96	1.78	0.52	0.74		
FST	8/28 (29%)	29/39 (74%)	204948_s_at	4.01	2.15	0.72	1.29		16367923
GPX1	2/3 (67%)	-	200736_s_at	5.57	2.70	0.41	0.42		17194187
HSPB1	8/9 (89%)	-	201841_s_at	4.30	1.79	0.45	0.41		
ID1	14/32 (44%)	40/42 (95%)	208937_s_at	3.63	1.47	1.50	0.93		
ID2	4/29 (14%)	28/43 (65%)	201565_s_at	4.59	2.34	2.02	1.34		
ID4	20/34 (59%)	38/42 (91%)	209291_at	4.29	2.72	1.35	0.97		15897910
IGFBP7	24/32 (75%)	-	201163_s_at	6.33	3.22	0.93	1.70		17334979
INHBB	23/37 (62%)	37/40 (93%)	205258_at	2.69	2.59	0.60	1.33		
ITPR3	1/5 (20%)	-	201189_s_at	2.18	1.74	0.85	1.29		
LGALS3	1/4 (25%)	-	208949_s_at	4.41	2.64	0.50	0.81		15734994
MAL	#		204777_s_at	#REF!	#REF!	1.85	2.59		16952549
MYO5C	4/6 (67%)	-	218966_at	3.29	2.03	1.52	1.77		
PROM1	#		204304_s_at	2.73	2.73	3.24	2.43		
RBBP7	2/9 (22%)	-	201092_at	3.69	1.11	0.36	0.39		
RHOBTB3	8/16 (50%)	-	216048_s_at	3.36	2.04	1.70	1.06		
SMAD5	12/31 (39%)	33/40 (83%)	205187_at	0.72	0.54	0.89	0.80		
SMAD7	13/32 (41%)	28/38 (74%)	204790_at	1.93	1.52	1.91	0.92		
SMURF2	12/33 (36%)	26/42 (62%)	205596_s_at	1.34	1.10	0.46	0.68		
TGFB2	22/33 (67%)	14/38 (37%)	220407_s_at	3.32	1.89	1.15	1.22		16778180
TGFBI	19/29(66%)	16/33 (48%)	201506_at	3.96	3.24	0.29	1.27		16651406
TGFBR2	7/32 (22%)	7/43 (16%)	208944_at	1.80	2.50	1.04	0.77		15895377
THBS1	11/41 (27%)	17/46 (37%)	201110_s_at	4.90	2.47	2.72	1.62		10359534
TPM2	6/8 (75%)	-	204083_s_at	4.05	1.74	0.54	1.72		
TUBB6	2/9 (22%)	-	209191_at	3.52	1.54	0.44	0.34		
UBB	6/9 (67%)	-	200633_at	8.55	3.27	0.22	0.48		

Table 5

GO:0009653 [3]: morphogenesis
GO:0009887 [4]: organogenesis
GO:0007275 [2]: development
GO:0009888 [5]: histogenesis
GO:0042127 [5]: regulation of cell proliferation
GO:0008285 [6]: negative regulation of cell proliferation
GO:0006915 [6]: apoptosis
GO:0012501 [5]: programmed cell death
GO:0042981 [6]: regulation of apoptosis
GO:0043065 [7]: positive regulation of apoptosis
GO:0043068 [6]: positive regulation of programmed cell death
GO:0007596 [4]: blood coagulation
GO:0050817 [3]: coagulation
GO:0007599 [5]: hemostasis
GO:0006928 [4]: cell motility
GO:0016477 [5]: cell migration
GO:0042330 [5]: taxis
GO:0006935 [6]: chemotaxis
GO:0001525 [6]: angiogenesis
GO:0007155 [4]: cell adhesion
GO:0030155 [4]: regulation of cell adhesion
GO:0006954 [5]: inflammatory response
GO:0009611 [5]: response to wounding
GO:0006952 [5]: defense response
GO:0006955 [4]: immune response

Table S1

Samples	Tumor origin	Pubmed ID
A549, H1299, H2347, H460, H1993	Lung cancer	17194187
AGS	Gastric cancer	16367923
HCT116	Colon cancer	16952549
HepG2	Hepatocellular carcinoma	16854234
MDA-MB231	Breast cancer	15662126
Primary culture (GLI56, GLI60, GLI72)	Glioma	16909125

Table S2

ABCB1	*CDH13*	*FABP3*	*MGMT*	*SFN*
ABCB4	*CDKN1B*	*FHIT*	*MLH1*	*SLC5A5*
ABL1	*CDKN1C*	*GJB2*	*MT1A*	*STK11*
ABO	*CDKN2A*	*GPC3*	*MT-CO2*	*TERT*
APC	*CDKN2B*	*GSTP1*	*MUC2*	*TES*
AR	*CFTR*	*H19*	*MYOD1*	*TGFBR1*
BRCA1	*CSPG2*	*HIC1*	*NEFL*	*THBS1*
CALCA	*DBCCR1*	*HOXA5*	*PAX6*	*TIMP3*
CASP8	*DDR1*	*IGF2*	*PGR*	*TJP2*
CAV1	*EDNRB*	*IGFBP7*	*PLAU*	*TLS3*
CCNA1	*EPHA3*	*IRF7*	*RARB*	*TUSC3*
CD44	*EPO*	*LRP2*	*RASSF1*	*VHL*
CDH1	*ESR1*	*LTB4R*	*RB1*	*WT1*

Table S3

Samples	Tissue origin	Number of methylated genes	Number of matched U133A probes	Pubmed ID
Cancer tissue	Ovary	40	61	12114427
I-87, Normal lung tissue	Lung	438	493	16407832
SW48, Normal colon tissue, SW38	Colon	18	19	16007088
HCT116	Colon	325	197	17041235
Caco-2, PC3, Colon tumor tissue	Colon+ Prostate	367	481	16444255
PC3, PC3M, PC3M-Pro4, PC3M-LN4, LNCaP, RWPE-1, 267B1, MIcsv40	Prostate	504	645	16207477
THP-1, KG-1, U937, Normal monocytes	Leukemia	131	60	16778185
	Total	**1140**	**1772**	

Table S4

Sample	Histology	Stage
OC1	Serous papillary adenocarcinoma	
OC5	Serous papillary adenocarcinoma	
OC6	Serous papillary adenocarcinoma	
OC7	Endometrioid adenocarcinoma	
OC10	Serous papillary adenocarcinoma	
OC14	Serous papillary adenocarcinoma	
OC15	Serous papillary adenocarcinoma	
OC16	Serous papillary adenocarcinoma	
OC18	Serous papillary adenocarcinoma	
OC20	Serous papillary adenocarcinoma	
OC22	Serous papillary adenocarcinoma	
OC26	Serous papillary adenocarcinoma	
OC27	Serous papillary adenocarcinoma	
OC2	Serous borderline tumor	
OC28	Serous borderline tumor	
NO1	Normal OSE from 5 individuals	
NO2	Normal OSE from 5 individuals	

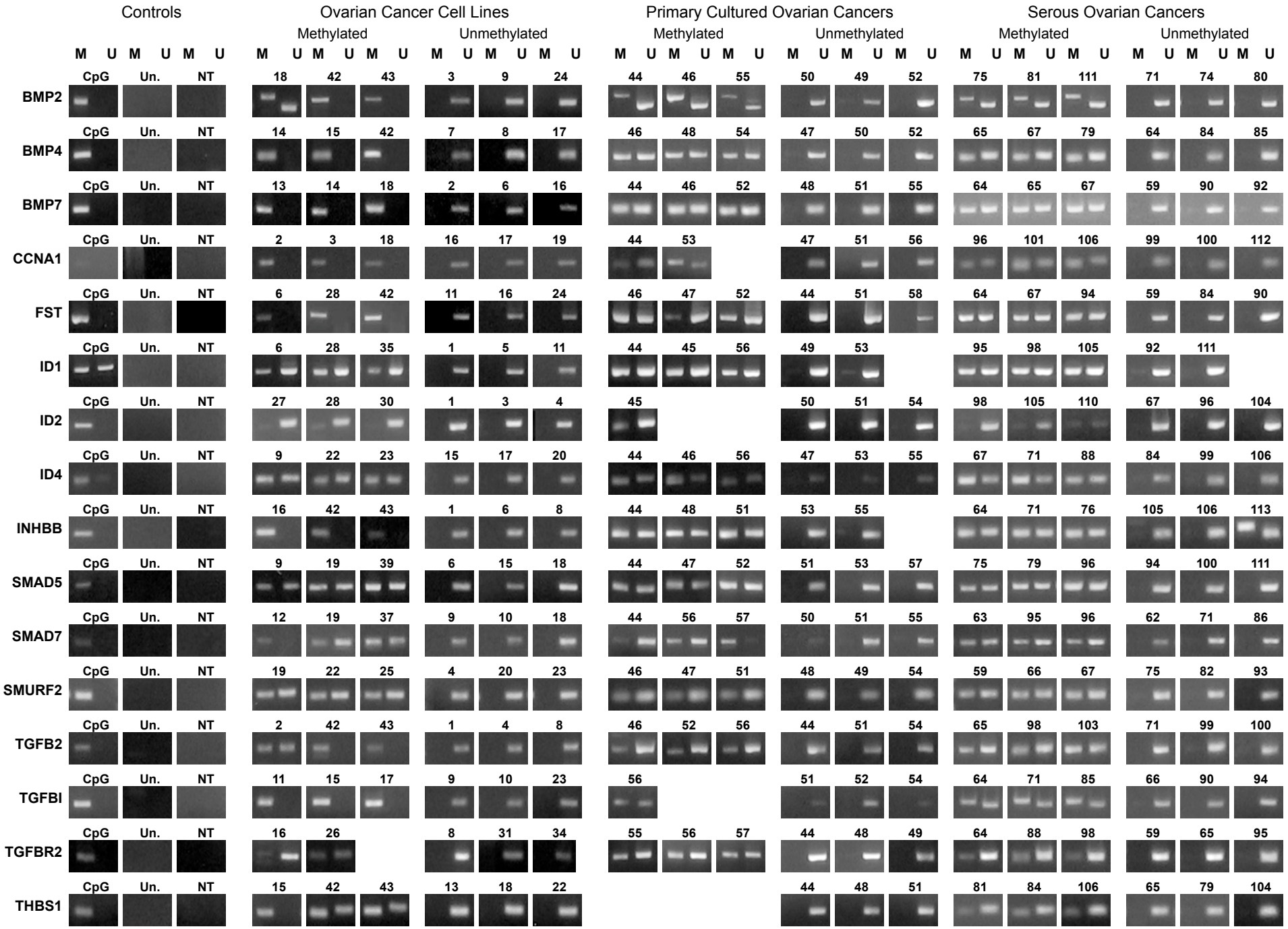
Controls
Ovarian Cancer Cell Lines
Primary Cultured Ovarian Cancers
Serous Ovarian Cancers
Methylated
Unmethylated
M U M U M U
CpG Un. NT
BMP2
BMP4
BMP7
CCNA1
FST
ID1
ID2
ID4
INHBB
SMAD5
SMAD7
SMURF2
TGFB2
TGFBI
TGFBR2
THBS1

Genome-wide targets of aberrant methylation in serous epithelial ovarian cancer cells

Dhani Biscocho[1] • Jessica J. Connelly[1] • Zhiqing Huang[2] • Simon G Gregory[1] • Susan K. Murphy[2]

[1]Department of Medicine and Center for Human Genetics, [2]Department of OB/GYN-Oncology
Duke University, Durham, NC

INTRODUCTION

The main focus of the epigenetic approach described here is to study genes that are misregulated in ovarian cancer due to changes in DNA methylation.

•In the United States in 2008, the American Cancer Society estimates that 21,650 new cases of ovarian cancer will be diagnosed and 15,520 women will die from this disease. The vast majority of women succumb due to recurrence of chemoresistant disease.

•Abnormal DNA methylation is a frequent finding in ovarian cancers and may provide opportunities to improve early disease detection and treatment. However, very little is known about why specific genes are targets of aberrant methylation and the breadth of these alterations that ultimately contribute to cancer.

•Unlike genetic mutations, aberrant DNA methylation is potentially reversible, generating great interest in epigenetic-based therapies. Non-invasive diagnostic tests may also be used in the future for detection of early disease, based on detection of disease-specific methylation in blood. This type of test is one of the most crucial needs for improving ovarian cancer patient prognosis and survival.

•Our long-term goals are therefore to develop a methylation-based screening test for detection of early stage ovarian cancer and to integrate epigenetic therapies into individualized treatment plans for ovarian cancer.

•Our central hypothesis is that normal ovarian surface epithelium has distinct patterns of genome wide methylation relative to epithelial ovarian malignancies that can be used to distinguish between normal and malignant tissues.

BACKGROUND

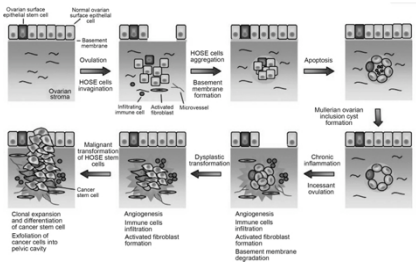

Figure 1. A Model of Ovarian Cancer Formation (from : Genomic analysis of epithelial ovarian cancer John Farley, Laurent L Ozbun and Michael J Birrer**).**

A model of disease formation is depicted in Figure 1:

1) Incessant ovulation and wound repair *increases the risk of genetic abnormalities*, leading to dysplastic changes in epithelial cells lining the mullerian inclusion cyst.

2) Stromal microenvironment in the form of activated fibroblast formation, microvessel proliferation, and growth factors contributes to dysplastic formation and eventual malignant transformation.

METHODS

DNA was isolated in triplicate from NOSE-06 and SKOV4 cells grown in culture. Methylated DNA was isolated (Figure 2).
Experimental control – NOSE-06 DNA was labeled with Cy5 and Cy3 and co-hybridized to the human genomic microarray (3X).
Experimental data set – NOSE-06 versus SKOV4 was labeled and co-hybridized to the microarray (3X).

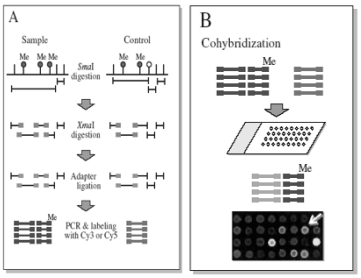

Figure 2. Comparative Methylation Hybridization.
(A) Enrichment of methylated region of the genome by restriction enzyme digestion and linker mediated PCR.
(B) Microarray hybridization of labeled, enriched regions.

Phenotyping of cells types

Assay	NOSE6	SKOV4
Population doubling time (hrs)	37.6 (35.8-39.5)	20.7 (19.5-22.1)
Anchorage-independent growth (colonies/ 20,000 cells plated)	0	1297±234.3
Invasion (# of invaded cells/ 100,000 cells plated)	0	292.5±24.6

DATA ANALYSIS

For each microarray clone, the mean and variance of the log2 ratio of the normalized intensity values were calculated across all three experiments for both the control set and the experimental set. An F-test was performed for each clone to determine if the difference in the variance between the experimental sets being compared was significant ($p<0.05$). A two-tailed t-test for equal or unequal variances, whichever appropriate, was then used to compare the control set to the test set for each clone. Clones were classified as being significantly ($p<0.01$) hypo- or hypermethylated compared to controls if the mean was greater than or less than the control mean, respectively.

Gene expression analysis was performed using the Illumina HumanHT-12v3 chip and expression software . One sample per cell type (NOSE6 or SKOV4) was hybridized per array.

RESULTS

SKOV4 Methylation Patterns across the Human Genome

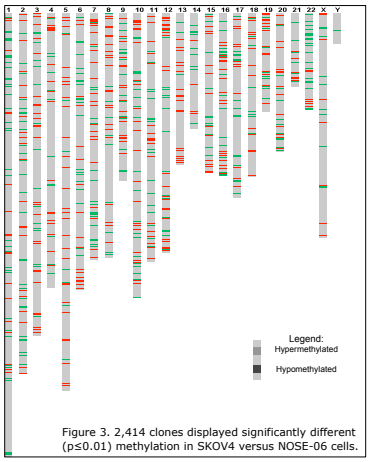

Figure 3. 2,414 clones displayed significantly different ($p \leq 0.01$) methylation in SKOV4 versus NOSE-06 cells.

Validation of methylated loci

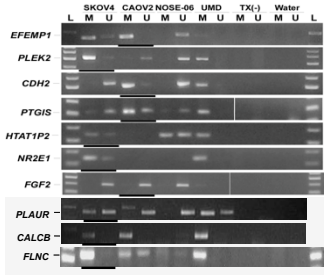

Figure 4. *MS-PCR for candidate methylated genes based on CMH analysis.* Bisulfite modified DNA from SKOV4, CAOV2 (a second ovarian cancer cell line) and NOSE-06 cell line DNA was analyzed, along with universally methylated DNA and untreated normal human genomic DNA [TX(-)]. L, ladder. Black underline designates cell line in which methylation of the promoter was expected from the CMH results.

Gene expression analysis of candidates

**methylation status previously implicated in ovarian cancer*
[‡]P-value ≤ 0.05

Pathway analysis of differentially methylated genes

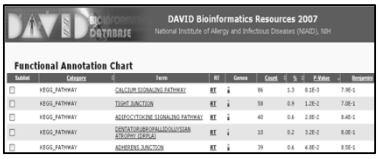

Pathways enriched in DNA methylation changes in ovarian cancer

Research has shown that signal transduction pathways in mammalian cells, which process chemical signals from the cellular environment through the membrane, contain many components that, when altered in quantity or structure, can lead to cancer growth.

A)

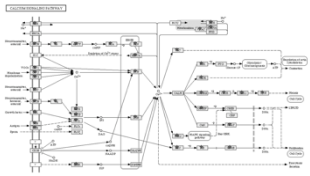

Intracellular calcium is needed to regulate many of the signaling pathways that underlie malignant progression, the idea of inhibiting calcium influx into cells seems to be a reasonable approach to stemming cancer growth.

B)

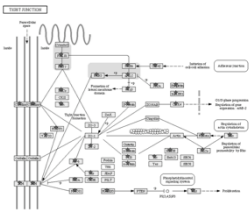

As OSE progresses toward malignancy, it loses its stromal appearance and acquires a more epithelial-like phenotype characterized by the formation of tight junctions.

C)

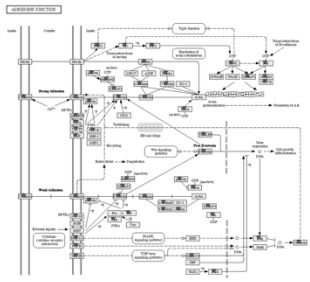

Epithelial tightness and apical/basolateral orientation are maintained through adherens and tight junctions (TJs). Alterations in junction formation and function could promote tumorigenesis via increased access to growth factors and cytokines.

D)

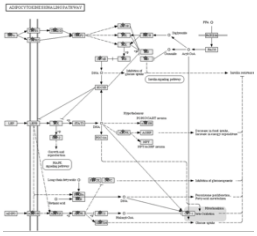

Adipocytokines play a significant role in obesity and numerous other functions of these hormones have been identified, including a potential role in the regulation of angiogenesis and tumor growth.

Figure 5. Significantly enriched pathways identified using differentially methylated candidate genes. Genes demarcated by red stars were found to be hypo- or hypermethylated in SKOV4 compared to NOSE6

CONCLUSIONS

1) Using genomic techniques and an *in-vitro* model, we defined a set of genes that are predicted to be differentially methylated in ovarian cancer.

2) DNA methylation changes and concomitant expression changes differentiate diseased and non-diseased surface epithelium.

3) Pathway analysis and molecular validation of loci is ongoing and will determine the important epigenetic players in the formation of this disease.

DUKE center for HUMAN GENETICS

2008 SGO Abstract

DNA Methylation in Ovarian Cancer is Related to Poor Prognosis and Suppression of the TGF-beta Signaling Pathway

Noriomi Matsumura[1,2], Zhiqing Huang[1], Tiffany Perry[1], Darby Kroyer[1], Tsukasa Baba[1,2], Seiichi Mori[3], Shingo Fujii[4], Andrew Berchuck[1,4] and Susan K. Murphy[1,3]

(1) Gynecologic Oncology, Duke University Medical Center, Durham, NC, USA
(2) Kyoto University, Kyoto, Japan
(3) Duke Institute for Genome Sciences and Policy, Durham, NC, USA
(4) National Hospital Organization, Kyoto Medical Center, Kyoto, Japan

Objectives: Deregulation of the TGF-beta signaling pathway is reported in many cancers but its basis is not understood. Analysis of ovarian cancer (OVCA) cells treated with DNA methyltransferase inhibitors identified candidate hypermethylated (HM) genes; among these were a sizeable number of TGF-beta pathway genes. Our objective was to determine if these genes are HM in ovarian cancer and how they impact phenotype.

Methods: Affymetrix U133A microarray data was generated for 43 ovarian cell lines and 13 primary OVCA cultures +/- 5-Aza-dC or 5-Aza-C, respectively. Probe set IDs were used to identify candidate HM genes based on standard deviations in expression values >1.8 and maximum fold-change in response to treatment >2.8, defined by analysis of a set of 63 genes known to be methylated in cancer. Promoter methylation was analyzed using methylation-specific PCR. Gene Set Enrichment Analysis (GSEA) was used to examine differences of *a priori* defined sets of genes in cancers or cells with divergent phenotypes, with a false discovery rate (q) <0.25 considered significant. Population doubling time and anchorage-independent growth were measured for the 43 ovarian cell lines. Microarray data for 57 stage III-IV OVCA tissue samples and for human fibroblasts treated +/- TGF-beta 1 were also used.

Results: 290 candidate HM genes (360 probes) were identified. 94% (15/16) of the genes tested showed HM in the OVCA cell lines and tissues. The Gene Ontology term, ”negative regulation of cell proliferation” ($p<0.0001$) and the KEGG-pathway, “TGF-beta signaling pathway” ($p<0.01$) were enriched among the candidate HM genes vs. the entire genome. Candidate HM genes are significantly suppressed in fast-growing cells ($q=0.185$), cells with increased anchorage independent growth ($q=0.054$), and OVCAs with poor prognosis ($q=0.208$). 5-aza-dC treatment of OVCA cell lines activates genes that comprise a TGF-beta pathway signature ($p=0.001$), defined based on induction of gene expression following TGF-beta1 treatment. Strikingly, many TGF-beta pathway genes, including *BMP2, BMP4, BMP7, FST, ID4, TGFB2, TGFBR2,* and *THBS1* were HM in OVCA.

Conclusions: This is the first report showing inactivation of multiple TGF-beta signaling pathway genes by HM in ovarian cancers. These results demonstrate that the methylation status of these genes is an important component in understanding inactivation of this pathway in OVCA, and that epigenetic-based therapies may have potential to restore this function.

Character count: 2229

Print this Page for Your Records Close Window

Control/Tracking Number: 08-AB-3477-AACR
Activity: Abstract Submission
Current Date/Time: 11/27/2007 9:53:46 AM

DNA methylation in ovarian cancer is related to poor prognosis and suppression of the TGF-beta signaling pathway

Short Title:
TGFB pathway methylation in cancer

Author Block: *Zhiqing Huang*, *Noriomi Matsumura*, *Tiffany Perry*, *Darby Kroyer*, *Tsukasa Baba*, *Seiichi Mori*, *Shingo Fujii*, *Andrew Berchuck*, *Susan K. Murphy*. Duke Univ. Medical Ctr., Durham, NC, Kyoto Medical Center, Kyoto, Japan

Abstract: **Purpose.** Deregulation of the TGF-beta signaling pathway is reported in many cancers but its basis is not understood. Analysis of ovarian cancer (OVCA) cells treated with DNA methyltransferase inhibitors identified candidate hypermethylated (HM) genes; among these were a sizeable number of TGF-beta pathway genes. Our objective was to determine if these genes are HM in ovarian cancer and how they impact phenotype.
Procedures. Affymetrix U133A microarray data was generated for 43 ovarian cell lines and 13 primary OVCA cultures +/- 5-Aza-dC or 5-Aza-C, respectively. Probe set IDs were used to identify candidate HM genes based on standard deviations in expression values >1.8 and maximum fold-change in response to treatment >2.8, defined by analysis of a set of 66 genes known to be methylated in cancer. Promoter methylation was analyzed using methylation-specific PCR. Gene Set Enrichment Analysis (GSEA) was used to examine differences of *a priori* defined sets of genes in cancers or cells with divergent phenotypes, with a false discovery rate (q) <0.25 considered significant. Population doubling time and anchorage-independent growth were measured for the 43 ovarian cell lines. Microarray data for 57 stage III-IV OVCA tissue samples and for human fibroblasts treated +/- TGF-beta 1 were also used.
Results. 290 candidate HM genes (360 probes) were identified. 94% (15/16) of the genes tested showed HM in the OVCA cell lines and tissues. The Gene Ontology term, "negative regulation of cell proliferation" ($p<0.0001$) and the KEGG-pathway, "TGF-beta signaling pathway" ($p<0.01$) were enriched among the candidate HM genes vs. the entire genome. Candidate HM genes are significantly suppressed in fast-growing cells ($q=0.185$), cells with increased anchorage independent growth ($q=0.054$), and OVCAs with poor prognosis ($q=0.208$). 5-aza-dC treatment of OVCA cell lines activates genes that comprise a TGF-beta pathway signature ($p=0.001$), defined based on induction of gene expression following TGF-beta1 treatment. Strikingly, many TGF-beta pathway genes, including *BMP2, BMP4, BMP7, FST, ID4, TGFB2, TGFBR2*, and *THBS1* were HM in OVCA.
Conclusions. This is the first report showing inactivation of multiple TGF-beta signaling pathway genes by HM in ovarian cancers. These results demonstrate that the methylation status of these genes is an important component in understanding inactivation of this pathway in OVCA, and that epigenetic-based therapies may have potential to restore this function.
:

Author Disclosure Information: **Z. Huang**, None; **N. Matsumura**, None; **T. Perry**, None; **D. Kroyer**, None; **T. Baba**, None; **S. Mori**, None; **S. Fujii**, None; **A. Berchuck**, None; **S.K. Murphy**, None.
Category and Subclass (Complete): CB06-02 DNA methylation
Primary Organ Site (Complete):
Organ Site Classification: Applicable. My abstract does refer to a specific primary organ site/tumor type as indicated below.

Primary Organ Site: Gynecological cancers: ovarian

Chemical Structure Disclosure (Complete):

Choose Chemical Structure Disclosure: YES, and I WILL DISCLOSE the complete chemical structures of the compounds used to generate the data in this abstract at the time of presentation.

Please explain (maximum 250 characters with spaces): : We treated cells with commercially available compounds, whose structures are already widely known.

Research Type (Complete): Basic research
Keywords/ Indexing (Complete): DNA hypermethylation ; Microarrays ; Signaling pathways
Sponsor (Complete):
2008 Travel Awards (Complete):
Payment (Complete): Your credit card order has been processed on Tuesday 27 November 2007 at 9:50 AM.
Status: Complete

***To log out, simply close your browser window. All information will be saved if you have hit the Continue button after each step.

If you have any questions or experience any problems with the 2008 AACR Abstract Submitter, please contact Customer Service at support@abstractsonline.com, or call (217) 398-1792.

Abstract/Session Information for Program Number 1204

Print Close window

Session Information

Session Title: Cancer Genetics **Session Type:** Poster

Session Location: Exhibit Hall C **Session Time:** Wed 4:30PM-6:30PM, Thu 4:30PM-6:30PM, Fri 10:30AM-12:30PM

Abstract Information

Poster Board Number: 1204/W **Presentation Time:** Wed, Nov 12, 2008, 4:30PM-6:30PM

Keywords: Cancer Genetics, KW012 - CANCER, KW025 - CHROMOSOMAL STRUCTURE/FUNCTION, KW151 - REGULATION OF TRANSCRIPTION, KW109 - METHYLATION, KW110 - MICROARRAYS

Abstract Content

Genome-wide targets of aberrant methylation in serous epithelial ovarian cancer cells. *D. Biscocho, J. J. Connelly, Z. Huang, S. K. Murphy, S. G. Gregory* Duke University, Durham, NC.

Ovarian cancer is an insidious disease that has usually metastasized prior to diagnosis. Abnormal DNA methylation is frequently found at specific loci in ovarian cancers and may provide opportunities to improve early disease detection and treatment. Unlike genetic mutations, aberrant DNA methylation is potentially reversible via epigenetic-based therapies. We have utilized DNA tiling path arrays to determine the genome-wide distribution of methylation in cell lines derived from spontaneously transformed normal ovarian surface epithelium (NOSE-06) and malignant ovarian cancer (SKOV4). 2414 regions of the genome were identified as differentially methylated ($p \leq 0.01$) in SKOV4 versus NOSE-06. Several regions contained genes known to be aberrantly methylated in ovarian cancer cells lines (*GSTP1*, *FLNC*, *CDH1*, *MAGEA3*, and *PYCARD*). Interestingly, loci previously identified as methylated in ovarian cancer cell lines were methylated in NOSE-06. It is not known how spontaneous immortalization and passaging in cell culture have influenced the methylation profiles of NOSE-06, but suggests the importance of defining normal methylation profiles of relevant tissues in order to serve as a basis for comparison to ovarian malignancy. We have validated the methylation state of several novel genes using methylation specific PCR (*CDH2*, *CDH4*, *PLAUR*, *CALCB*, *PLEK2*, *FN1*, *NR2E1*). Correlative gene expression analysis identified two genes that exhibit a decrease in gene expression and an increase in promoter methylation in two separate ovarian cancer cell lines. Interestingly, these genes, fibronectin 1 (*FN1*) and alpha-actinin 1 (*ACTN1*), both play a role in cell adhesion and migration. Pathway analysis of the genes contained within differentially methylated regions indicated enrichment of pathways involved in tight junction ($p=0.01$) and adherens junction ($p=0.05$) formation. Disturbance of the integrity of intercellular junctions promotes invasiveness and mobility of cancer cells. Taken together this information indicates the role DNA methylation may play in the integrity of intercellular junctions and implicates a reversible cellular process in the oncogenic transformation of a cell.

Print Close window

The American Society of Human Genetics
9650 Rockville Pike, Bethesda, MD
Phone: 301-634-7300, Fax: 301-634-7079
Questions and Comments: kkoziol@ashg.org

BIGH3, target of methylation in ovarian cancer, is up-regulated in omental metastasis

Shogo Yamamura, Noriomi Matsumura, Masaki Mandai, Tsukasa Baba, Junzo Hamanishi, Ken Yamaguchi, Ikuo Konishi
(Kyoto University, ObGyn)

Coauthor; Susan Murphy, Zhiqing Huang, Andrew Berchuck (Duke University, IGSP)

[Objective]This study aims to identify epigenomic patterns and genes that accelerate omental metastasis of ovarian cancer.
[Method]A list of 290 candidate methylation genes, that we previously generated by analyzing microarray data of 43 ovarian cancer cell lines adding 5Aza-dC, was used. Microarray dataset, that contains 46 serous advanced ovarian cancers and 28 omenatal metastasis derived from serous ovarian cancers, was obtained from website (GSE 2109). Methylation specific PCR was used to examine methylation of *BIGH3*.
[Results]The methylation gene list was up-regulated in omental metastasis (FDR q value < 0.250). *BIGH3*, which was up-regulated in omental metastasis ($p < 0.05$), was methylated in 19/29 (65.5%) ovarian cancer cell lines and 16/33 (48.5%) advanced ovarian cancer tissue samples.
[Discussion]Our result suggests that many methylated genes, including *BIHG3*, are upregulated, probably by demethylation, in omental metastasis of ovarian cancer. BIHG3 may enhance the metastatic potential of cancer cells because BIGH3 is known to be an important mediator that accelerates colon cancer metastasis.

卵巣癌におけるメチル化は予後不良と相関し、TGFβ経路の抑制をもたらす

[目的]
TGFβ経路の異常は多くの癌で報告されているが、そのメカニズムの詳細は不明である。本研究は、卵巣癌におけるメチル化の臨床的意義やTGFβ経路との関連を調べることを目的とした。
[方法]
43種類の卵巣癌細胞株に5Aza-dCを添加し、マイクロアレイを施行した。細胞の倍加時間と足場非依存性増殖を調べ、進行卵巣癌組織57症例のデータも用い、遺伝子リストの発現との相関をGene Set Enrichment Analysisで検討し、false discovery rate q値<0.25を有意とした。またヒトfibroblastにTGFβ1を添加したデータから、Binary Regressionによってコンピューター上でTGFβ活性を調べた。メチル化はMethylation Specific PCRで評価した。
[成績]
5Aza-dC添加による発現亢進が大きい360プローブ(290遺伝子)を選んだところ、94%（15/16遺伝子）で、卵巣癌細胞株や組織でメチル化を認めた。その遺伝子リストには、ゲノムと比べ"negative regulation of cell proliferation"というgene ontology termが濃縮し($p<0.001$)、"TGFβ signaling pathway"が濃縮していた($p<0.01$)。その遺伝子リストの発現は、増殖が早い細胞、足場非依存性増殖能の高い細胞、予後不良の癌で有意に抑制されていた(それぞれ$q=0.185$, 0.054, 0.208)。コンピューター上の解析では、5Aza-dC添加によりTGFβ活性が上昇し($p<0.001$)、実際、細胞株や組織において、TGFβ経路に属する*BMP2, BMP4, BMP7, FST, ID4, TGFB2, TGFBR2, THBS1*がメチル化されていた。
[結論]
卵巣癌において、予後不良の腫瘍で発現が抑制され、腫瘍抑制遺伝子を多く含むメチル化遺伝子群を同定した。また、TGFβ経路はメチル化により抑制されていると考えられた。

卵巣癌における治療個別化に向けたBioinformaticsの応用 –化学療法感受性に関わる分子メカニズムの解明と新規分子標的薬剤の同定–

[目的] 卵巣癌患者の予後を改善するため、患者ごとの薬物療法の個別化、すなわちオーダーメイド治療が求められている。そのためには、抗癌剤の作用メカニズムに基づき感受性を予測し患者ごとに最適な抗癌剤を選択すること、および、個々の癌で標的となるシグナル伝達機構を解明し新規分子標的薬剤による個別化を目指すことが不可欠である。近年のDNAマイクロアレイとBioinformatics技術の発達により、癌で生じている多くの遺伝子の複合的な異常を正確に把握し、臨床に反映させることが可能となってきた。本研究では、卵巣癌治療の個別化を目指し、マイクロアレイを利用した研究を行った。

[方法]〈研究１：卵巣癌におけるパクリタキセル感受性バイオマーカーの同定とその分子メカニズム〉 7年以上の長期生存24例と3年以内の短期死亡33例の進行漿液性卵巣癌計57例のマイクロアレイデータをwebsiteより入手した。プロモーター領域の転写因子結合モチーフ解析を用いて、E2Fのcofactorとして働く転写因子YY1の下流遺伝子を同定した。２種の卵巣癌細胞株(HEY, BG1)を用いて、siRNAを用いたYY1のknockdownが、シスプラチン感受性、パクリタキセル感受性に与える影響を調べた。また培養細胞にE2F3を過剰発現させたマイクロアレイデータをwebsiteより入手し、微小管を構成する遺伝子群(GO#5874 microtubuleに含まれる遺伝子)の発現変化を検討した。

〈研究2：卵巣明細胞腺癌の発生メカニズムに基づく新規分子標的療法剤の同定〉 卵巣癌99例(漿液性腺癌41例、類内膜腺癌37例、粘液性腺癌13例、明細胞腺癌8例)のマイクロアレイデータをwebsiteより入手した。また、卵巣癌39細胞株(漿液性腺癌13株、類内膜腺癌4株、粘液性腺癌4株、明細胞腺癌13株、未分化癌5株)を用いてマイクロアレイ解析を行った。それらのデータセットにおいて、SAM(Significance Analysis of Microarrays)により、明細胞腺癌を特徴付ける遺伝子群を抽出し、RT-PCRで確認した。不死化OSE細胞株を用いて、チョコレート嚢腫内溶液、あるいはFeを添加して、マイクロアレイを行った。他臓器癌のデータセットをwebsiteより入手して解析した。

〈研究3：卵巣癌播種性転移の分子メカニズムに基づく新規分子標的療法剤の同定〉 43種類の卵巣癌細胞株にDecitabineを添加しマイクロアレイを施行した。Decitabineによる発現上昇の程度の大きい遺伝子群をメチル化候補遺伝子群と定義し、Methylation specific PCRによりメチル化の頻度を調べた。卵巣癌細胞株(SKOV4, HEY, A2008, OVCAR3)のTGFβ活性を、リン酸化SMAD2/3抗体を用いたWestern blottingおよび、SMAD3レポータープラスミドを用いたルシフェラーゼレポーターアッセイで評価した。卵巣漿液性腺癌Ⅲ期およびⅣ期の原発巣46例と大網転移巣28例のマイクロアレイデータセットをwebsiteより入手した。培養ヒトfibroblastに

TGFβを添加したデータセットを用いて、Binary regression法により臨床サンプルのTGFβ活性を評価した。

[成績]<研究1> YY1は予後良好の進行卵巣癌で高発現していた(p<0.001)。卵巣癌においてYY1と正に相関する遺伝子にはYY1結合モチーフやE2F結合モチーフをもつ遺伝子が集まり(それぞれp<0.0001)、YY1/E2Fはその下流遺伝子の発現を亢進させていることが判明した。そのターゲット遺伝子群の発現亢進は、パクリタキセルを使用した症例では予後良好と相関した(p<0.05)が、パクリタキセルを使用していない症例では予後との関連がなかった。卵巣癌細胞株においてYY1をknockdownすると、パクリタキセルに対して抵抗性となった(p<0.01)が、シスプラチンに対する感受性は変化しなかった。微小管を構成する遺伝子群においては、YY1結合モチーフを持つ頻度が高く(p<0.01)、E2F3過剰発現により発現が亢進し、YY1/E2Fによる微小管阻害剤特異的な感受性との関連が示唆された。本研究により、卵巣癌の摘出標本でYY1発現を調べることで、パクリタキセルを使用すべきか否かを決定し、化学療法のレジメンを選択できる道が開けた。

<研究2> 卵巣癌組織および細胞株のデータから、明細胞腺癌を特徴づける230遺伝子(Clear Cell Signature)(発現上昇229遺伝子と発現低下1遺伝子)を同定し、RT-PCRで10個の遺伝子が実際に明細胞腺癌組織で高発現していることを確認した。Clear Cell Signatureは、不死化OSE細胞にチョコレート嚢胞内溶液あるいはFeを添加することによって発現が上昇した(p<0.001)。Clear Cell Signatureには腎臓の発生に関連した遺伝子が集まり(p<0.01)、クラスタリングによって卵巣明細胞腺癌は腎細胞癌に極めて類似していることが明らかとなった。したがって、腎細胞癌に対し有用なマルチキナーゼ阻害剤SorafenibとSunitinibは、明細胞腺癌の治療にも有用である可能性があると考えられる。

<研究3> 卵巣癌細胞株43種類のいずれかでDecitabine添加後の発現上昇が顕著なメチル化候補360遺伝子を同定し、その中の20/20遺伝子(100%)で実際にメチル化を認めた。メチル化候補遺伝子には、TGFβ経路に関わる遺伝子が集まっていた(p<0.01)。卵巣癌細胞株にDecitabineを添加すると、TGFβ活性が亢進した。大網播種性転移巣では、原発巣に比して、メチル化候補遺伝子群の協調した発現上昇および、TGFβ経路の活性化が認められた(p<0.01)。このことより、卵巣癌の進展においては、エピジェネティックに制御された遺伝子の協調した発現上昇がTGFβ経路の活性化をもたらして、播種性転移を促すと考えられた。近年開発されたTGFβ阻害剤は、卵巣癌の播種性転移に対して有用と考えられる。

[結論] マイクロアレイを用いて、卵巣癌のパクリタキセルに対する感受性メカニズム、さらに、卵巣明細胞腺癌の発生や卵巣癌の播種性転移に関わる分子機構が明らかになった。これらの知見は、患者ごとに最適な化学療法剤を選択し、新たな分子標的治療薬を探索するために有用と思われる。